AD NUMBER

AD900576

NEW LIMITATION CHANGE

TO

Approved for public release, distribution unlimited

FROM

Distribution authorized to U.S. Gov't. agencies only; Test and Evaluation; FEB 1972. Other requests shall be referred to Air Force Flight Dynamics Lab., Wright-Patterson AFB, OH 45433.

AUTHORITY

AFFDL ltr, 27 Aug 1973

AFFDL-TR-71-12-Pt-2

MULTIWHEEL LANDING GEAR–SOILS INTERACTION AND FLOTATION CRITERIA – PHASE III

PART II

Final rept. 18 Dec 70 - 15 Dec 71,

DAVID C. KRAFT,
HENRY LUMING,
J. RICHARD HOPPENJANS
FRED BOGNER

UNIVERSITY OF DAYTON
RESEARCH INSTITUTE
DAYTON, OHIO

F33615-70-C-1170

TECHNICAL REPORT AFFDL-TR-71-12, PART II

AF-1369

JAN [redacted] 72

220P.

136908

AIR FORCE FLIGHT DYNAMICS LABORATORY
AIR FORCE SYSTEMS COMMAND
WRIGHT-PATTERSON AIR FORCE BASE, OHIO

105 400

NOTICE

When Government drawings, specifications, or other data are used for any purpose other than in connection with a definitely related Government procurement operation, the United States Government thereby incurs no responsibility nor any obligation whatsoever; and the fact that the government may have formulated, furnished, or in any way supplied the said drawings, specifications, or other data, is not to be regarded by implication or otherwise as in any manner licensing the holder or any other person or corporation, or conveying any rights or permission to manufacture, use, or sell any patented invention that may in any way be related thereto.

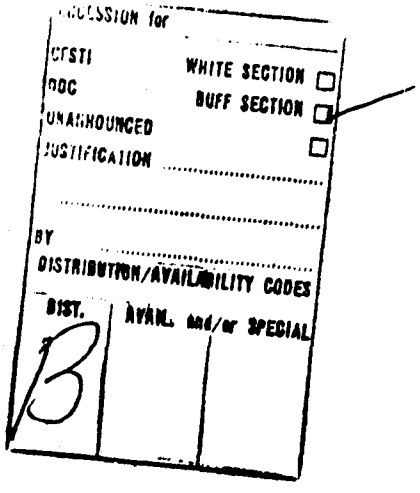

Copies of this report should not be returned unless return is required by security considerations, contractual obligations, or notice on a specific document.

AIR FORCE: 5-6-72/250

AFFDL-TR-71-12
PART II

MULTIWHEEL LANDING GEAR–SOILS INTERACTION AND FLOTATION CRITERIA – PHASE III

PART II

DAVID C. KRAFT
HENRY LUMING
J. RICHARD HOPPENJANS
FRED BOGNER

AFFDL-TR-71-12
PART II

FOREWORD

This report was prepared by the Aerospace Mechanics Group of the University of Dayton Research Institute under USAF Contract F33615-70-C-1170. The contract was initiated under Project No. 1369, "Launching and Alighting Systems for Military Aircraft," Task No. 136908, "Aircraft Surface Operation on Soil." This work was conducted under the direction of the Vehicle Equipment Division, Air Force Flight Dynamics Laboratory, Wright-Patterson Air Force Base, Ohio, Mr. George Sperry (AFFDL/FEM) Project Engineer.

This report covers work conducted from 18 December 1970 to 15 December 1971.

The authors wish to thank Mr. Sperry for his efforts and assistance in integrating the research program toward Air Force objectives. This report was submitted by the authors in January 1972.

Publication of this technical report does not constitute Air Force approval of the reported findings or conclusions. It is published only for the exchange and stimulation of ideas.

K. N. Digges

KENNERLY H. DIGGES
Chief, Mechanical Branch
Vehicle Equipment Division
Air Force Flight Dynamics Laboratory

ABSTRACT

The design and utilization of military aircraft in forward area situations has required a continual investigation of those factors which define the aircraft flotation performance and surface operating capability on semi- and unprepared soil runways. This report summarizes these efforts conducted under Phase III - Part II of a continuing research program in landing gear/soil interaction.

Phase III - Part II consisted primarily of a comprehensive investigation of the flotation variable of braking and how braked tire/soil interaction influences flotation performance. A series of full scale braked tire tests were conducted in a sand and clay type soil. An analytical study of braked tire/soil interaction was also made using a lumped parameter technique to simulate the soil. The results of these investigations resulted in two braking analysis equations which can be used to predict the braked tire drag ratio, R_B/P (where R_B = braked drag force, P = vertical tire load), for aircraft type tires operating in sand and clay type soils. Both the braking tests results and analysis equations apply to a limited speed range (0 to 15 knots).

Additional studies were also made, on a preliminary basis, of the flotation variables of multipass and speed. An update of the Aircraft Flotation/Operation Summary Guide, initially presented in the Phase III - Part I Final Report, is also presented.

TABLE OF CONTENTS

ILLUSTRATIONS

Illustrations (Continued)

Illustrations (Continued)

LIST OF TABLES

List of Tables (Continued)

List of Tables (Continued)

LIST OF SYMBOLS

Symbol	Definition	First Page Referenced	Page Defined
A	Tire contact area (rigid surface)	7	7
A_{Cone}	Cone base area	188	188
A_Z	Area of equivalent plane of contact at sinkage Z	18	18
B	A variable related to the stress invariants	159	159
b	Tire section width	4	12
CBR	California bearing ratio	2	10
C_{DI}	Soil inertia drag coefficient	62	62
CI	Mobility cone penetration test or resistance	10	10
CI_{avg}	Average cone index of soil over 0" to 6" depth	2	64
CI_{tot}	Average cone index of all layers	87	189
CI_{layer}	Average cone index of a layer	87	188
c	Cohesion of soil	18	18
c_1	Dilatational wave propagation velocity	164	164
D	Tire outside diameter	4	12
d'	Tire deflection in percent	8	8
d	Tire deflection in inches (rigid surface)	12	12
E	Young's modulus	46	46
FI	Flotation index	195	195
F_{plate}	Resistance of plate	94	94
f	Yield function	158	158
G	Modulus of rigidity	159	159
h	Space mesh size	45	45
I	First invariant of the stress tensor	158	158
i	Location identifier (column)	45	45
J	Second invariant of the deviatoric stress tensor	158	170

LIST OF SYMBOLS (Continued)

Symbol	Definition	First Page Referenced	Page Defined
j	Location identifier (row)	45	45
K	Constant clay soil	20	20
K_1	Constant sand soil	29	29
K_2	Torque constant	36	36
k	Shear yield stress	46	46
L	Hydrodynamic lift	63	63
ℓ	Tire footprint length (rigid surface)	7	7
ℓ_Z	Length of equivalent plane of contact	17	17
M'	Number width mesh points	45	45
m	Fraction of tire diameters (spacing/tire diameter)	68	68
N'	Number depth mesh points	45	45
OI	Operations index	195	195
P	Vertical load	7	7
P'	Vertical load minus hydrodynamic lift	64	64
P_s	Vertical soil reaction	17	17
PR	Tire ply rating	7	7
p	Tire contact stress or prescribed surface pressure	68	68
p_{max}	Peak surface pressure	44	44
p_n	Uniform vertical pressure	41	42
p_s	Uniform shear distribution	41	42
Q	Constant for incremental stress-strain relation use	159	159
R	Rolling drag resistance to forward motion	7	7
R_1, R_2, R_3	Cone penetrometer penetration resistance in pounds	188	188
RMI	Relative merit index	1	1
R_B	Braked tire drag force	7	17

LIST OF SYMBOLS (Continued)

Symbol	Definition	First Page Referenced	Page Defined
R_R	Horizontal soil resistance to forward motion exclusive of shear resistance during braking	16	17
R_T	Horizontal component of net shear force resistance	16	16
$(R/P)_M$	Multiple wheel drag ratio	2	2
(R_B/P)	Braking drag ratio	40	41
r	Rate of penetration (in/sec)	78	78
ΔR	Incremental change in rolling drag resistance	63	63
ΔR_R	Incremental change in resistance to forward motion exclusive of shear resistance	16	17
S	Percent tire slip	7	17
T	Tangential shear force	16	17
T'	Braking torque	7	17
t	Elapsed time	44	44
t_c	Characteristic time related to time variable	164	164
t_d	Time duration of load pulse	44	44
t_r	Rise time	68	68
Δt	Time increment	46	46
$U, \dot{U}, \ddot{U}$	Displacement, velocity, acceleration in η direction	45	45
$u, \dot{u}, \ddot{u}$	Displacement, velocity, acceleration in the x-direction	45	45
ΔU	Incremental radial displacement in η direction	45	45
$V, \dot{V}, \ddot{V}$	Displacement, velocity, acceleration in the ζ-direction	45	45
V_a	Horizontal velocity of the aircraft and wheel axle	7	7
V_W	Peripheral speed of wheel	7	17

LIST OF SYMBOLS (Continued)

Symbol	Definition	First Page Referenced	Page Defined
$v, \dot{v}, \ddot{v}$	Displacement, velocity, acceleration in the y-direction	45	45
ΔV	Incremental velocity in the ζ-direction	45	45
W	Moisture content of soil (percent)	13	13
ΔW	Incremental work done on the soil medium	70	159
$w, \dot{w}, \ddot{w}$	Displacement, velocity, and acceleration in the z-direction	45	45
w_s	Surface deflection of a mass point	73	73
Δw	Incremental vertical displacement in z-direction	45	45
x	x-coordinate, horizontal axis	45	45
Z	Instantaneous soil sinkage	7	17
z	z-coordinate, vertical axis	45	45
Z_R	Rut depth	7	7
ΔZ	Incremental sinkage	63	64
ΔZ_{lift}	Incremental sinkage due to lift	63	64
$\Delta Z_{inertia}$	Incremental sinkage due to inertia	63	64
(Z/D)	Sinkage ratio	4	4
α	Ratio of vertical load to tire contact area P/A	25	25
α_1	Soil parameter related to the friction angle	158	158
β	Constant used to define loading and unloading	46	159
$\Delta\gamma_{\eta\zeta}$	Shear strain increment in the η-ζ direction	158	158
$\Delta\epsilon_\eta, \Delta\epsilon_\zeta, \Delta\epsilon_\xi$	Normal strain increment in the η, ζ, and ξ directions	158	158
ζ	Coordinate system axis label	45	45
η	Coordinate system axis label	45	45

LIST OF SYMBOLS (Concluded)

Symbol	Definition	First Page Referenced	Page Defined
η_c	Stress correction equation parameter	160	160
λ	Lame's constant	159	159
μ_0	Coefficient of rolling friction on a rigid surface	62	62
$\mu(S)$	Nonlinear function which varies with slip	16	16
ν	Poisson's ratio	46	46
ρ	Mass density of soil	46	46
γ_d	Dry soil density	13	13
$\bar{\sigma}$	Effective normal stress	18	18
$\sigma_x, \sigma_y, \sigma_z, \sigma_\eta, \sigma_\zeta$	Normal stresses in the x, y, z, η, and ζ directions	157	157
$\tau_{xz}, \tau_{xy}, \tau_{\eta\zeta}$	Shear stresses in the x-z, x-y, and η-ζ directions	157	157
θ	Angle defining equivalent plane of contact	17	18
ϕ	Friction angle of soil	18	18

SECTION I

INTRODUCTION AND AIRCRAFT FLOTATION/ OPERATION SUMMARY GUIDE

A number of comprehensive efforts[1-7] have been conducted in recent years in studying the problems associated with the operation of military aircraft on forward area soil runways. The results of these efforts have led to an identification of what have been termed the primary and secondary variables which influence aircraft flotation/operation performance. The primary variables are aircraft surface drag, sinkage, multiple wheel effects, braking, soil surface type and strength, and tire size and contained air pressure. Secondary variables include multipass, speed, turning, landing impact, surface roughness, texture, and stress hardening characteristics.

The current research effort described in this report is a part of a continuing research program sponsored by the United States Air Force. The objective of this continuing research program is to: (1) analytically define landing gear-soil interaction; (2) develop a system for comparing and rating the flotation capacity and surface operating capability of landing gear contact elements and landing gear systems during aircraft operations on soil runways; and (3) to develop systematic design procedures for optimizing the flotation and surface operating capability of future aircraft. Phase I[6] of this program included a survey of the flotation problem, establishment of the critical parameters, and an investigation of available flotation data leading to the development of a flotation analysis equation. Phase II[2] included the development of an empirical sinkage prediction equation, development of a lumped parameter simulation sinkage prediction technique, conducting the Rolling Single Wheel Verification Tests, and the development of the Single Wheel Relative Merit Index (RMI) system for defining comparative flotation capacity (see Figure 1 for a typical comparative rating). Phase III - Part I[1] consisted of the development of the multiwheel sinkage-drag analysis equations, conducting the Multiwheel Verification Tests, and the development of a lumped parameter iteration technique for simulating the

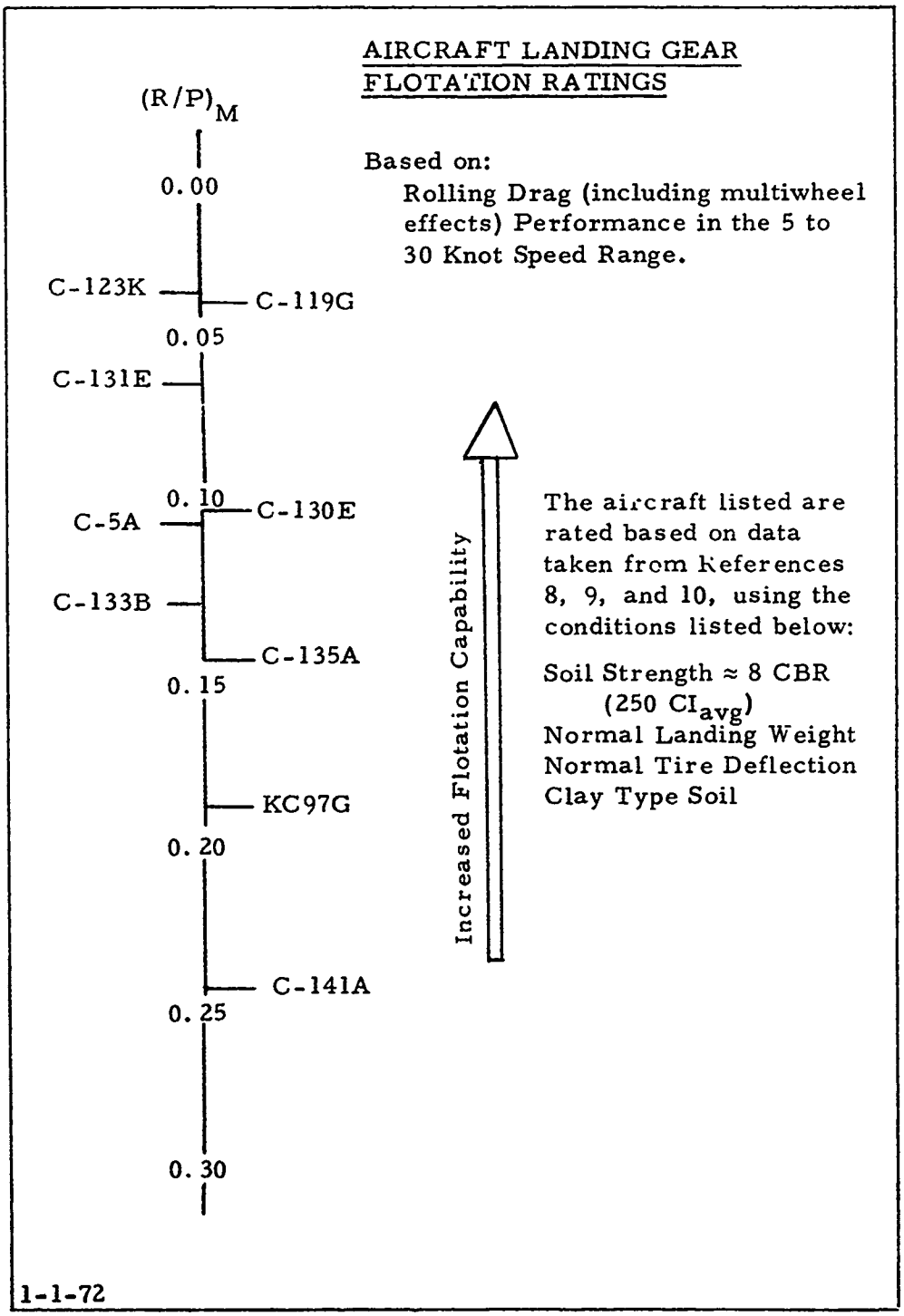

Figure 1. Cargo Type Aircraft Landing Gear Flotation Ratings

interaction of dual tires on soil. Phase III - Part II, described herein, included:

- Braked Wheel Verification Tests
- Lumped parameter braking simulation technique computer program
- Development of braking analysis equations for defining braking drag ratios
- Preliminary studies of multipass and speed effects.

The results of the tire/soil interaction studies conducted to date, as well as the results of numerous mobility studies, were used to develop the Aircraft Flotation/Operation Summary Guide presented in Table I. The information contained in Table I provides an up to date review of flotation information for aircraft operations and design personnel. The details of the development of this information are available in past reports[1-7]. Reference to Table I indicates that considerable progress has been made to date (1971) in establishing and verifying the criteria for the primary flotation variables of sinkage, drag, multiwheel, and braking. Based on these criteria it is now possible to develop systematic landing gear design procedures. One such system[11] which was recently developed is detailed in Figure 2. The basis of the design approach uses drag and sinkage as the optimizing variables in selecting candidate landing gear designs. Each design is then further evaluated by the multipass analysis procedure and the resulting information is used to select the finalized landing gear design. As additional information becomes available on landing gear loads, aircraft turning interactions, landing gear storage volumes, and weight trade-offs, a full optimization design procedure will be developed.

TABLE I

QUICK REFERENCE-TIRES ON SOIL FLOTATION GUIDE

FLOTATION VARIABLE	SINKAGE AND DRAG	VELOCITY
Single Wheel	- Drag Ratio (R/P) correlates with sinkage ratio (Z/D) R/P = 0.018 + 3.23(Z/D), all soils, Region II velocity range (see Reference 2) - Sinkage prediction techniques available for sand and clay, Region II velocity range UDRI WES - High speed (Region III) sinkage/drag theory preliminarily defined by UDRI - Low speed (Region I) sinkage/drag relationship not important - Flotation performance improves with: increasing tire diameter increasing tire deflection increasing soil strength decreasing tire load	3 Regions of sinkage/drag variance Approximate 0 ≤ Region I ≤ 5 knots 5 knots ≤ Region II ≤ 40 knots 40 knots ≤ Region III (see Reference 2)
Multiple Wheel Twin Tandem-Tracking Tandem-Nontracking	Optimum spacing based on drag minimization (Region II velocity range) (see Reference 1) - 1.75 b to 2.5 b, sand - 2.5 b to 3.5 b, clay - ≤ 1.75 D or ≥ 2.5 D, sand - 1.5 D to 2.5 D, clay - > 1.25 b > 1.25 D all soils	Velocity influence on optimum multiple wheel spacing is not known. Very likely optimum spacing not influenced by Region I and III velocities.
Braked Wheel	- Braking drag ratio (R_B/P) analysis equations available (see page 51) - Braking drag ratio (R_B/P) independent of initial sand soil strength - Sinkages increase markedly for braking in sand - Sinkages increase moderately for braking in clay - Braking drag ratio increases with: increasing sinkage, sand and clay increasing slip, sand and clay	**Velocity is known not to effect the R_B/P for clay soils in the 3 to 15 knot range. Velocity does affect the braked sinkage in sand in the 3 to 15 knot speed range. The effects of higher speeds on braking has not been established as of 1-1-72. (see page 33)**

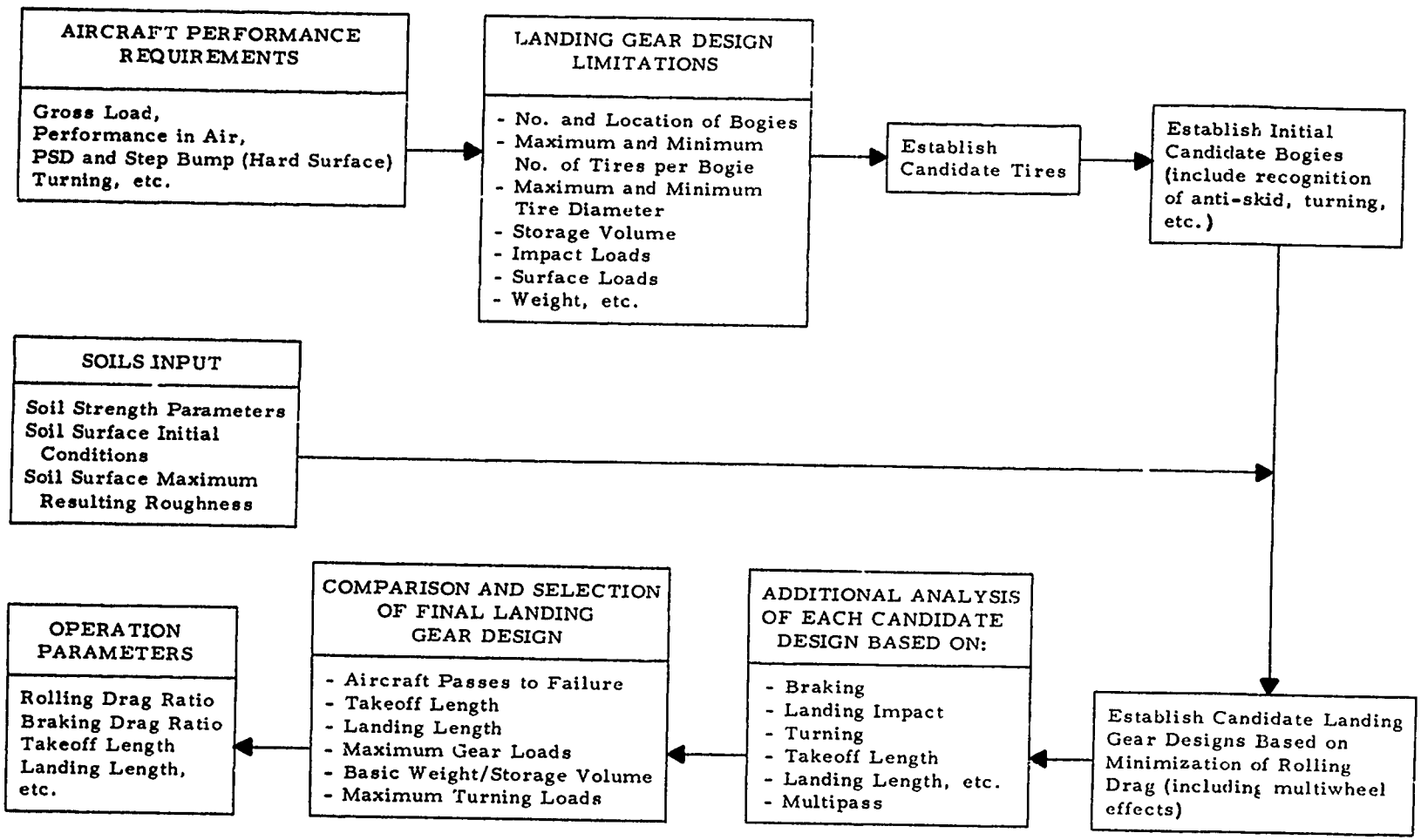

Figure 2. Landing Gear System Design for Aircraft Flotation/Operation on Soil Runways

SECTION II
BRAKING SINKAGE AND DRAG ANALYSIS

A. BRAKING VERIFICATION TESTS

Purpose and Objectives

The purpose of the braked tire on soil test program was to obtain data for the further study and development of theories concerned with predicting the influence that braking action has on aircraft tire performance on soil. Verification and possible modification of the previously developed semi-analytical braking theory[1] was of primary interest. The specific objectives include:

1. Verify the variation of sinkage with increasing percent negative slip (braking) for tires operating in sand and clay type soils.
2. Further establish the variation of the shear force at the tire soil interface with percent negative slip (braking).
3. Study the influence of speed, in the limited velocity range of 5 to 20 fps, on braked tire drag and sinkage in sand and clay type soils.
4. Comparatively study test data with braked tire drag ratio prediction equations and also the lumped parameter iteration braking solution.
5. Evaluate the influence of high tire deflection on braked tire drag and sinkage in sand and clay type soils.

Test Program

Based on a previous experimental braking study[3], speed was observed to influence both sinkage and drag for aircraft tires braking in soil. Due to current funding limitations, however, only a limited velocity range was studied in this test program, while also accomplishing the previously listed objectives. The test program was designed to give drag and sinkage data that was in the range of application to aircraft flotation

analysis. The test program which is summarized in Tables II and III for the clay and sand type soil was run with a 7:00-6, 6PR Type III tire, and a 8:50-10, 8PR Type III tire. Both of these tires had been used in the previous flotation test programs, and therefore, offered the best conditions for correlation of the current test data with that information obtained previously. The following parameters were measured for each test:

Vertical Load (P)
Drag Load - Rolling (R) and Braked (R_B)
Braking Torque (T')
Wheel Velocity (Peripheral) (V_W) } for calculation of % slip (S)
Carriage Velocity (V_a) }
Wheel Axle Vertical Movement (Z_a)
Soil Strength (CI_{avg})
Rut Depth (Z_R)

In addition to the variables mentioned above, complete sets of tire data including such items as measured rigid surface contact area (A), and footprint length (ℓ) were taken for both tires. Soil strength data including density, moisture content, and cone index values were obtained periodically during the testing. The instantaneous soil sinkage (Z) can be determined using the measured values of axle movement and rut depth.

Test Equipment

All braked wheel validation tests in this program were conducted at the U. S. Army Waterways Experiment Station (WES), Vicksburg, Mississippi, at the model wheel facility of the Mobility and Environmental Division between the dates of April 14, 1971 and May 12, 1971. WES modified their basic dynamometer slightly during the program to accomplish the tests. Initially, the tests were to be of a programmed slip type, but the equipment that was to apply the braking torque to the tire was not capable of completely stopping the tire from rolling. As a consequence of this, the test procedure was modified slightly, in that the slip (braking)

TABLE II

BRAKED WHEEL VERIFICATION PROGRAM - CLAY

7:00-6, Type III tire
8:50-10, Type III tire

Tire	Tire Deflection, % (d')	Vertical Load, lbs. (P)	Forward Velocity, fps (V_a)	Soil Strength, (CI_{avg})
7:00-6	35	900	5	40
7:00-6	35	900	10	40
7:00-6	35	900	20	40
7:00-6	42	1100	5	40
7:00-6	42	1100	10	40
7:00-6	42	1100	20	40
8:50-10	35	1500	5	40
8:50-10	35	1500	10	40
8:50-10	35	1500	20	40
8:50-10	42	1700	5	40
8:50-10	42	1700	10	40
8:50-10	42	1700	20	40

TABLE III

BRAKED WHEEL VERIFICATION PROGRAM - SAND

7:00-6, Type III tire
8:50-10, Type III tire

Tire	Tire Deflection, % (d')	Vertical Load, lbs. (P)	Forward Velocity, fps (V_a)	Soil Strength, (CI_{avg})
7:00-6	35	400	5	40
7:00-6	35	400	10	40
7:00-6	35	400	20	40
7:00-6	42	450	5	40
7:00-6	42	450	10	40
7:00-6	42	450	20	40
8:50-10	35	600	5	40
8:50-10	35	600	10	40
8:50-10	35	600	20	40
8:50-10	35	1000	5	40
8:50-10	35	1000	10	40
8:50-10	35	1000	20	40
8:50-10	42	700	5	40
8:50-10	42	700	10	40
8:50-10	42	700	20	40

is not a linearly increasing function along the test track. Figure 3 shows the dynamometer with the 8:50 x 10 tire mounted.

Test Tires

As mentioned above, two previously used tires were chosen for this test program. The tires were the 7:00-6, 6 PR Type III and the 8:50-10, 8 PR Type III. The tire geometry data for these two tires can be found in Table IV.

Soil Tests and Preparation

The two soil types chosen for these braking tests were buckshot clay and mortar sand, both of which were used in the previous multiwheel and single wheel testing programs. Two purposes were fulfilled by the soil tests conducted, first to insure an accurate description of the test soil and its uniformity, second to allow possible correlation to other tire soil interaction theories by collecting an optimum amount of information describing the soil. The soil tests that were conducted are moisture and density determination, mobility cone penetration resistance (CI), and the California Bearing Ratio (CBR). A complete description of each soil test is given in Appendix I. The summary of the correlation data taken to relate CBR and CI_{avg} is presented in Table V. The summary of the moisture-density determination is in Table VI.

Test Results - Buckshot Clay

The finalized test results for the 21 tests run in buckshot clay are presented in Tables 16 through 36 which are presented in Appendix II. The data presented represent average values of the measured quantities, as obtained by plotting the test parameters versus the test bed length and then reading off the values of load, tire drag, sinkage, and braking torque for even values of slip. A typical plot from one of the clay tests is shown in Figure 4. As can be seen in this figure, the slip was continually varied throughout the test in order to study the variation in braking drag with slip.

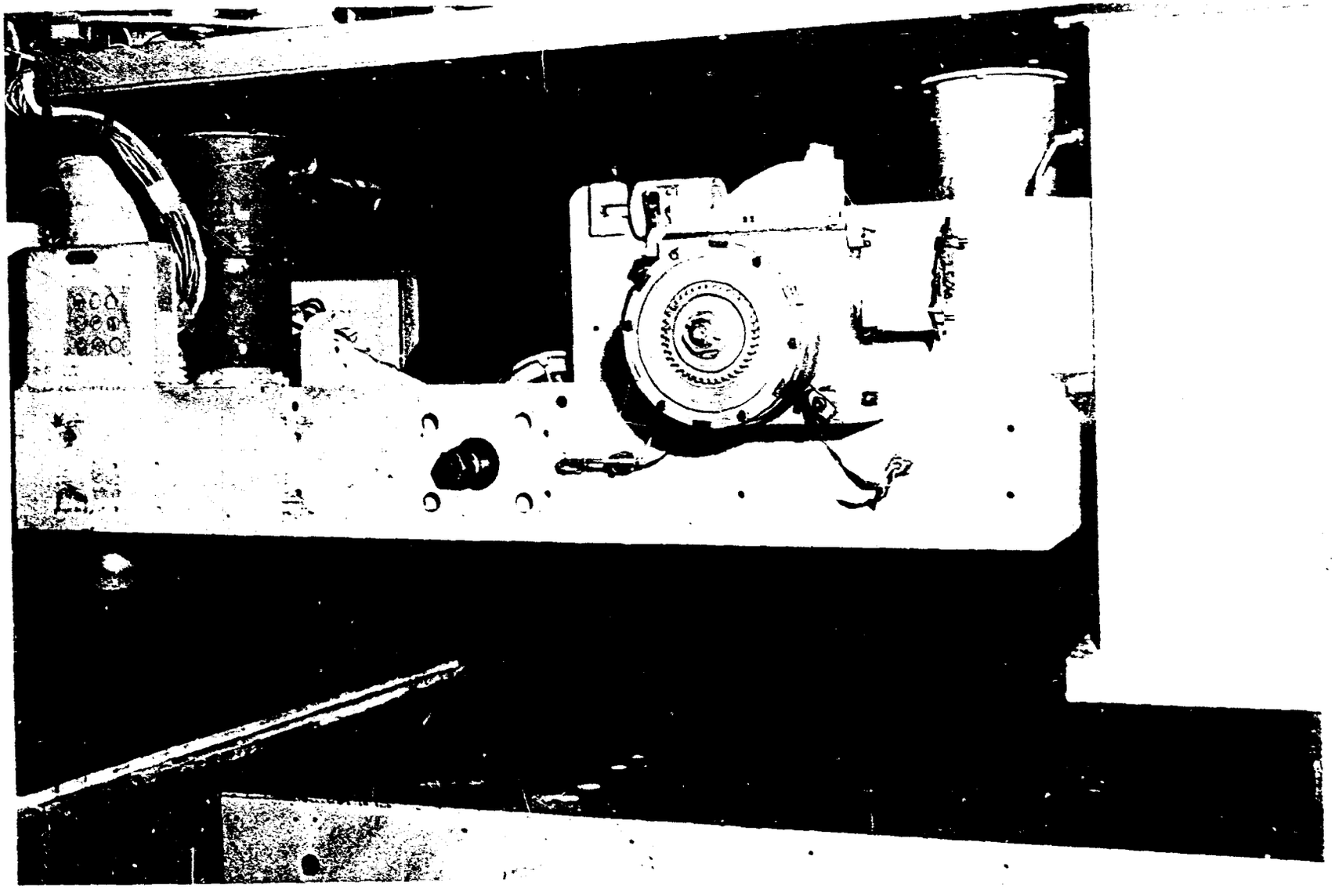

Figure 3. Braked Tire Test Dynamometer

TABLE IV

BRAKING TESTS - TIRE DATA (MEASURED)

Tire Type	Deflection d[%]	Wheel Load P[lbs]	Carcass Dia. D[in]	Contact Area * A[sq. in]	Tire Print		Deflection d[in]	Inflation Pressure		Section Height		Section Width	
					Length* l[in]	Width * b[in]		Unloaded [psi]	Loaded [psi]*	Unloaded [in]	Loaded [in]*	Unloaded [in]	Loaded [in]*
7:00-6, 6PR Type III	35	400	17.76	43.41	8.63	5.60	1.80	3.80	4.60	5.13	3.33	6.73	7.84
	35	900	17.98	43.48	8.80	5.58	1.83	15.80	16.50	5.24	3.41	6.76	7.79
	42	450	17.74	49.45	9.50	5.55	2.15	3.00	4.00	5.12	2.97	6.73	8.19
	42	1100	17.94	50.38	9.69	5.60	2.19	14.80	15.50	5.22	3.03	6.75	8.15
8:50-10, 8PR Type III	35	600	24.52	73.52	11.67	6.95	2.19	2.00	2.65	6.26	4.07	8.00	9.36
	35	1000	24.68	70.85	11.54	6.98	2.22	7.15	7.95	6.34	4.12	8.01	9.30
	35	1500	24.74	72.67	11.75	6.95	2.22	14.00	14.90	6.37	4.15	8.02	9.28
	35	1600	24.76	72.66	11.80	6.96	2.23	14.55	15.80	6.38	4.15	8.01	9.27
	42	700	24.48	87.11	13.16	7.02	2.62	1.10	2.10	6.24	3.62	8.01	9.67
	42	1700	24.70	85.65	13.02	7.00	2.66	11.05	12.40	6.35	3.69	8.02	9.67

* Data taken with tire loaded on a rigid surface. All other data is for unloaded inflated tire.

TABLE V

TEST BED SOIL CONDITIONS

Soil Type	Design Soil Strength CI_{avg} (0" to 6")	CI_{avg} 0" to 6"	$CBR_{0.1"}$	$CBR_{0.2"}$
Buckshot Clay	40	38.9	1.13	0.88
Mortar Sand	40	43.9	1.86	1.48

TABLE VI

MOISTURE-DENSITY DATA SUMMARY

Soil Type	Design Soil Strength CI_{avg} (0" to 6")	Average Conditions: Dry Density γ_d (pcf)	Average Conditions: Moisture Content W (%)
Buckshot Clay	40	77.5	41.9
Mortar Sand	40	100.4	less than 1.0

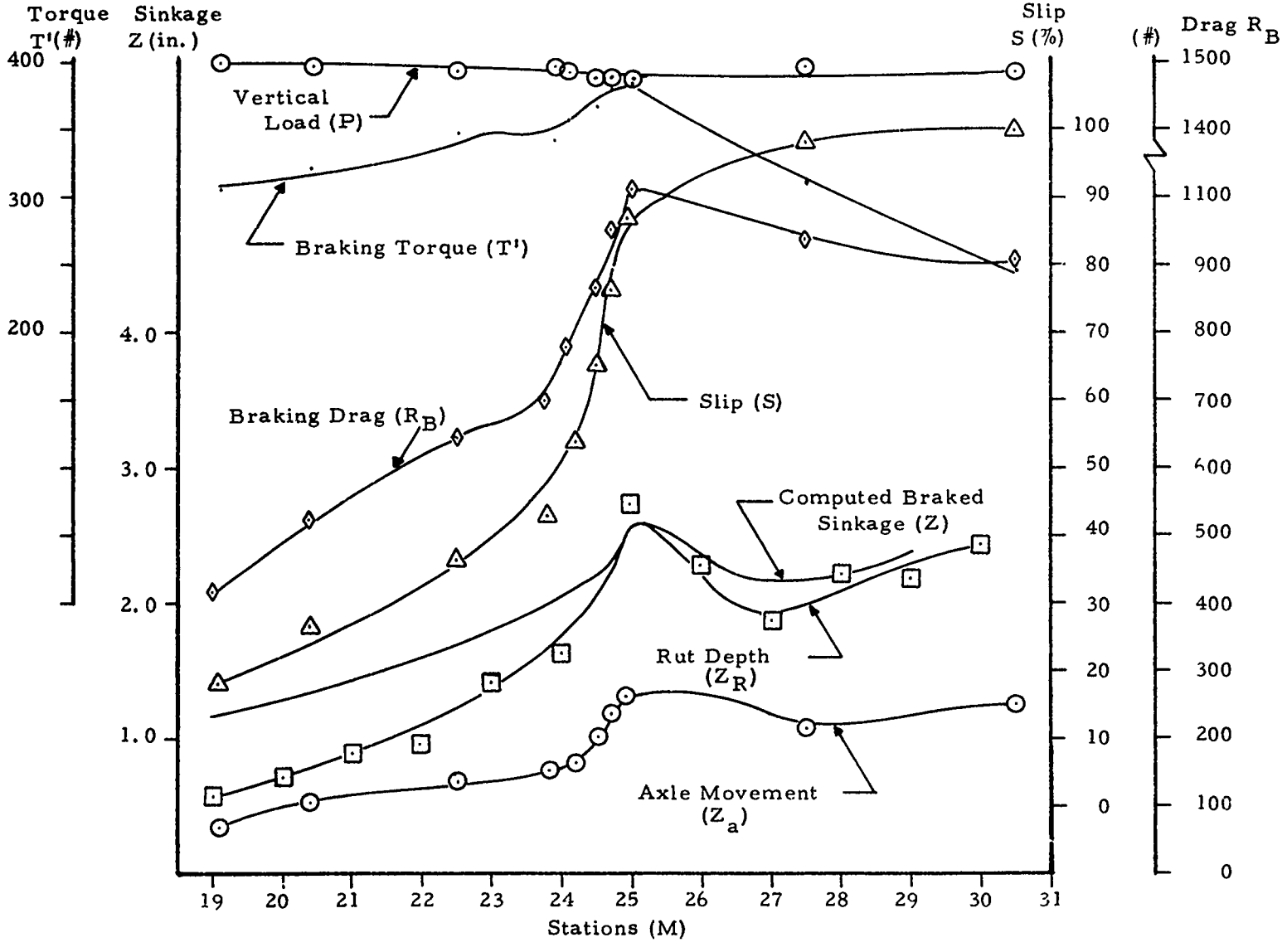

Figure 4. Typical Results - Clay Test # 10 (8.50-10, 8PR)

All the tests were run with the slip varying from approximately 10% to 100% (100% slip is a fully braked tire). All tests did not reach 100% slip. This was accomplished by holding the carriage speed constant while reducing the peripheral tire velocity during each test run. The CI value given in the tables in Appendix II represents the average value of five before-traffic tests and is given as the average penetration resistance over the first six inches of soil profile in psi. The sinkage values reported were arrived at through empirical relationships relating tire sinkage to both rut depth and axle movement. Soil strength measurements made in the tire ruts after each test are included in Appendix I.

Test Results - Mortar Sand

The finalized test results for the 19 tests run in mortar sand are presented in Tables 37 through 55 which are presented in Appendix II. As with the clay data, the values given in these tables for the various parameters were obtained by plotting the test parameters versus the test bed length and reading the values of load, tire drag, sinkage, and braking torque for even values of slip. Each test was a variable slip test, where the tire started at zero slip (free rolling) and was braked to a value of 100% slip (fully braked). All tests did not reach 100% slip. The soil strength of each test section was measured by five cone penetration tests before the test run, and the average penetration resistance over the first six inches of soil profile is presented. The sinkage values reported were arrived at through empirical relationships between tire sinkage and both rut depth and axle movement. Soil strength measurements made in the tire ruts after each test are included in Appendix I. These results of the Braking Verification Tests are used in the next section to further develop braking analysis equations suitable for predicting braked tire on soil drag ratios (braking coefficients).

B. BRAKING ANALYSIS EQUATIONS

Previous investigations[1, 2] have indicated that in both sands and clays, the total drag resistance (R_B) on a braked tire is a function of two

components:

$$R_B = R_R + R_T \tag{1}$$

the horizontal soil resistance to forward motion, exclusive of soil shear resistance, during braking (R_R), plus the horizontal component (R_T) of the net shearing force resistance (T) between the tire and the soil as a function of slip. Figure 5 shows the forces and interface conditions for such a braked tire. It was shown during these preliminary investigations[1, 2] that the R_R term was independent of slip and could be determined from a rolling resistance formula as a function of sinkage,

$$\frac{R_R}{P} = f(Z/D) \tag{2}$$

The R_T term however is a function of both slip and sinkage, and a relationship between R_T and various tire parameters including slip and sinkage were determined semi-analytically based on experimental data which existed at that time (1970).

Summary of Previous Braking Analysis Equations - Cohesive Soils

Using this braking theory, the following preliminary braking prediction equation for cohesive soil was developed using data developed by WES[12] and compared to data produced by Lockheed[3] prior to the testing program described in this report.

$$\frac{R_B}{P} = \frac{R_R}{P} + \frac{R_T}{P} = 3.85\,(Z/D) + \frac{K\,CI_{avg}\cdot D^2}{P}\,(Z/D)^{1/2}\mu(S) \tag{3}$$

where $\mu(S) = (\frac{S}{100})^{1/2}$, and

D = tire outside diameter S = percent tire slip

Z = instantaneous soil sinkage P = vertical load

K = 0.11 CI_{avg} = average cone index over 0-6" depth

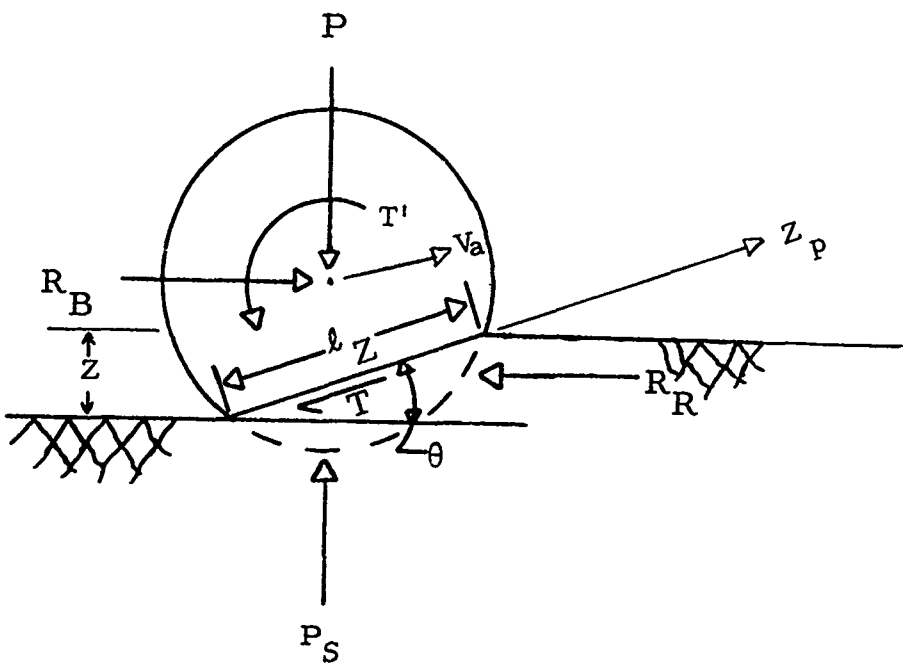

V_a = horizontal velocity of axle

V_W = peripheral speed of wheel

Z = instantaneous soil sinkage

θ = angle defining plane of contact

P = vertical load

R_B = braking drag

T' = braking torque

R_R = forward motion soil drag

P_S = vertical soil reaction

T = tangential shear force

ℓ_Z = length of equivalent plane of contact

$$S = \text{percent negative slip (braking)} = \left(\frac{V_W}{V_a} - 1\right) \times 100$$

Figure 5. Braked Tire/Soil Interface Conditions

The R_R term was developed from rolling tire data for clay type soils as previously reported[2]. The R_T term was developed from the horizontal component of tangential force (T) shown in Figure 5. The tangential force is calculated based on the Coulomb theory for shear force at an interface as

$$T = A_Z (c + \bar{\sigma} \tan\phi) \mu(S) \tag{4}$$

where

A_Z = area of equivalent plane of contact at sinkage Z

c = soil cohesion

$\bar{\sigma}$ = effective normal stress

ϕ = angle of internal friction of soil

$\mu(S)$ = nonlinear function of slip.

The horizontal component of T is given by

$$R_T = A_Z (c + \bar{\sigma} \tan\phi) \mu(S) \cos\theta \tag{5}$$

where

$$\theta = 90° - [\sin^{-1}(1 - \frac{2Z}{D}) + \frac{1}{2}\cos^{-1}(1 - \frac{2\ell Z}{D^2})]$$

where ℓ = tire footpring length (rigid surface). Knowing that $\ell = 0.45D$ for most aircraft tires, Figure 6 was developed which gives θ as a function of Z/D. For cohesive soils, the $\tan\phi$ is zero and the cohesion, c, can be replaced by the average cone index, CI_{avg}. Assuming that the equivalent contact area A_Z is a function of the tire diameter squared and the sinkage ratio, (Z/D), R_T was shown to be represented as follows:

$$R_T = K \cdot CI \cdot D^2 \cdot (Z/D)^{1/2} \cdot \mu(S) \cdot \cos\theta \tag{6}$$

where

K = constant.

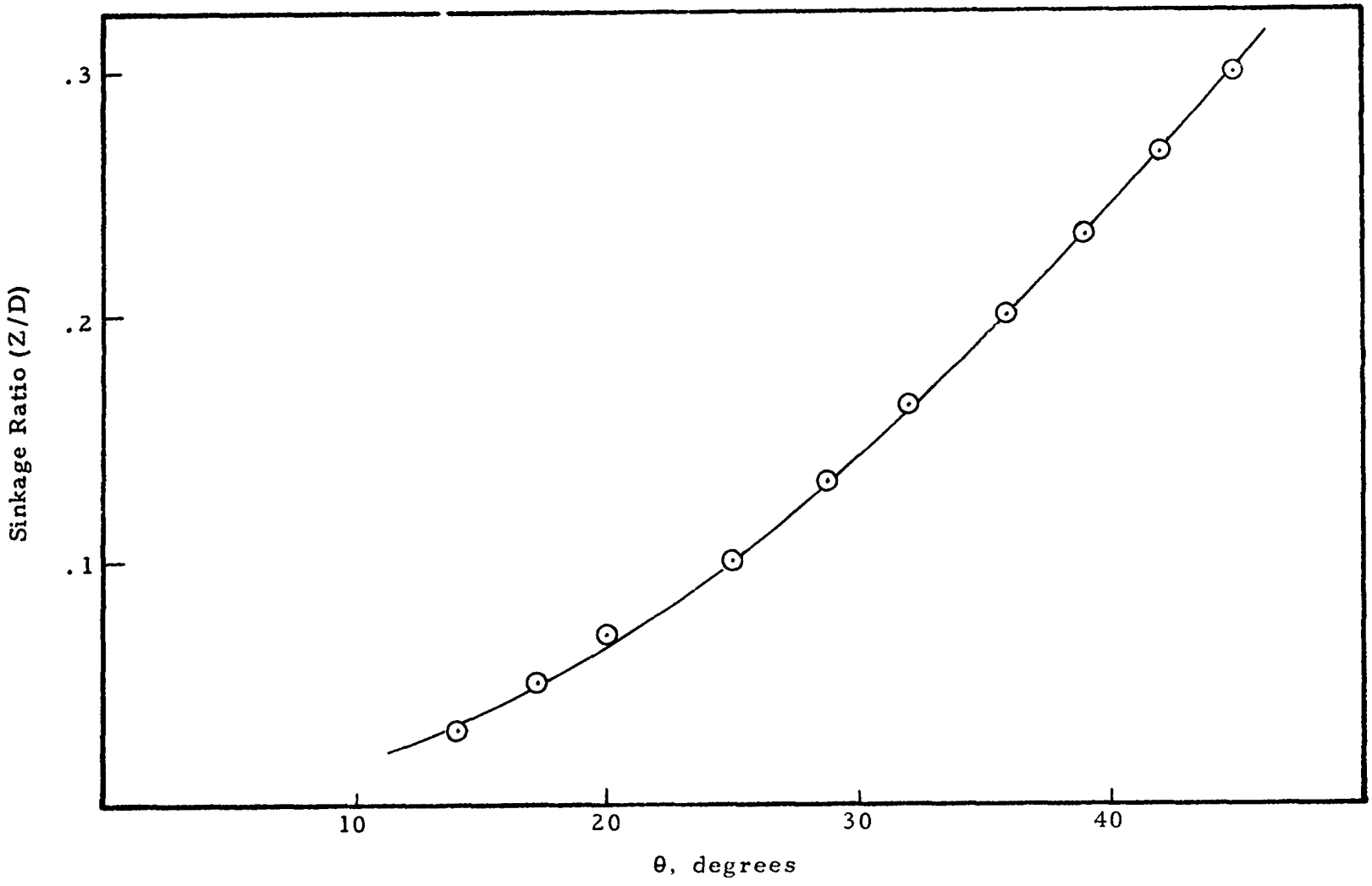

Figure 6. Angle Defining Plane of Contact, θ vs. Z/D for Use in Equation 5

It was further assumed that θ was relatively small ($\cos\theta \simeq 1.0$) and $\cos\theta$ was dropped from the prediction equation which results in the form given in Equation (3).

Analysis of Braking Verification Tests - Clay Soil

In order to further study the empirical constant, K, contained in the R_T term in Equation (6), Figure 7 was developed which shows a plot of the experimentally determined R_T component of the braking drag divided by the numeric, $[CI \cdot D^2 \cdot (Z/D)^{1/2} \cos\theta]$, versus slip as taken from the results of the Braking Verification Tests. R_T was determined by subtracting the rolling drag, R_R, from the total measured braking drag. This was accomplished by calculating R_R as a function of Z/D based on single wheel rolling tests previously conducted on buckshot clay by UDRI[2]. As can be seen from Figure 7 the limiting value reached by $R_T/CI \cdot D^2 \cdot (Z/D)^{1/2} \cos\theta$ depends somewhat on the forward speed but in general is less than the K value of 0.11 previously established and given in Equation (3). Although coefficients could be selected for each forward speed, a K value of 0.08 would seem appropriate in representing an average response over the 5 fps to 20 fps speed range for higher percent slips.

The results of the Braking Verification Tests were also used to further study the rate of growth of the R_T term as determined by plotting the value of R_T at each slip divided by $(R_T)_{max}$ versus percent slip as shown in Figure 8. Keeping the simple form of $\mu(S)$ given in Equation (3) in mind, Figure 8 indicates that the growth of R_T is faster than that previously indicated, and the revised function which is applicable for negative slip rates greater than approximately 15% can be given as:

$$\mu(S) = \left(\frac{S}{100}\right)^{1/3} \qquad (7)$$

where

K = constant.

Figure 7. Variation in R_T with Slip - Braking Verification Tests, Clay

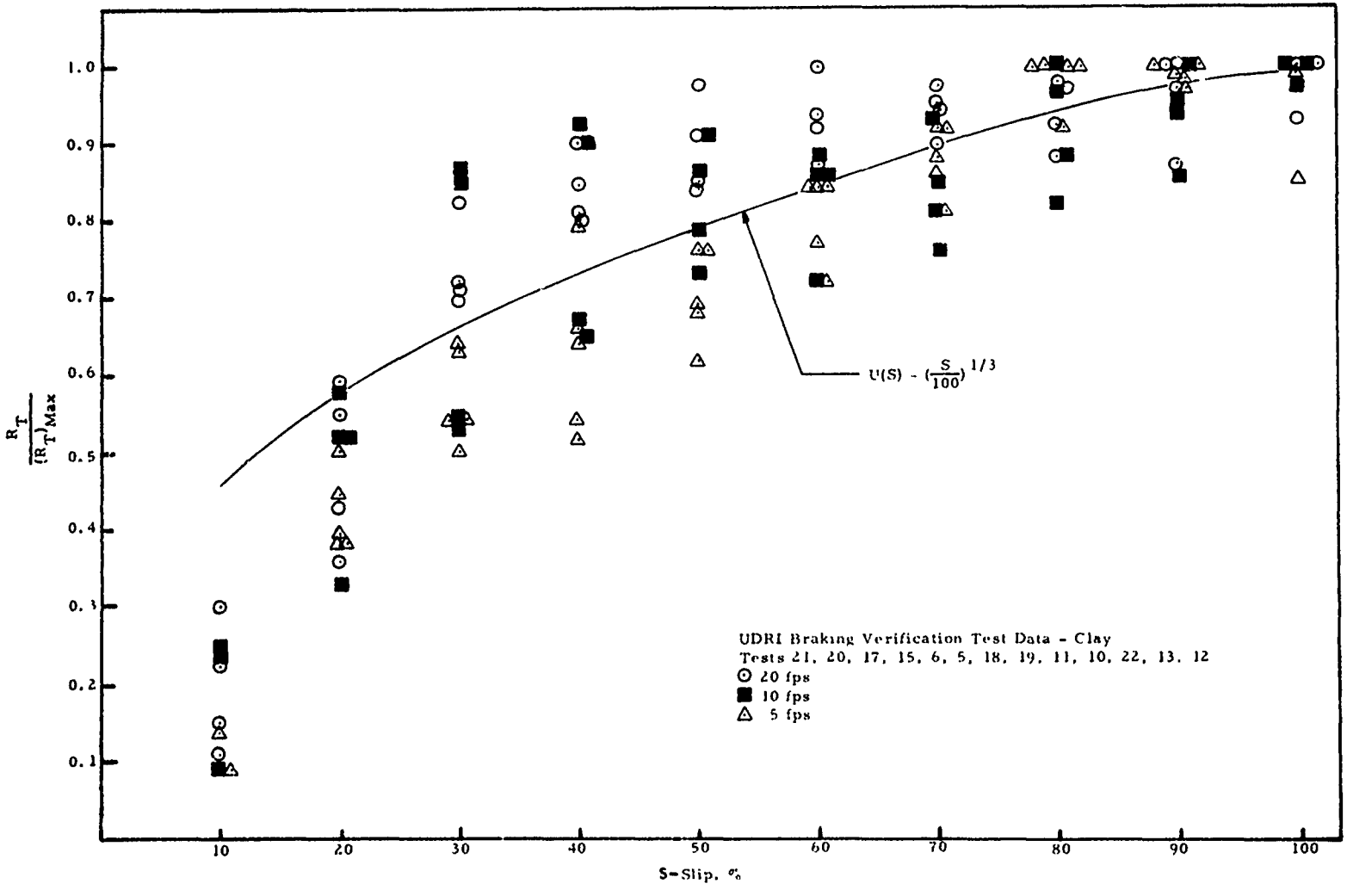

Figure 8. $\frac{R_T}{(R_T)_{Max}}$ vs. Percent Slip - Braking Verification Tests, Clay

Based on this analysis of the verification tests, the braking prediction equation for buckshot clay would take the form:

$$\frac{R_B}{P} = \frac{R_R}{P} + \frac{R_T}{P} = f(Z/D) + \frac{0.08CI \cdot D^2}{P}(Z/D)^{1/2}\mu(S)\cos\theta \qquad (8)$$

for 5 fps ≤ Velocity ≤ 20 fps and $0.01 \leq Z/D \leq 0.10$

where

$f(Z/D) = \frac{R}{P}$ for buckshot clay (see Reference 2)

$$\mu(S) = \left(\frac{S}{100}\right)^{1/3}$$

Note that the cosθ has been retained here for completeness.

Using Equation (8), the predicted braking drag ratio was compared to the actual measured data as shown in Figure 9. Reference to Figure 9 indicates an approximate ±10% scatter which is due to: (a) the use of an average K over a velocity range, and (b) the use of a slip function, μ(S), only approximately describes the rate of growth of the R_T term for the 5 fps to 20 fps velocity range. No information is currently available defining the slip function for speeds greater than 20 fps.

Equation (8) can only be used if the braked sinkage can be calculated. One preliminary method of braked sinkage prediction is to consider the braked sinkage as a function of the free rolling sinkage. From a review of all existing braking data, including WES, Lockheed, and UDRI (see Appendix II), the maximum braked sinkage is between 1.5 and 3 times larger than the free rolling sinkage. Therefore, as an approximation, the braked drag can be calculated from the above equation assuming that

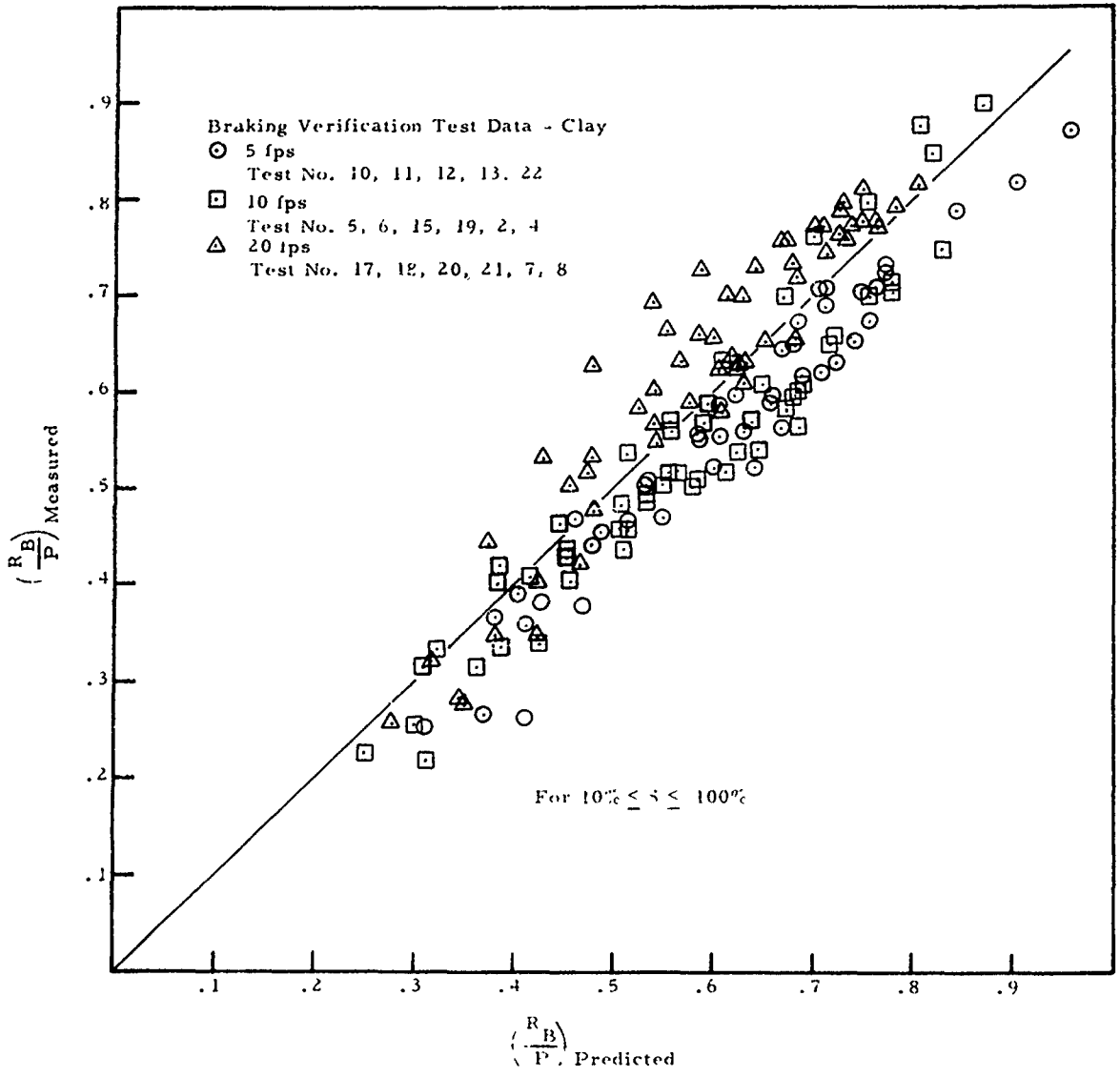

Figure 9. Comparison of Predicted (Equation 8) and Measured Braking Drag Ratios, Buckshot Clay

$$(Z_{\text{Braked}})_{\text{max}} = 2.5\, Z_{\text{Rolling}} \quad . \tag{9}$$

The torque measurement results for the braked tire tests on clay are represented by the curves presented in Figure 10. No torque prediction theory has been developed, however, it is interesting to note that the torque required to brake a tire on soil increases rapidly for low slip values, and reaches its maximum value at between 25 and 50% slip as compared to the braking drag which continuously increases throughout the entire slip range. As seen in Figure 10 the trend is for the torque to reach its maximum value at or about 50% slip and then to remain constant or decrease in value as the slip increases. The relationship between torque and velocity for the clay braking tests is seen in Figure 11, where the average torque for 35% and 42% deflection at 90% slip for each tire is plotted versus velocity. The torque requirement increases slightly with velocity.

Summary of Previous Braking Analysis Equations - Cohesionless Soils

The following preliminary braking prediction for cohesionless soil was developed using data from WES[12] and compared to data produced by Lockheed[3] prior to the testing program.

$$\frac{R_B}{P} = \frac{R_R}{P} + \frac{R_T}{P} = 0.048 + 2.77(Z/D) + \frac{\alpha D^2}{K_1}\,\mu(S) \tag{10}$$

where

$\alpha = P/A$, $\qquad K_1 = 29$

$\mu(S) = \left(\frac{S}{100}\right)^{1/2}$,

and A = rigid surface tire contact area.

The R_R term was developed from rolling tire data for sand type soils as previously reported. The R_T term is the horizontal component of the tangential force (see Equation (4)) at the tire soil interface and is given by

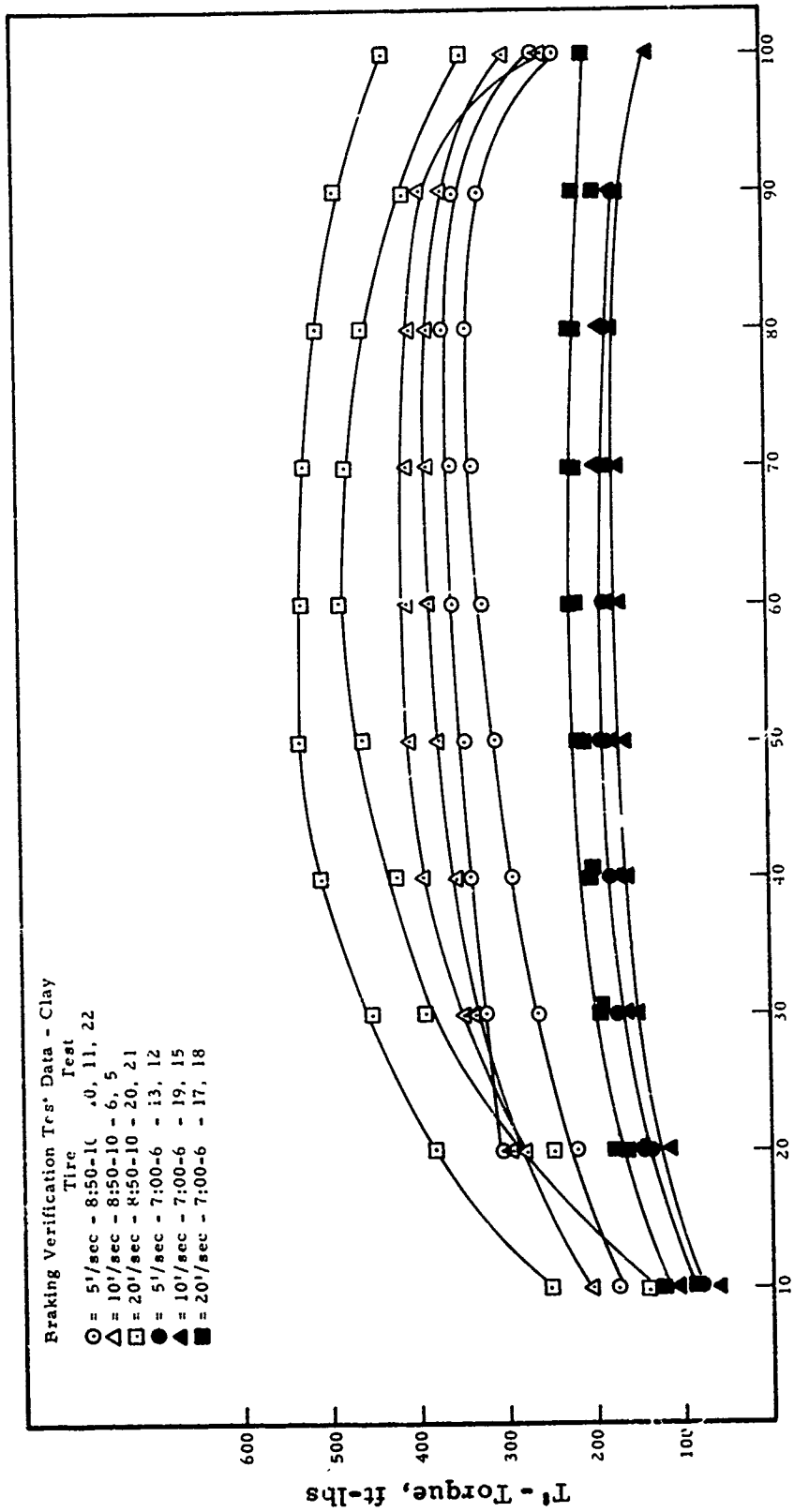

Figure 10. Braking Torque vs. Percent Slip - Braking Verification Tests, Clay

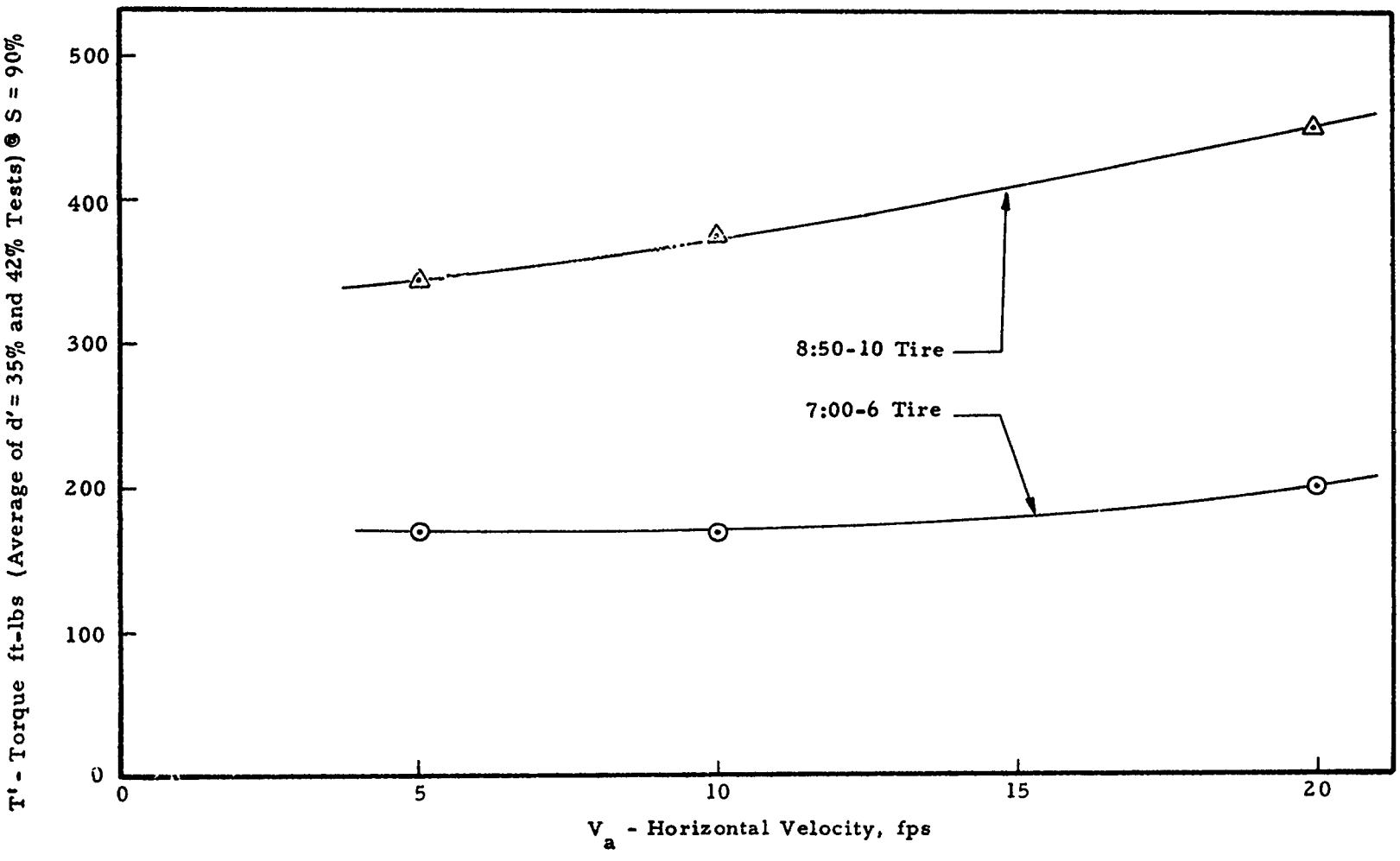

Figure 11. Braking Torque vs. Horizontal Velocity - Braking Verification Tests, Clay

$$R_T = A_Z (c + \bar{\sigma} \tan\phi)\, \mu(S) \cos\theta \quad . \tag{11}$$

In the cohesionless soils, the cohesive term, c, in this equation is zero. Replacing $\bar{\sigma}$ by $\alpha = P/A$, where A is the rigid surface tire contact area, and A_Z by $[D^2 \cdot (Z/D)^n]$, Equation (11) can be written as,

$$\frac{R_T}{D^2 (Z/D)^n} = \alpha \cdot \tan\phi \cdot \mu(S) \cdot \cos\theta \tag{12}$$

Initial analysis of sand data[1] developed from data in the 0 fps to 5 fps velocity range, indicated that R_T was only a weak function of Z/D and was therefore deleted from the above equation. It was further observed during braking in sand, that considerable sand flow takes place not only at the tire soil interface but also ahead of the tire. Based on this observation, it can be reasoned that the R_T term might very well be independent of the initial soil strength since the sand disturbance and flow very likely causes the shearing strength to be determined by some large deformation equilibrium void ratio condition rather than the initial strength. Therefore a preliminary relationship developed from Equation (12) and the WES braking data[1] was found to be

$$R_T = \frac{\alpha D^2}{K_1} \mu(S) \cos\theta \tag{13}$$

where K_1 = constant for sand.

It was assumed that θ was relatively small ($\cos\theta \simeq 1.0$) and $\cos\theta$ was dropped from the prediction equation which results in the form given in Equation (10).

Analysis of Braking Verification Tests - Sand Soil

Reference to Table III and Table IV indicates that for the braking tests conducted in sand that D^2/A was approximately constant for all the tests (both 7:00-6 and 8:50-10 tires). Additionally the Z/D's for each test

resulted in cosθ's which were approximately equal. For the sand braking tests at S = 100%, Equation (13) can be written as

$$\frac{R_T}{P} = \frac{D^2}{AK_1} \cos\theta \qquad (14)$$

which implies that their R_T/P values should also be approximate'y equal. Table VII shows this R_T/P comparison at each velocity for the 7:00-6 and 8:50-10 tires for sand soil. R_T was determined by subtracting R_R, determined as a function of sinkage for mortar sand, from the actual measured braked drag.

TABLE VII

R_T/P COMPARISON, SAND BRAKING TESTS

V_a Velocity [FPS]	R_T/P 7:00-6 Tire	R_T/P 8:50-10 Tire
5	0.45, 0.52	0.50, 0.45
10	0.58, 0.59	0.61, 0.58, 0.56
20	0.77, 0.74	0.79, 0.74, 0.74, 0.72

A review of the above table indicates a definite trend in R_T/P with velocity. The R_T/P term increases with increasing velocity which indicates that D^2/AK_1 is not the same for all velocities. Therefore, K_1 must vary with velocity in sand.

In order to establish a velocity constant for each velocity, the measured R_T values were plotted versus the predicted R_T values using the previously established $K_1 = 29$ (see Equation (10)), as shown in Figure 12, 13, and 14 for velocity ranges of 5, 10, and 20 fps. Using a best fit line through the plotted data, a correction was applied to the constant K_1 to account for the variation in predictions for each velocity range. The adjusted values for K_1 are presented in Table VIII.

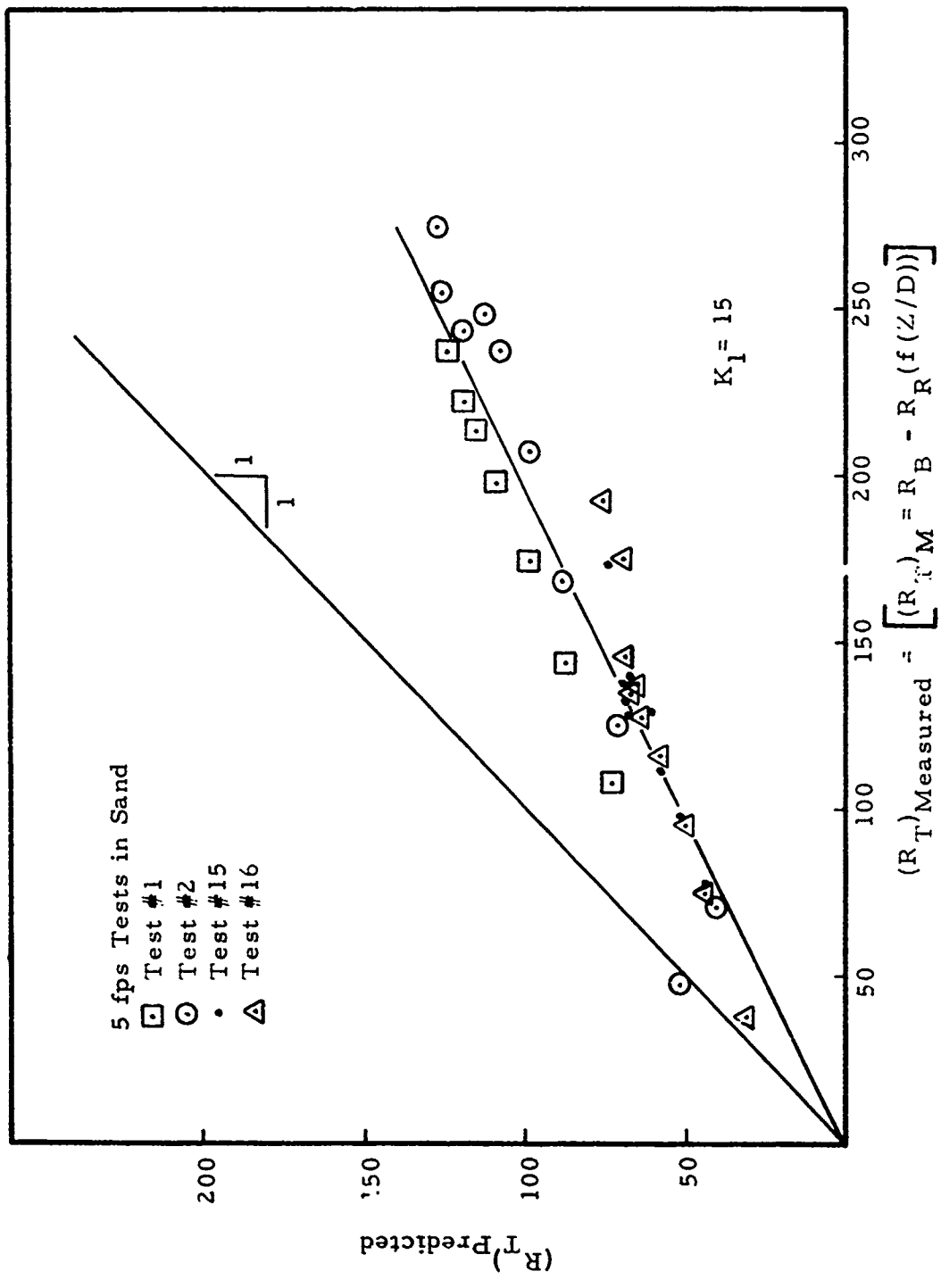

Figure 12. Comparison of Predicted Horizontal Component of Net Shear Force, R_T (Equation 10) and Measured R_T in Sand, 5 fps

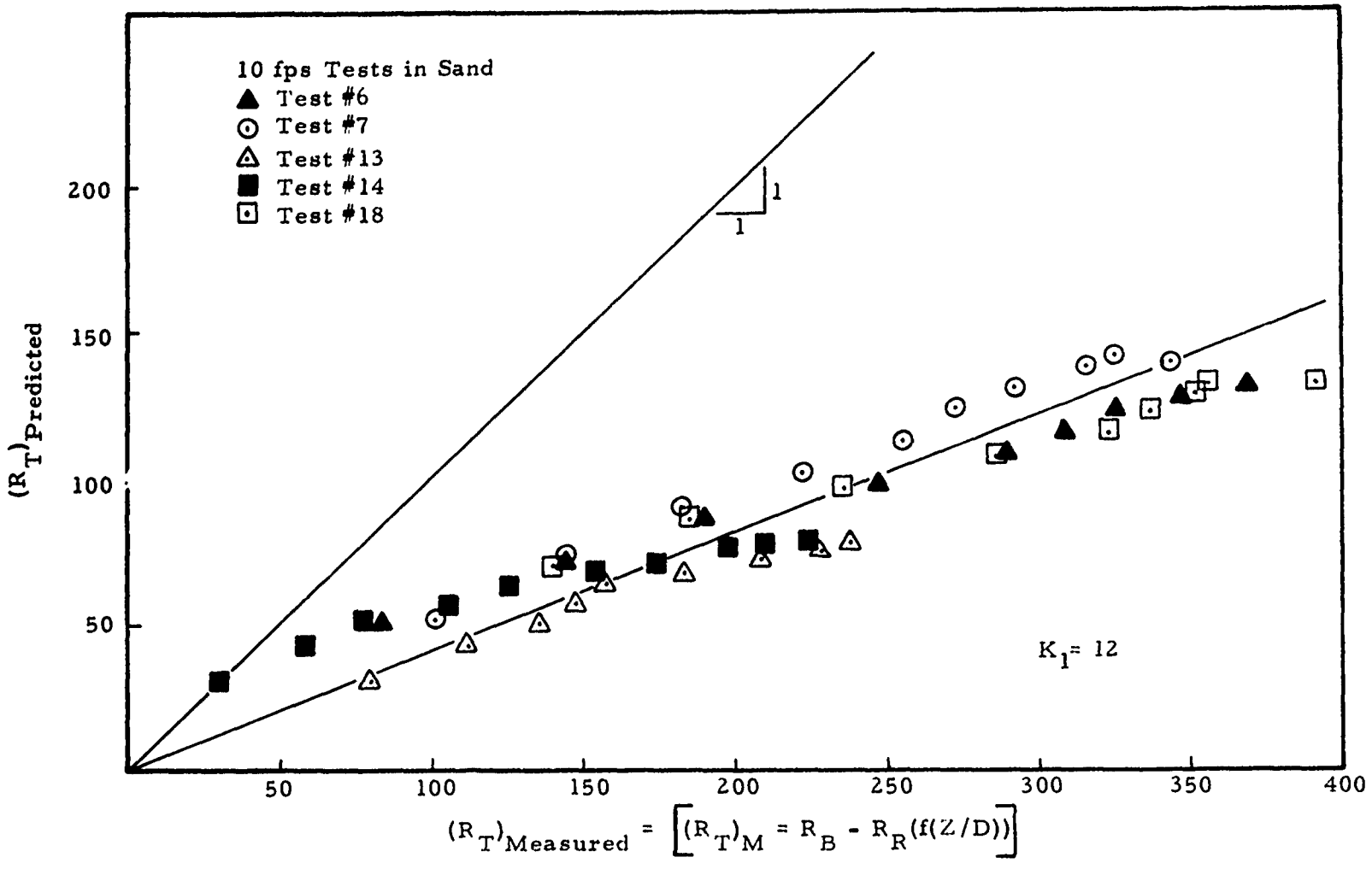

Figure 13. Comparison of Predicted Horizontal Component of Net Shear Force, R_T (Equation 10) and Measured R_T in Sand, 10 fps

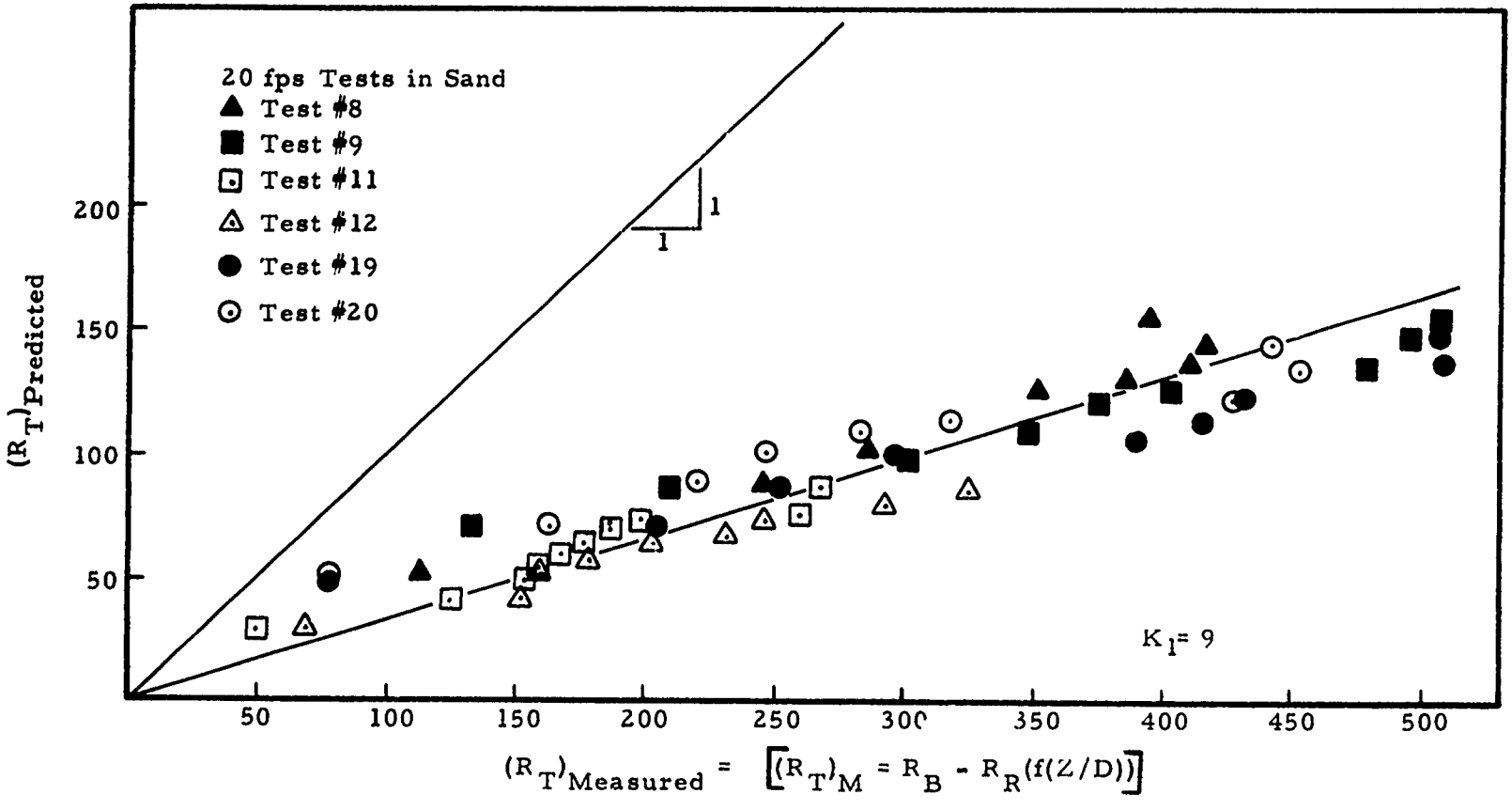

Figure 14. Comparison of Predicted Horizontal Component of Net Shear Force R_T (Equation 10) and Measured R_T in Sand, 20 fps

TABLE VIII

VELOCITY CONSTANT FOR SAND
BRAKING TESTS

Velocity, V_a (fps)	K_1 Value
5	15
10	12
15	9

The variation of $R_T/R_{T_{max}}$ for sand was also examined based on the results of the verification tests and the result is given in Figure 15. Figure 15 shows some scatter of the data by forward velocity but in general indicates that for slips greater than about 15%, the relationship

$$\mu(S) = \left(\frac{S}{100}\right)^{1/2} \tag{15}$$

adequately describes the variation of R_T with percent slip.

Using the verification test data analysis, the braking prediction equation for the mortar sand would take the form

$$\frac{R_B}{P} = \frac{R_R}{P} + \frac{R_T}{P} = f(Z/D) + \frac{\alpha D^2}{K_1 P}\,\mu(S)\cos\theta \tag{16}$$

for 5 fps ≤ Velocity ≤ 20 fps and $0.01 \le Z/D \le 0.10$

where

K_1 = function of velocity (see Table VIII)

$f(Z/D) = R/P$ for mortar sand (see Reference 2), and

$\mu(S) = \left(\frac{S}{100}\right)^{1/2}$.

Equation (16) was then used to predict the braked tire drag ratio and compared to the measured braked tire drag ratio as shown in Figure 16.

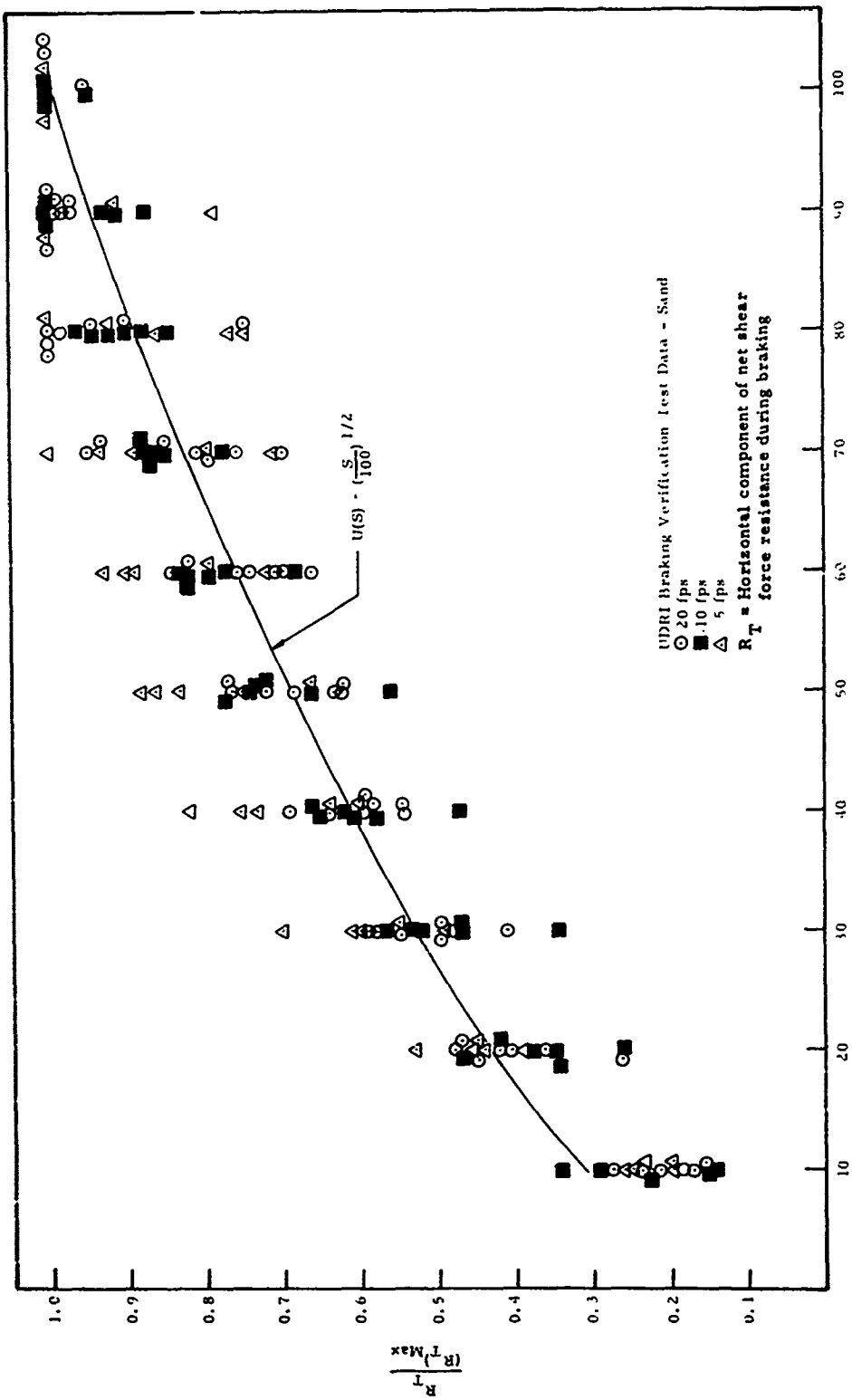

Figure 15. Variation in R_T with Percent Slip - Braking Verification Tests, Sand

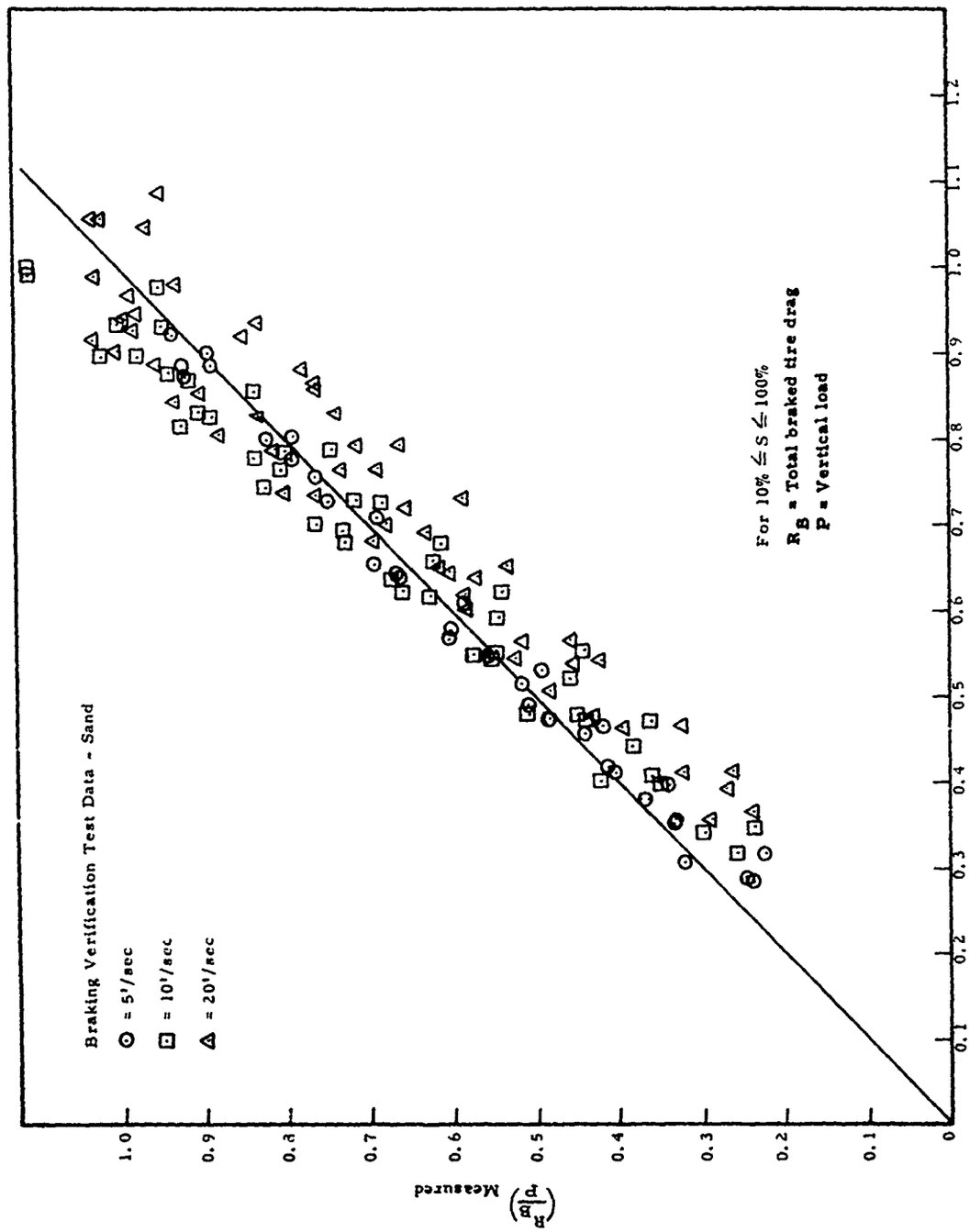

Figure 16. Comparison of Predicted and Measured Braking Drag Ratios, Mortar Sand

The scatter in the data is attributed primarily to the use of the approximate expression for $\mu(S)$ for the entire velocity range of 5 fps to 20 fps.

As for cohesive soils, no torque prediction equation has been developed, since however the R_R portion of R_B is the resistance to forward motion and would be present even if no braking torque were applied, the R_T components in the force relationship acting on the wheel is the force which balances the applied torque in a steady state braking condition. That is:

$$T'(\text{torque}) = \text{moment arm} \times R_T.$$

For sand the R_T relationship is given by

$$\frac{R_T}{P} = \frac{D^2}{AK_1} \tag{17}$$

which is a constant for a given velocity range in the verification test data. The torque would then be given by

$$T' = \text{moment arm} \times (P \times \text{constant}) \quad .$$

If it is assumed that the moment arm is proportional to the tire diameter ($= K_2 D$), then the torque becomes

$$T' = (K_2 D)(P \times \text{constant}) = \text{constant} \times PD.$$

Reference to this equation indicates that the braking torque for tires in sand would vary linearly with the product of the vertical tire load (P) and the tire diameter (D). Table IX shows the results of such a comparison for the 7:00-6 and the 8:50-10 tires for the verification tests and indicates that such a relationship is approximately valid.

TABLE IX

COMPARATIVE TORQUE (AT 90% SLIP) SUMMARY,
SAND TESTS

Velocity, V_a, (fps)	Predicted $\frac{(T')_{8:50-10}}{(T')_{7:00-6}} = \frac{(P \times D)_{8:50-10}}{(P \times D)_{7:00-7}}$	Measured $\frac{(T')_{8:50-10}}{(T')_{7:00-6}}$
5	2.16	2.23
10	2.17	2.39
20	2.20	2.26

Figure 17 shows the variation of the torque required for braking in sand as influenced by the percent slip. Unlike braking in clay, the torque requirements in sand continually increase throughout the slip range. The influence of forward velocity on the braking torque requirements in sand is examined in Figure 18 which shows some increase in braking torque as the forward velocity of the wheel increases.

As for clays, the resulting drag ratios for braked tires in sand can only be predicted if the instantaneous braked sinkage is known. Unlike clays, however, the ratio of the braked sinkage (Z_{max} at S = 100%) to rolling sinkage (Z_R at S $\simeq$ 0%) ranges from approximately 4 to 15 for sand type of soils. On the basis that the fully braked sinkages are controlled by the resulting large deformation soil strength, it is logical to expect the ratio of Z_{max}/Z_R will be in the upper range (approximately 8 to 15) for high values of α/CI_{avg}, while Z_{max}/Z_R will be in the lower range (4 to 10) for low values of α/CI_{avg}. This trend in the variation of Z_{max}/Z_R was noted previously in the analysis of WES's braking data[1]. While the results of the Braking Verification Tests do not confirm the absolute numbers previously established[1], the trend in the data was confirmed.

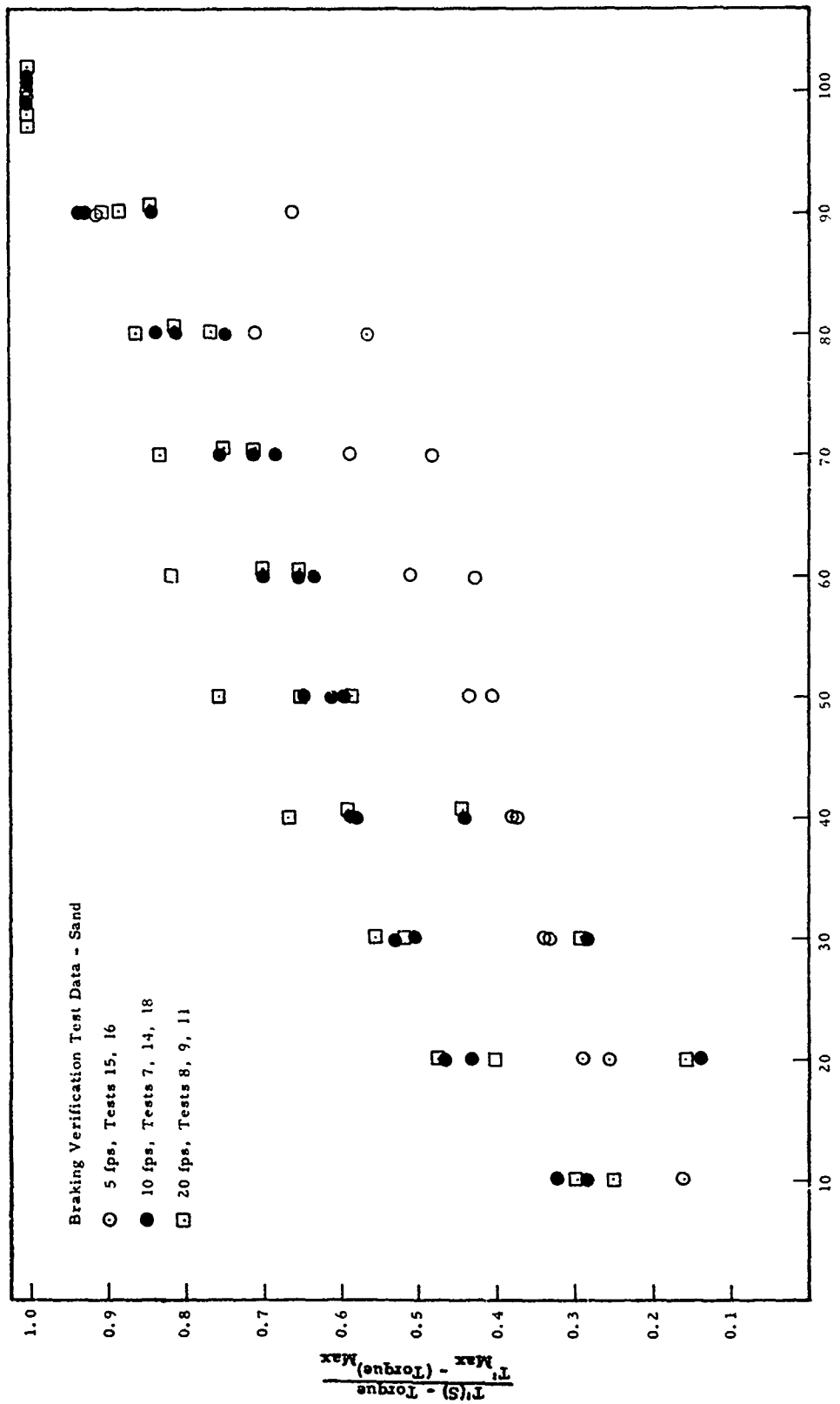

Figure 17. Torque Requirements vs. Percent Slip for Braking in Sand

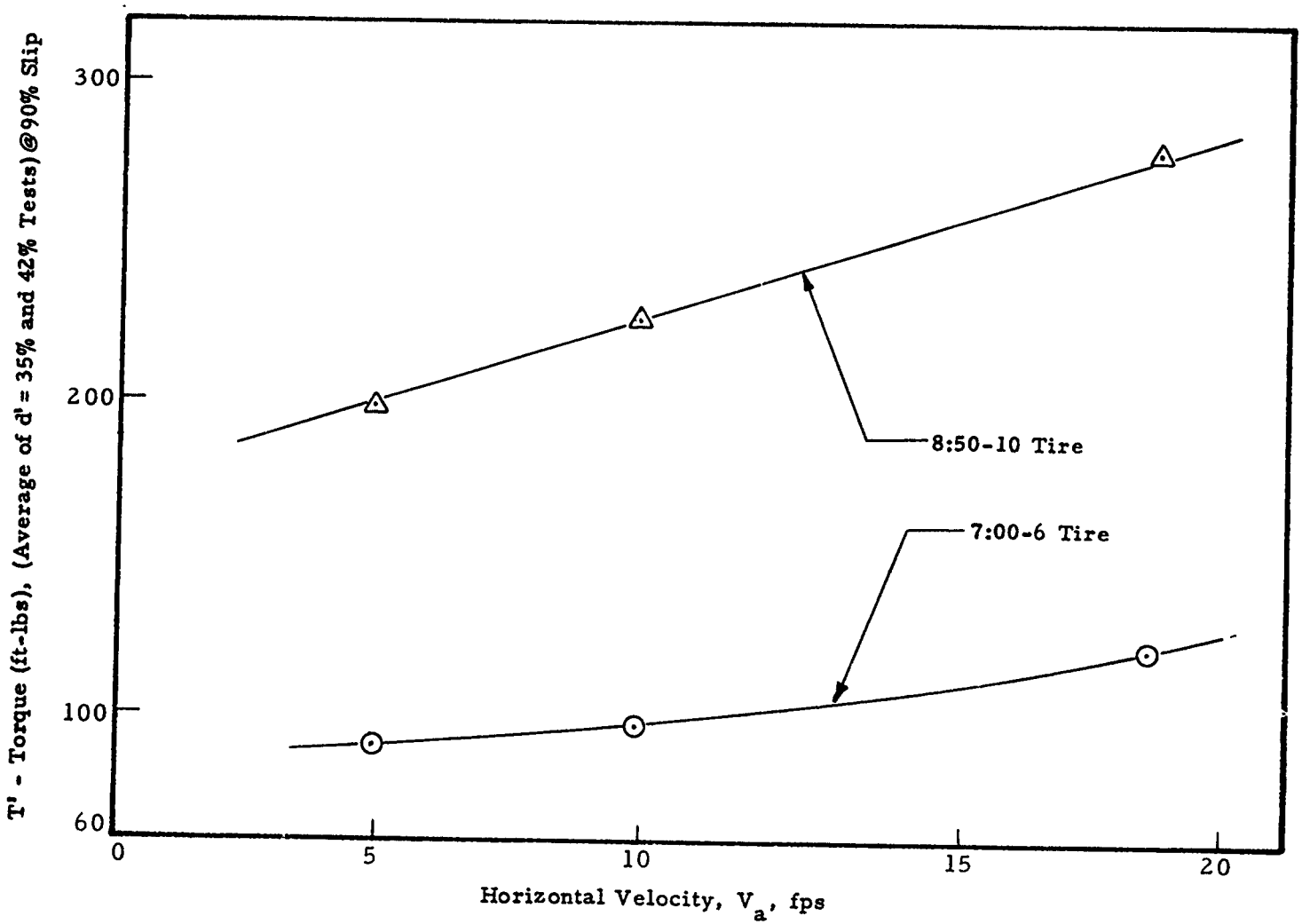

Figure 18. Torque Requirements vs. Horizontal Velocity for Braking in Sand

C. ANALYTICAL BRAKING ANALYSIS (LUMPED PARAMETER TECHNIQUE)

This section contains a description of the analytical/numerical approach utilized to approximate the sinkage of a braked aircraft tire into a soil runway. The approach used is not the same as was originally proposed due to accuracy difficulties which were encountered. Originally it was intended to use a finite element mathematical model based on the Reissner energy formulation of deformable solids. This approach was programmed and tested on a completely elastic problem for which the solution is known. The stress results obtained with this program compared quite favorably with the known stress; however, the displacements were considerably in error. Since displacements (sinkages) are of greatest importance for this project it was decided to abandon (temporarily at least) the originally proposed approach. Therefore, the analytical/numerical approach which was utilized is the lumped parameter iteration approach which has proved to be successful for other aspects of this program.

Problem Definition

The idealized problem which was considered is defined below by listing the assumptions which were made and discussing the loading, region of solution, and boundary conditions.

Assumptions

- A single wheel is in contact with the sample of soil under consideration.

- Only vertical loading and horizontal shear loading are applied to the soil surface.

- The deformation of the soil material due to the loading considered results in a state of plane strain; thus, the problem is considered to be two-dimensional.

Loading

Figure 19 shows the portion of the soil surface which is loaded by a uniform vertical pressure, p_n, and a uniform shear distribution, p_s. The indicated loading is intended to represent the effective loading applied by an aircraft tire during braking.

Region of Solution

The loading shown in Figure 19 is applied to a soil surface which is infinite in length and depth. In order to obtain a solution by numerical means, the extent of the region affected by the loads must be restricted to be finite. Figure 20 shows the region of the soil medium considered in the computations. The dimensions of the considered region were selected such that the applied loading has negligible effect on the displacements at the extremities of the region.

Boundary Conditions

- Under the applied loads the normal stress is equal to the applied vertical pressure and the shear stress is equal to the applied shear stress.

- The shear and normal stresses are zero on the remainder of the soil surface.

- The displacements are zero on the artificial boundaries which limit the extent of the soil medium (Figure 20).

Mathematical Model

As in the cases in which the lumped parameter approach was used previously to model tire/soil interaction, the soil medium was taken to be elastic-perfectly plastic with the elastic deformations governed by Hooke's law, the plastic deformations governed by an incremental stress-strain relation based on the normality flow rule, and the plastic yielding governed by the Drucker-Prager yield criterion. The soil parameters of the model consist of the elastic Young's modulus, the cohesion and the friction angle.

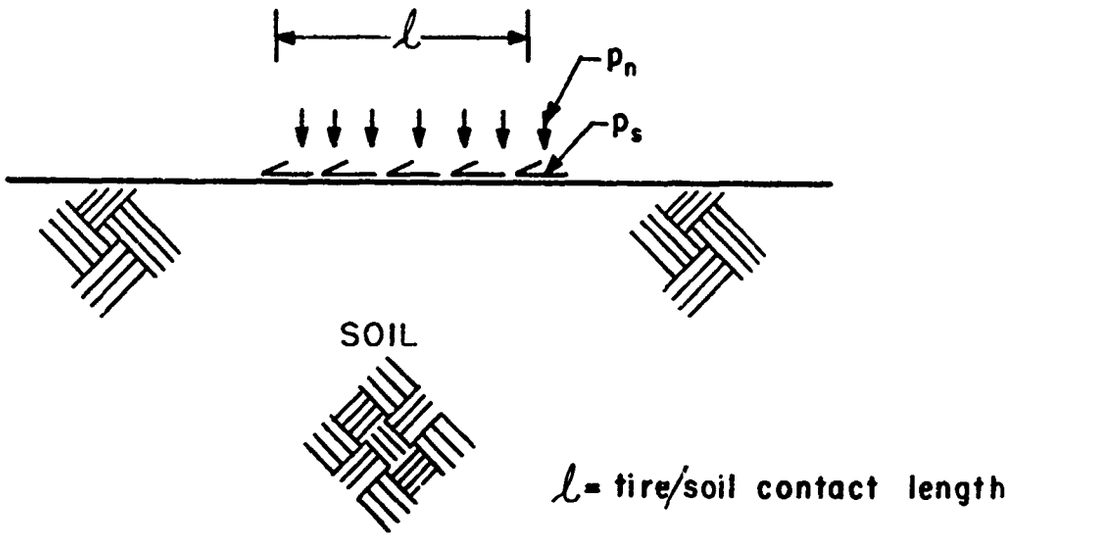

Figure 19. Simulated Loading During Braking

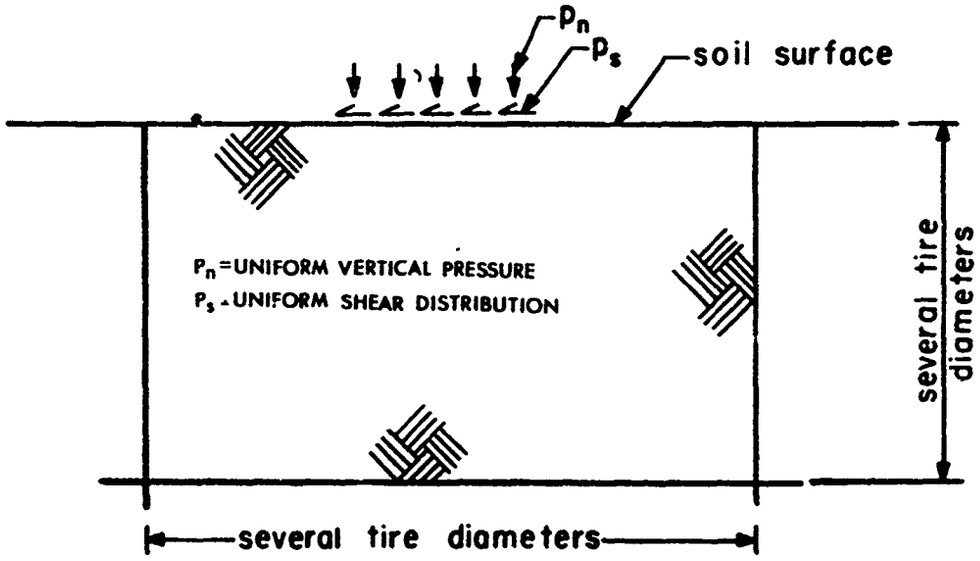

Figure 20. Region of Solution

The vertical pressure-time curve is shown in Figure 21; this is the same pressure pulse used previously. For the case in which braking effects are present, the horizontal shear loading (Figure 19) is taken to have the same time variation as the vertical load (Figure 21) and the magnitude of the shear load is expressed as a percentage of the vertical pressure.

The soil region shown in Figure 20 was modeled by the lumped parameter technique (see Figure 22) used previously to solve the single-wheel, vertical pulse loading problem[2] and the multiwheel and tandem wheel problems[1,13]. The reader is referred to References 1 and 2 for a detailed description of the lumped parameter approach. The mathematical relations, which govern the behavior of the lumped parameter model of a soil medium subjected to surface loading, are summarized in Appendix III.

Computer Program and Results

A FORTRAN IV computer program has been written to implement the braked-wheel/soil-interaction mathematical model on the CDC 6600 computer at Wright-Patterson Air Force Base. The program computes the instantaneous sinkage of a simulated, braked aircraft tire into a soil runway. To date, only one braked condition has been processed with this program. Therefore, a detailed description of the program (FORTRAN IV source deck listing, input data instructions, output irterpretation, etc.) is being deferred until sinkages have been predicted for a range of braking conditions. When the complete series of data have been processed, a separate report will be submitted. This report will contain a complete discussion of the analytical braking analysis, the computer program and the results, and will be entitled "Braked Wheel Sinkage Prediction Technique and Computer Program."

The results of the single condition, on cohesive soil, which has been processed with the braked wheel sinkage prediction computer program are presented in this section. The particular braking condition considered was the case when the horizontal shear load applied to the soil surface is 25% of the applied vertical normal pressure. All other parameters were taken to be

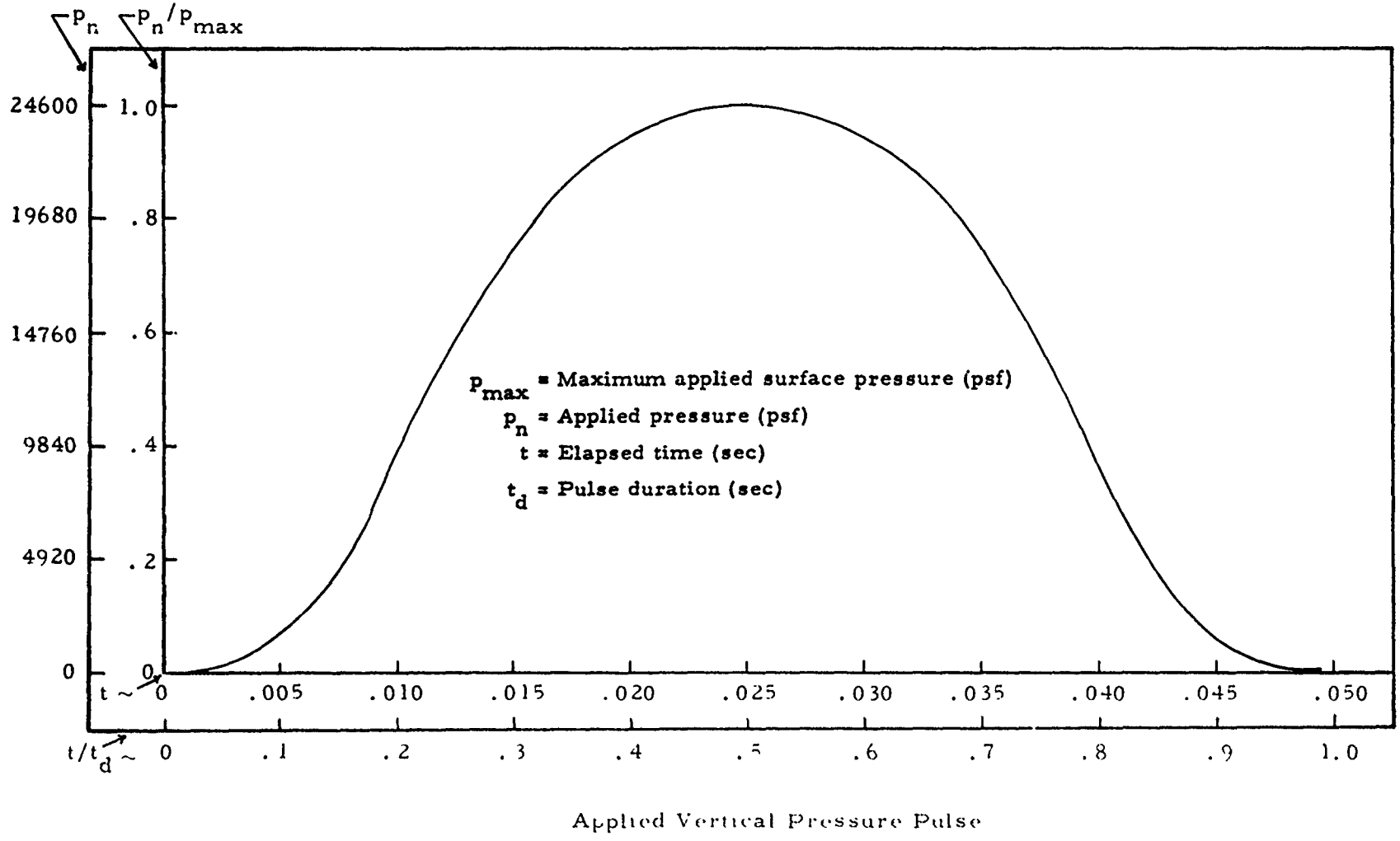

Applied Vertical Pressure Pulse

Figure 21. Applied Vertical Pressure Pulse - Braking Problem

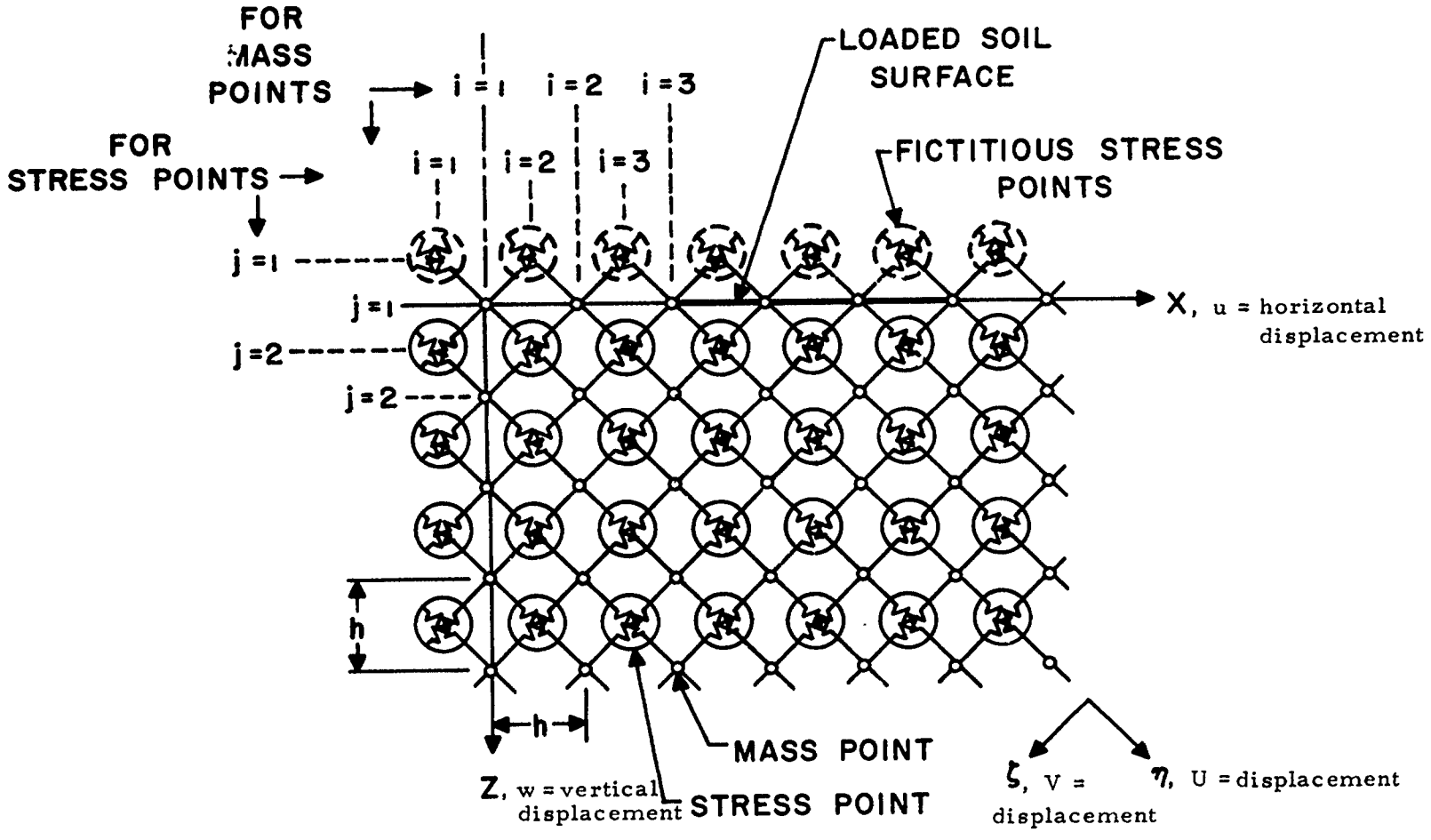

Figure 22. Lumped Parameter Model for Plane Strain

the same as those utilized in the multiwheel solutions so that comparisons could be made. In particular, the various computational parameters are:

Soil Parameters:

Density	ρ = 130 lb/cu. ft.
Poisson's Ratio	ν = 0.45
Young's Modulus	E = 8950 psi
Cohesion	c = 2000 psf
Friction Angle	$\phi = 15^{\circ}$
Shear Yield Stress	k = 2440 psf

(This set of soil parameters corresponds approximately to a clay soil with CBR = 8-10.)

Load Parameters:

Tire Footprint Length	ℓ = 12.0 in
Peak Surface Pressure	p_{max} = 24600 psf
Pulse Duration	t_d = 0.05 sec
Load Ratio (shear to normal)	β = 0.25

Computational Parameters:

Time Increment	$\Delta t = 6.25 \times 10^{-5}$ sec
Space Mesh Size	h = 3.0 in
No. Width Mesh Points	M' = 47
No. Depth Mesh Points	N' = 27

Figures 23, 24, and 25 summarize the results obtained using the braked wheel sinkage prediction computer program for the case when the braking shear stress is 25% of the vertical pressure load. Figure 23 shows the vertical deflection of the soil surface at three isolated times during the application of the load pulse shown in Figure 21; Figure 24 shows the horizontal displacement of the soil surface at three particular times; and Figure 25 traces the complete time history of the vertical deflections of Stations 23, 24, 25, and 28.

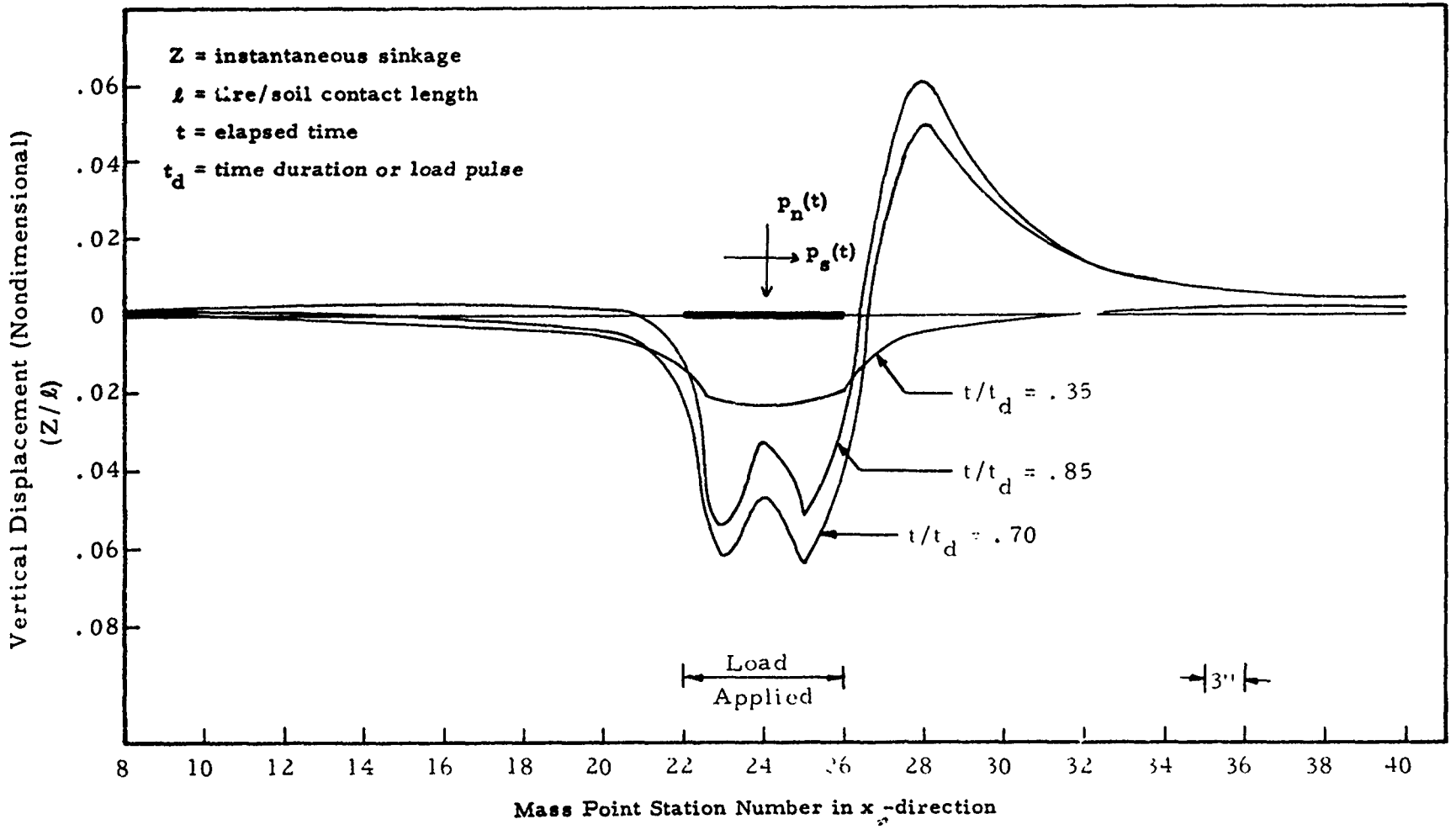

Figure 23. Vertical Displacement of Soil Surface

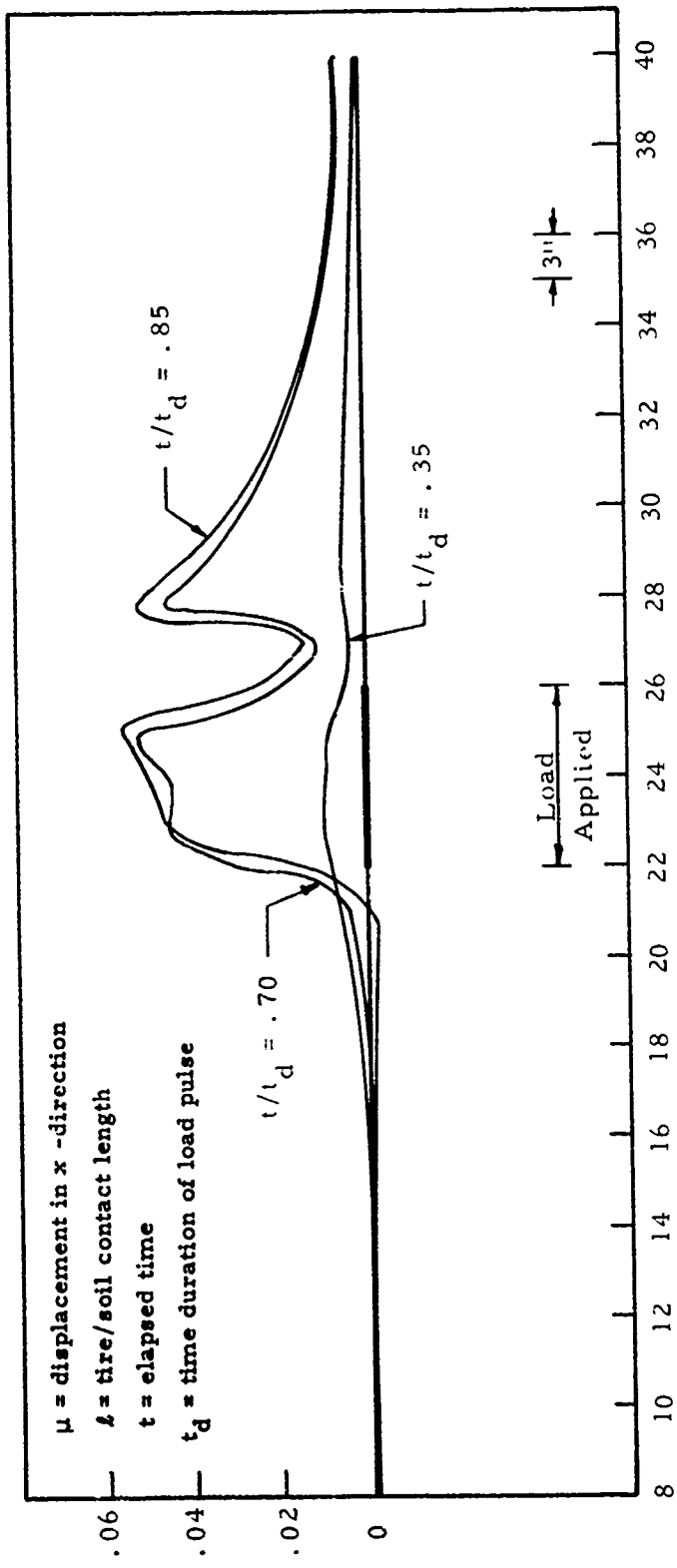

Figure 24. Horizontal Displacement of Soil Surface

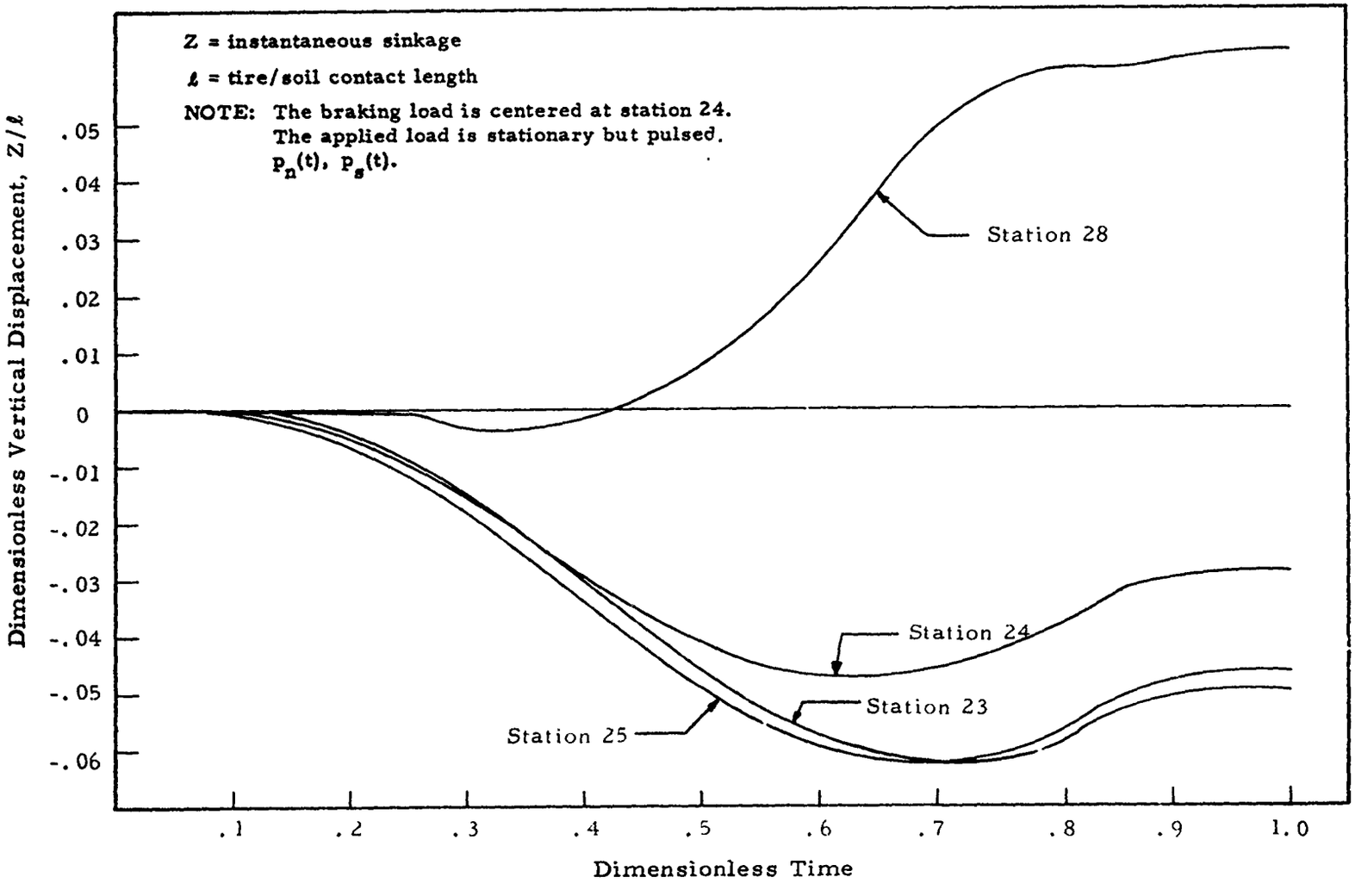

Figure 25. Vertical Displacements of Mass Points 23, 24, 25, and 28 With Time

The sinkage profile under the loaded region (Stations 22-26) did not appear too realistic at first glance since that is not what one would expect if a metal plate were subjected to the same loading. However, it must be realized that a metal plate is very stiff and would resist such a deformation, whereas the idealized problem considered actually corresponds to the case when the loading is transmitted to the soil through a thin flexible membrane since the soil surface is completely free to deform. When this is taken into consideration it is not too difficult to imagine the displacement profile shown under the applied loading in Figure 23. Figure 23 also indicates that there is a substantial build-up of soil immediately in front of the braked tire; this certainly is an expected phenomenon.

Figure 24, the plot of horizontal displacements, is not particularly illuminating since the horizontal displacement distribution is difficult to visualize. Reference to Figure 24 indicates that the greatest horizontal displacement occurs directly under the loaded region and directly under the soil build-up in front of the loaded region. Other points of the soil surface experience very little horizontal displacement.

Figure 25 shows clearly the "rebound effect" which occurs under the loaded region (Stations 23, 24, 25); that is, as time increases the vertical displacement first grows to a maximum value and then diminishes until a permanent steady state sinkage is attained. Figure 25 also shows the vertical displacement time history of Station 28, the point at which maximum build-up of soil occurs in front of the loaded region. For small times, this point behaves as though no braking were present (the displacement of this point is in the same direction as the points under the load for small times) and then pile-up begins. The upward displacement of Station 28 also increases to a maximum value, but instead of decreasing to a steady state value, it increases further until steady state is reached. Apparently, the rebounding of the soil under the load causes additional pile-up of soil in front of the loaded region.

The maximum and permanent sinkages (or build-up) of Stations 23, 24, 25, and 28 are as follows:

$$\text{Station 23} \quad \begin{cases} Z_{max} \approx 0.76" \\ Z_{perm} \approx 0.59" \end{cases}$$

$$\text{Station 24} \quad \begin{cases} Z_{max} \approx 0.57" \\ Z_{perm} \approx 0.35" \end{cases}$$

$$\text{Station 25} \quad \begin{cases} Z_{max} \approx 0.75" \\ Z_{perm} \approx 0.55" \end{cases}$$

$$\text{Station 28} \quad \begin{cases} Z_{max} \approx 0.72" \\ Z_{perm} \approx 0.76" \end{cases}$$

The results indicate that the maximum sinkage and the maximum soil build-up are about the same magnitude, while the permanent build-up is greater than the permanent sinkage. Also, the maximum sinkage obtained for a single wheel without braking under similar conditions is about 0.5"; that is, $(Z_{max})_{braked} > (Z_{max})_{unbraked}$. The ratio of $(Z_{max})_{braked}$ to $(Z_{max})_{unbraked}$ for this case is 1.5+ which compares to the range of 1.5 to 3.0 for cohesive soils from the Braking Verification Tests previously described.

The total computer run time to compute the permanent steady state sinkage by incrementing the load to its maximum value and then completely removing it was approximately 37 minutes.

D. BRAKING SUMMARY

The results of the previous braking studies[1, 3, 12], the Braking Verification Tests, and the analytical study of braked tire/soil interaction now permit the establishment on a preliminary basis the following braked tire drag ratio prediction equations. The value of K = 0.09 as given for Equation (18) was selected based not only on the results of the Braking Verification Tests but also on the previous work of WES[12] and Lockheed[13].

Cohesive Soil

$$\frac{R_B}{R_P} = \frac{R_R}{P} + \frac{R_T}{P} = 3.85\left(\frac{Z}{D}\right) + \frac{K\,CI \cdot D^2}{P}\left(\frac{Z}{D}\right)^{1/2}\left(\frac{S}{100}\right)^{1/3} \qquad (18)$$

where

Z = braked tire sinkage, $K = 0.09$

and

$$\frac{Z_{max}\,(S \simeq 100\%)}{Z_R\,(S \simeq 0\%)} \simeq 2.0 \text{ to } 2.5$$

and

2 knots $\leq$ Forward Velocity $\leq$ 15 knots,

and

$$0.01 \leq \frac{Z}{D} \leq 0.20$$

Cohesionless Soil

$$\frac{R_B}{P} = \frac{R_R}{P} + \frac{R_T}{P} = 0.048 + 2.7\left(\frac{Z}{D}\right) + \frac{\alpha D^2}{K_1 P}\left(\frac{S}{100}\right)^{1/2} \qquad (19)$$

where

Z = braked tire sinkage

and

$$\frac{Z_{max}\,(S \simeq 100\%)}{Z_R\,(S \simeq 0\%)} \simeq 8 \text{ to } 15 \text{ for } \frac{\alpha}{CI_{avg}} \text{ high}$$

$$\frac{Z_{max}\,(S \simeq 100\%)}{Z_R\,(S \simeq 0\%)} \simeq 4 \text{ to } 10 \text{ for } \frac{\alpha}{CI_{avg}} \text{ low}$$

and

$K_1 = 15$ for Velocity $\simeq 2$ knots

$K_1 = 12$ for Velocity $\simeq 6$ knots

$K_1 = 9$ for Velocity $\simeq 12$ knots

and

$$0.01 \leq \frac{Z}{D} \leq 0.20$$

It should be recognized that the braked tire drag ratio prediction equations are based primarily on experimental braking tests conducted to date (1971) which includes only a limited range of tire diameters, tire loads, soil types, forward speed, etc. They can be used, however, to provide preliminary estimates of braking drag ratios within the stated range of limitations and to conduct comparative studies of braking efficiency for various tire parameters.

SECTION III

MULTIPASS AND SPEED - PRELIMINARY

A. MULTIPASS

Efficient and effective use of forward area airfields by the Air Force depends upon the development of a multipass criteria which will specify the useful life of these runways. The two areas of importance associated with multipass operations are runway deterioration (roughness) and aircraft drag load. A thorough review of the existing multipass flotation performance on soil runways has been completed, and the following presents the results of this review.

Existing Multipass Data

The major portion of the existing data was developed by the U. S. Army Waterways Experiment Station[5] for the purpose of updating the multipass design criteria for the C-5A aircraft. One of the major difficulties of previous multipass testing was the inability to discern consistent trends from the resulting data. This inability is partially attributable to the test programs lacking duplicate testing procedures to verify accuracy. Additionally many of the data sources were not specifically designed to generate multipass flotation criteria as such, and therefore, many times did not adequately describe important flotation parameters necessary for an analysis. Other sources of multipass data are the following: C-122 Flotation Test Program[14]; Douglas Aircraft Company research; Waterways Experiment Station research[15, 16]; a combined research effort of WES and Boeing Aircraft Company[4]; C-141 Flight Test Program[17]; and finally, research conducted by I. C. Holm[18]. All of the above data was collected on cohesive type soils with the exception of the C-141 program, and some of the WES data by Nuttal which were test programs using tires on cohesionless soil. Only the WES-C-5A program and the Douglas tests were conducted for large numbers of multiple passes,

usually determined by some preset failure condition. The test variables for all this data varies considerably, from small-scale model tests in the WES programs to the full size flight testing of the C-122 and C-141. A wide range of tire sizes, soil strengths, and types of testing (small model, full scale model, actual prototype) were conducted. Unfortunately, the tests were not conducted in such a manner as to evaluate the important multipass variables, and therefore, do not represent a collection of data sufficient to develop a complete multipass analysis.

Multipass Flotation Analysis

It should be pointed out that as the data described above was being collected, the researchers,in many cases, were lacking considerable information concerning the important multipass flotation variables. Additionally, the various definitions of several important variables, such as sinkage and rut depth, were not clearly understood. In fact, sinkages and rut depth were taken to be one in the same by many researchers. An additional area of concern was the method of applying multipass operations. Some investigators felt that each pass of a test tire had to be in the previous tire's rut, while others tried to distribute the passes over some finite width of the test track. As a consequence of the above mentioned difficulties, the following analysis will only be able to indicate trends in the existing data.

Cohesive Type Soil

Shown in Table X is a summary of the trends in the multipass data that have been accumulated to date. It is evident that in each test series, independent of the method of rut depth determination, that the accumulated rut depth increased at a decreasing rate for increasing coverages. This is particularly true of the test series where the subsequent passes of the test vehicle or carriage were distributed over a general area rather than in the exact same rut each time. The increase in rut depth per pass after the first pass in all cases was less then the first pass rut depth,

TABLE X

MULTIPASS DATA RESULTS - CLAY TYPE SOIL

Test Program Parameter	C-122	Douglas	WES	WES-Boeing (not a test program)	WES C-5A	C-141	Holm
Drag, R	No data.	Multipass drag loads decreased (much scatter).	Multipass drag increases slightly.	Multipass drag for same soil strength decreases.	Multipass drag increases greatly. (much scatter) (data inconsistent)	No data.	Multipass drag decreases.
Rut Depth, Z_R	Decreasing rate of increase in accum. rut depth with increasing passes.	Decreasing rate of increase in accum. rut depth with increasing passes.	Decreasing rate of increase in accum. rut depth with increasing passes.	Multipass sinkage decreases for same soil strength.	Decreasing rate of increase in rut depth with increasing passes. (much scatter) (data inconsistent)	Second pass rut depth smaller than twice the first pass rut depth.	Decreasing rate of increase in rut depth with increasing passes.
Soil Strength	No data.	Indicates increasing soil strength.	Possible 5% decrease in soil strength.	Not applicable.	Not consistent.	No data.	Increasing soil strength.
Soil Type	Harper's Lake Clay	Silty Clay	Buckshot Clay	Buckshot Clay	Buckshot Clay	Harper's Lake Clay	Sandy Loam
Maximum No. of Passes	6	Varied Some > 300	5	3	Varied Some > 600	2	4

yet the tests by WES, WES-Boeing, and Holm indicated only a very slight decrease in the rate of rutting after the second pass. In the tests where the subsequent passes of the tire were distributed to obtain some type of coverage pattern, the soil surface was being releveled by the multipass operations and the results are predictable. Again note that the definition of rut depth varied considerably, and therefore much of the quoted data is subject to possible improper interpretation. Using this data, however, Figure 26 was developed to indicate the trend in the accumulative rut depth with increasing passes. (Note: In tests where coverages were given instead of passes, coverages were assumed to equal passes.) As would be expected, the data scatter for such a plot was progressively larger for increasing passes. It should be noted that the number of data points which contributed to the curve shown in Figure 26 was not equal from each test program (see Table X), therefore each test program was not equally weighted. The previous results were based on a limited amount of data and should be viewed as preliminary.

The trends in the multipass drag data are a little harder to define. However, when considering the Douglas, WES-Boeing, and Holm data, it is noted that the multipass drag decreases while the soil strength increases. It appears, therefore, that the multipass drag is a function of the change or lack of change in strength of the soil surface for clay type soils.

Cohesionless Type Soil

The only two sources of multipass data on sand are the WES-Boeing program and the report by Nuttal. Both clearly indicate that the multipass drag in sand will be less than the first pass drag, and that incremental sinkage also decreases if the soil strength does not change. The soil strength change, however, is probably a function of the critical void ratio in sand. That is, sand type soils tend to reach an equilibrium soil strengths when subjected to large deformations. Therefore, a normal loose sand would become stronger after the first pass, and a dense sand would weaken.

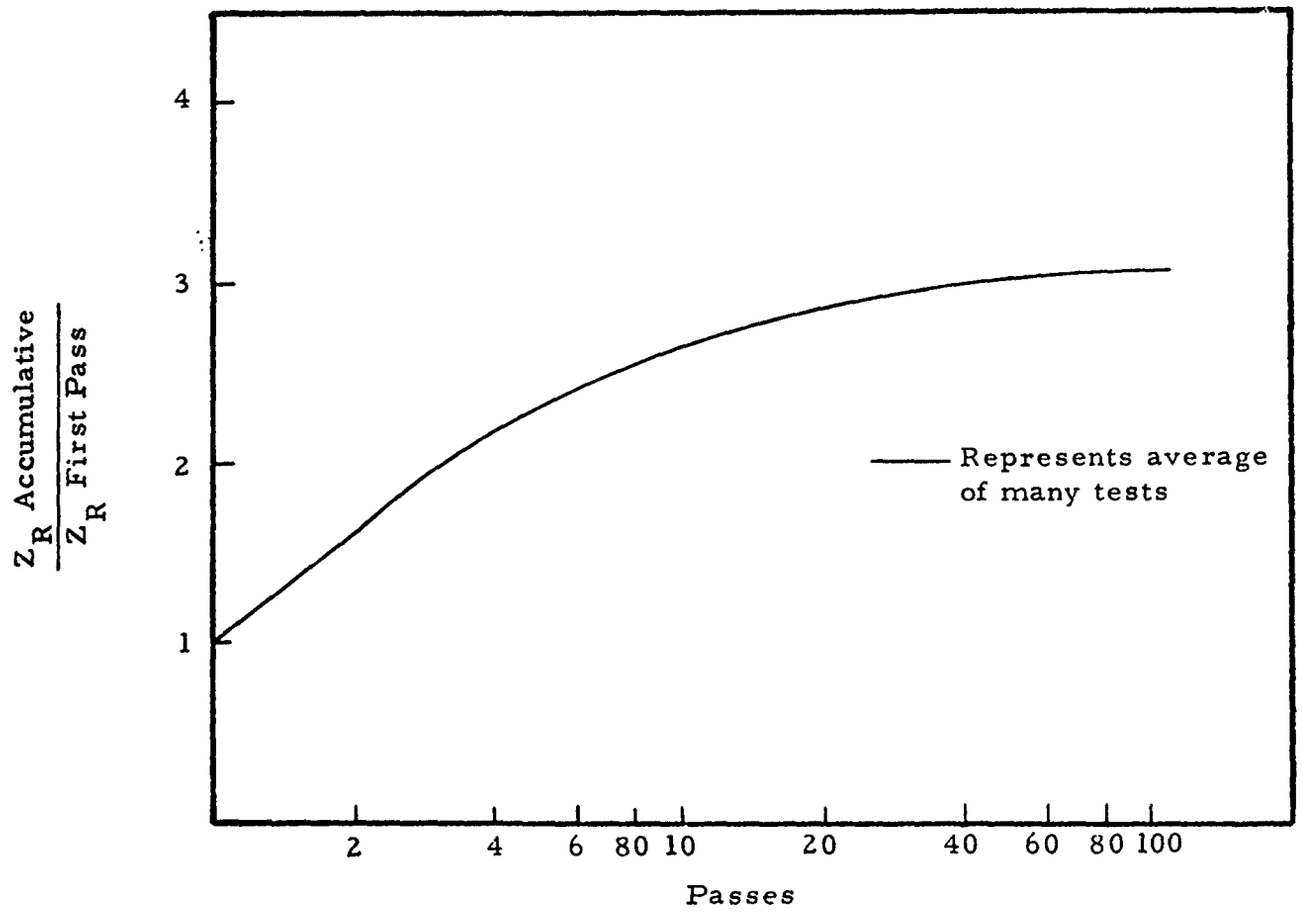

Figure 26. Accumulative Rut Depth Increases versus Passes - Clay Soil

Therefore, as in clay, the multipass drag is probably a function of the soil strength change, or lack of it.

Multipass Flotation Criteria

The criteria currently used by the Air Force which was developed by the U. S. Army Waterways Experiment Station[19], specifies multipass operations in terms of coverages, where a coverage is defined as sufficient passes of tires in adjacent tire paths to completely cover a given width of runway area one time. However, even though this procedure is the accepted standard, it is generally conceded that it needs considerable improvement. One of the difficulties with this current procedure is the somewhat arbitrary nature of its development. In order to specify coverages for an aircraft, a runway failure criteria and a given runway width must be specified. Both of these factors are given set values in the Air Force procedure and are not related to specific aircraft. The runway failure criteria is set at 3 inches of permanent rut depth or 1.5 inches of elastic sinkage, and the runway width in which 75% of the aircraft passes must be performed is given as 80 inches plus the width of one main gear bogie. This procedure also ignores the differences in the performance characteristics of twin and tandem tire arrangements does not consider the effects of speed and braking and has only a limited criteria for sand type soils. In general, the current criteria generates an unreasonable number of coverages for some aircraft, and lacks any ground roughness criteria. In reviewing the multipass data and criteria, it was observed that the present multipass criteria was developed by heavily relying on engineering judgement and past experience with multipass flexible pavement criteria, and it is difficult therefore to define the accuracy of the current multipass criteria. Also it is evident that a new and more meaningful multipass criteria cannot be developed without further experimental work.

Based on the above study, an effort to define aircraft flotation and multipass performance in terms of ground vehicle performance has been proposed. This method is based on the theory that aircraft first pass

performance can be predicted by developing a relationship between first pass ground vehicle rut depth and soil strength. Based on the ground vehicle rut depth, the aircraft performance can be predicted for the first landing and takeoff. Subsequent operation prediction would then be made based on the observations (rut depths) of the first aircraft operation. This experimental program is essential to the development of a more meaningful multipass criteria which will provide insight into the above mentioned problems and take into account ground induced vertical and drag loads.

B. SPEED

Intrcduction and Background

Although aircraft in their takeoff runs go through a large velocity range (0 to approximately 120 knots), early flotation studies and design criteria presumed that rolling aircraft tire drag due to sinkage in soil was a constant throughout the velocity range. In 1964, Boeing[4] conducted a number of full scale tests designed to observe the influence of speed on the aircraft rolling drag ratio. These tests were conducted at Harpers Lake, California on a lean clay. Although these results provided only preliminary information on speed effects, they were important since they showed a significant variation of the rolling drag ratio with speed for aircraft operating on soil runways. More recently the Air Force again sponsored a series of full scale speed tests conducted by Lockheed[3] at the NASA test track. As shown in Figure 27, the results to date indicate speed has a significant influence on the rolling drag ratio for low strength soils but only small influence for operations on high strength soil.

Both Boeing[4] and Lockheed[3] in attempting to develop a drag prediction model noted the similarity in the shape of the drag ratio vs. velocity relationship (see Figure 27) to that observed in tire hydrodynamics studies on water and proposed the use of the same basic equation:

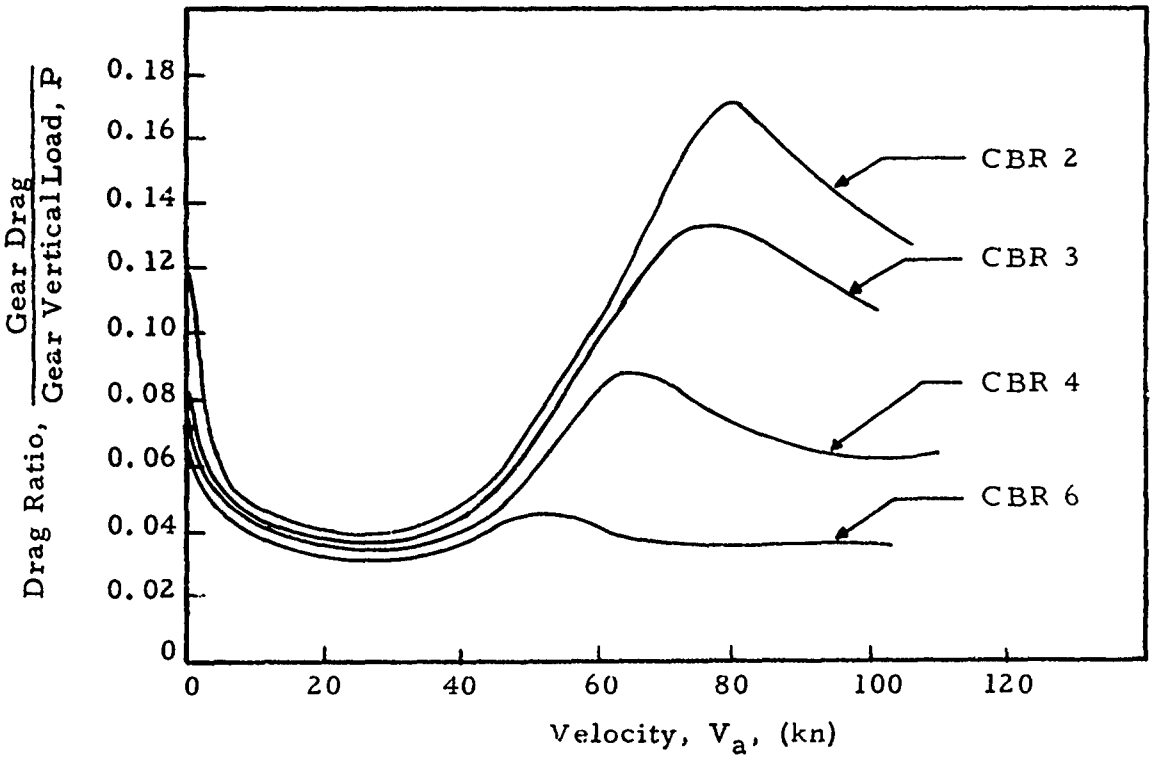

Figure 27. Effect of Velocity on Main-Gear Drag Ratio (Harper Lake Tests), Boeing[4] Test Program

$$R = P(\mu_o + \tan\theta) + \frac{C_{DI}}{2} \rho b Z V_a^2 \qquad (20)$$

where

R = total rolling drag

P = total vertical load

μ_o = coefficient of rolling friction on a rigid surface

$\tan\theta = Z/\ell$

C_{DI} = soil inertia drag coefficient (a function of the planing velocity)

b = tire width

and

V_a = forward velocity of the tire

ℓ = tire footprint length

ρ = soil density.

Reference to the above equation indicates that the total drag is made up of a term which is independent of velocity and a drag term which is a function of velocity squared (inertia) but is independent of the vertical load. Based on the normal values of ρ, b, and Z encountered for aircraft tires on soil, the inertia drag term normally does not become significant until the forward velocity reaches 20 to 30 knots.

Comparisons between measured drag and the drag predicted by Equation 20 or its modified form[3] have been less than satisfactory and have led to the introduction of several empirical coefficients to better curve fit the experimental data. The primary reason for these poor results in the comparative studies is that in a high speed rolling drag situation, four unknowns are present (rolling drag, sinkage, soil inertia drag coefficient, and planing velocity). Since only one analytical equation exists (see Equation 20), the other three unknowns must be determined empirically. Sufficient data is not available to date (1971) to accurately define these other unknowns.

Preliminary Speed Analysis

It is generally accepted that at low velocities (0 to approximately 5 knots, Region I velocity range), the viscosity of the soil significantly influences the magnitude of the sinkage and drag. As previously indicated, at high speed (greater than 20 to 30 knots, Region III velocity range), viscous effects no longer predominate but soil inertia becomes a critical factor in influencing sinkage and drag. At intermediate velocities (Region II velocity range), neither viscosity or soil inertia are important considerations in defining sinkage and drag. One approach to developing a drag prediction equation including velocity effects would be to recognize that the sinkage and drag effects are interactive and given by

$$Z_{(\text{instantaneous})} = Z_{\text{Region II}} + \Delta Z_{\text{inertia drag}} - \Delta Z_{\text{lift}} \qquad (21)$$

Existing theory[2] can be used to determine the sinkage in Region II. For example, Equation 22 gives an approximate drag/sinkage relationship usable for both sand and clay and is based on the results of numerous tests:

$$\frac{R}{P} = 0.018 + 3.23\left(\frac{Z}{D}\right) \qquad (22)$$

for $0.01 \leq \frac{Z}{D} \leq 0.12$

where

D = tire diameter

Applying the hydrodynamic equations at the tire soil interface gives a lift as defined by

$$L = \rho b Z V_a^2 \sin\theta \cos\theta \qquad (23)$$

and an inertia drag term as given by

$$\Delta R = \rho b Z V_a^2 \sin^2\theta \qquad (24)$$

where

θ = angle defining the effective plane of contact at the tire/soil interface.

Using Equation 22 as a basic relationship between drag, vertical load, and sinkage, the increment of sinkage associated with inertia drag becomes

$$\Delta Z_{\text{inertia drag}} = 3.23D \left[\frac{\Delta R}{P'} - .018 \right] \tag{25}$$

where

P' = total load on the tire minus the lift (L).

The increment of sinkage, $-\Delta Z_{lift}$, can be determined by using the previously established sinkage prediction equations[2] which are of the form

$$\frac{Z}{\ell} = C_1 + C_2 \frac{\alpha}{CI_{avg}} \tag{26}$$

where

ℓ = tire footprint length

C_1 and C_2 = constants

$\alpha = P/A$

and

P = vertical load

A = tire contact area

CI_{avg} = average cone index over 0" to 6" depth

which for the incremental case would be given by

$$-\Delta Z_{lift} = \frac{C_2 L \ell}{A CI_{avg}} \tag{27}$$

Using the above approach, an interactive computer program was written and used to make comparisons between measured drag and predicted drag for the Lockheed high speed test data[3]. The results of one such comparison is given in Figure 28. Other comparisons have been made and the results were equally favorable. These results, which have been encouraging, indicate that as the velocity increases into Region III, the ΔZ due to inertia drag is greater than the $-\Delta Z$ due to lift. As the speed continues to increase, this relationship is reversed and the sinkage-velocity curve peaks and begins to decrease with further increases in velocity. The results are viewed as sufficiently promising to warrant further research into the drag-velocity relationship using the above approach.

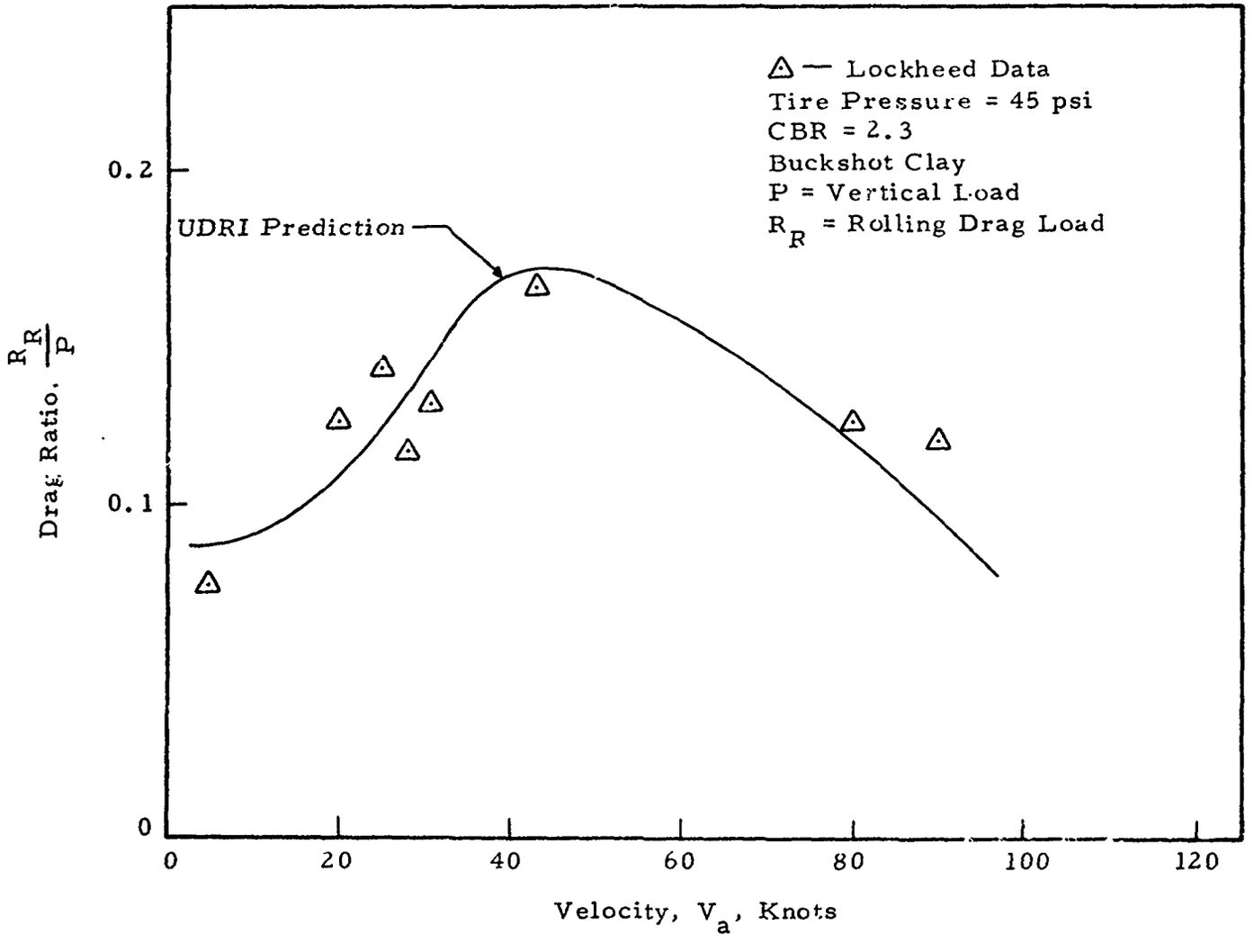

Figure 28. Predicted Rolling Drag, R_R, Versus Measured Drag

SECTION IV

ADDITIONAL STUDIES IN TIRE/SOIL INTERACTION

A. ROLLING TANDEM WHEEL - ANALYTICAL STUDY

In the report for Pa ' One of Phase III of this research program[1], an analytical approach for studying the sinkage and drag effect of tandem tracking wheels was discussed. In that discussion, the following items were included: (a) the actual three-dimensional problem of the rolling tandem-tracking wheels; (b) the two-dimensional plane strain approximation using two moving infinite surface pressure strips (a diagram of the plain strain problem is shown in Figure 29); (c) the lumped parameter iteration method of solution and the simulation of the moving pressure strips; and (d) the method of evaluation of the multiwheel effects. The reader is referred to References 1 and 20 for complete details. In Appendix III the governing equations, figures of the lumped parameter model, and the numerical procedures are presented without derivations. The detailed development of the equations and the procedures is given in References 2, 21, and 22. The computer program for the numerical procedure and the results of the test cases will be presented in this section.

Computer Program and Test Cases

A computer program was written based on the governing equations and the numerical procedure given in Appendix III. A general flow chart of the computer program is shown in Figures 30 and 31. A Fortran IV source program listing of the computer program, a sample set of input data, a list of definitions of symbols, and some remarks about running the computer program are given in Appendix IV.

Three test cases were run with the computer program. All the cases have the same soil, load, and computational parameters, which are listed below. This set of parameters is that of a typical multiwheel aircraft tire-soil interaction.

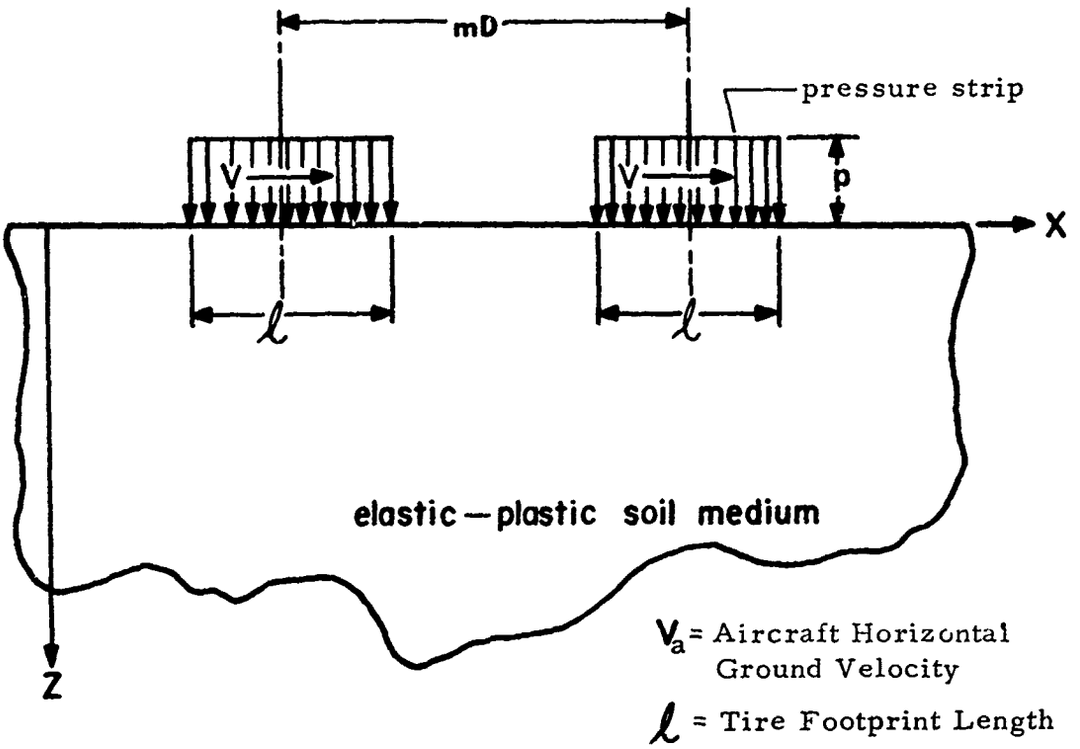

(a) Soil Medium with Moving Strip Pressure

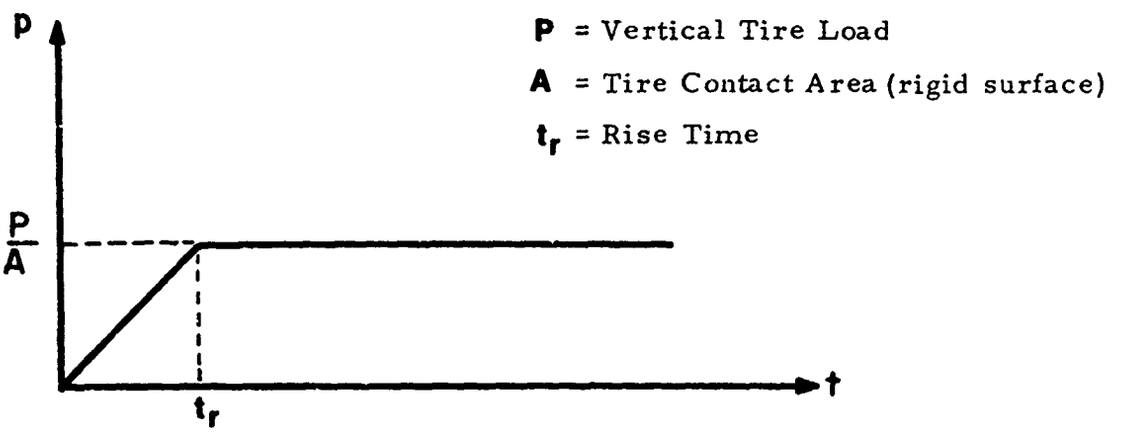

(b) Pressure-Time Curve

Figure 29. Rolling Tandem-Wheel Interface Boundary Condition

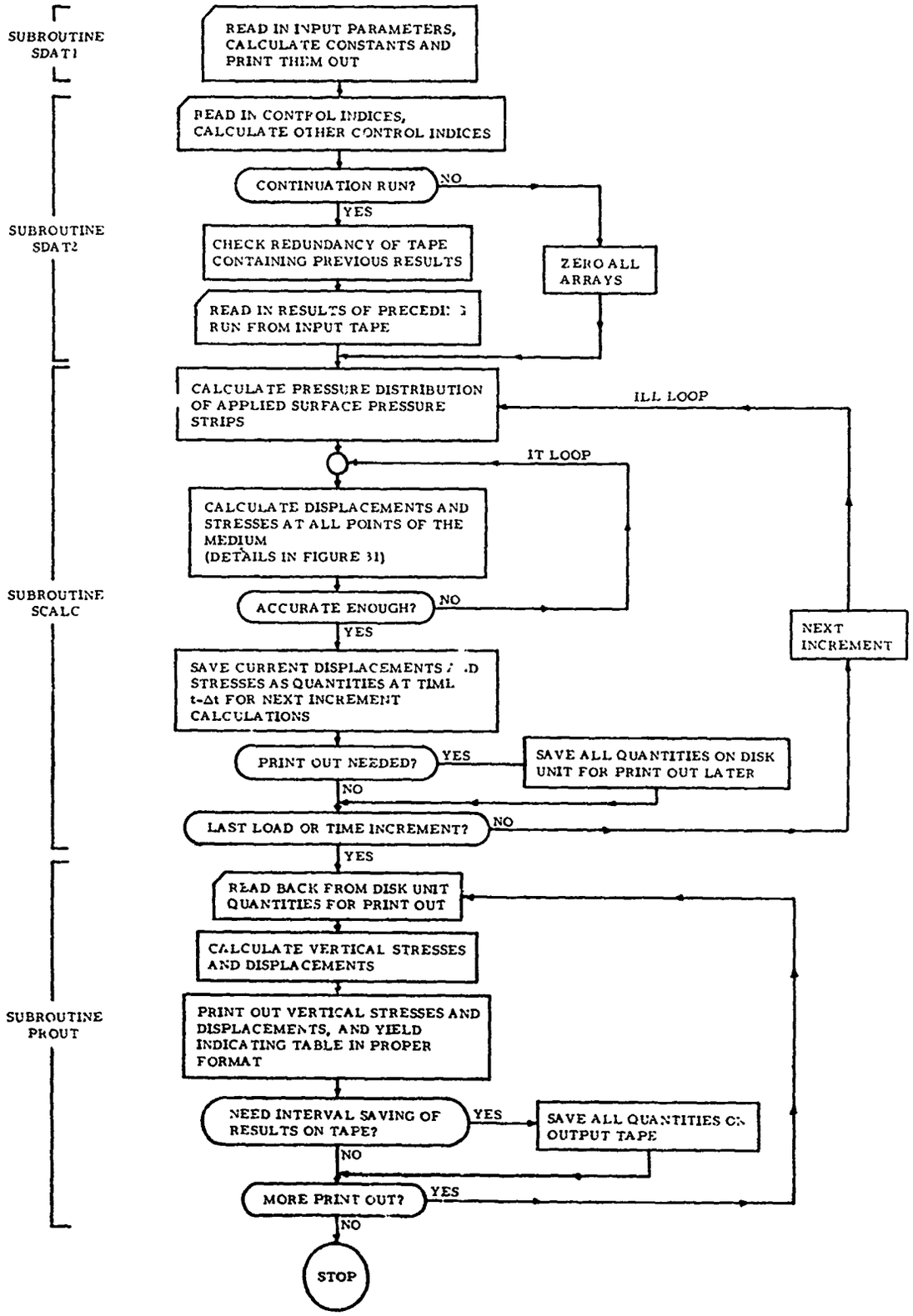

Figure 30. General Flow Chart of Computer Program

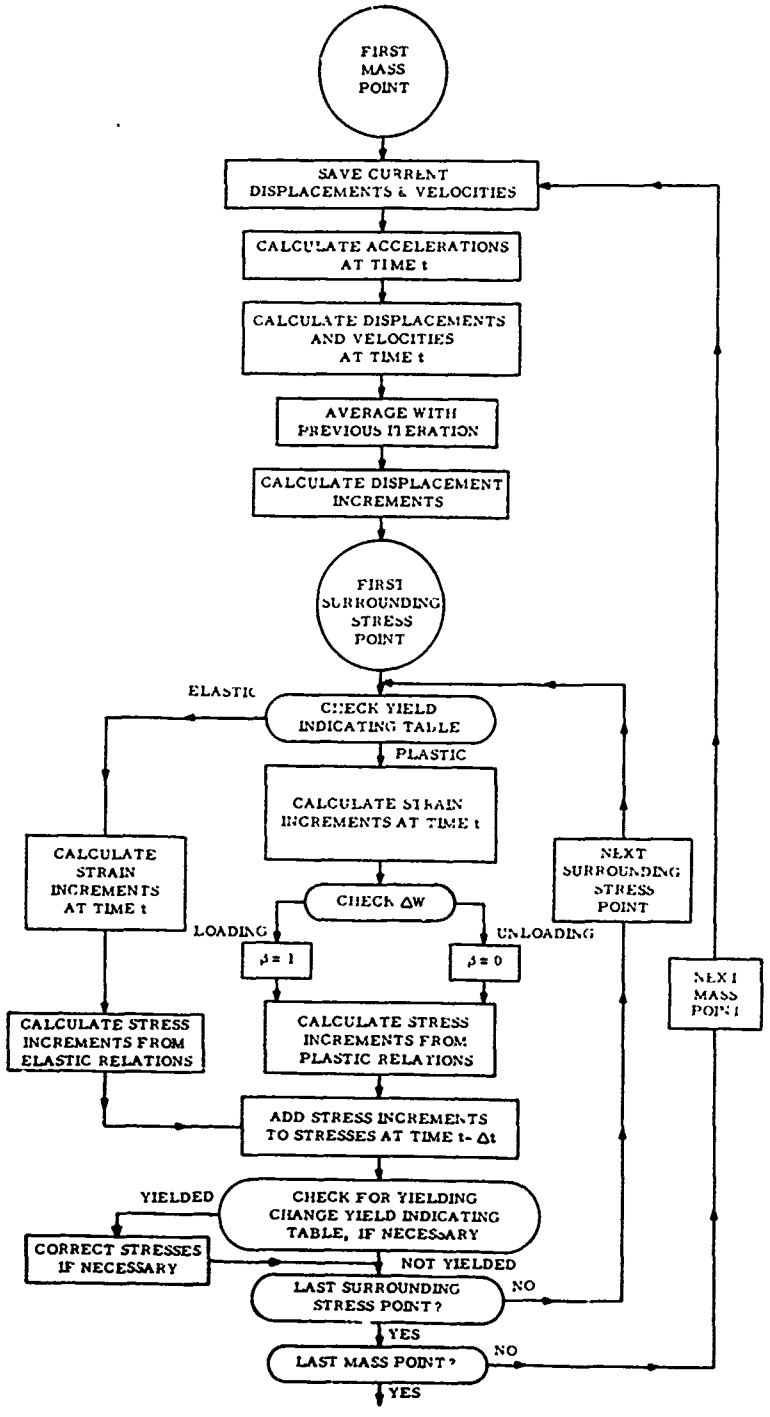

ΔW = Incremental work done on the soil medium

β = a variable related to the stress invariants

Figure 31. Part of Program for Calculation of Displacements and Stresses

Soil Parameters:

Density	ρ = 130 lb/cu ft
Poisson's Ratio	ν = 0.45
Young's Modulus	E = 8950 psi
Cohesion	c = 2000 psf
Friction Angle	ϕ = 15°
Yield Stress in Shear	k = 2440 psf

(This set of soil parameters corresponds approximately to a clay soil with CBR = 8 to 10.)

Load Parameters:

Tire Footprint Length	ℓ = 18.0 inches
Peak Contact Pressure	p_{max} = 24600 psf
Rise Time of Pressure	t_r = 0.0075 sec.
Aircraft Ground Velocity	V_a = 45 knots (approx.)
Tire Outside Diameter	D = 42.8 inches

Computational Parameters:

Space Mesh Size	h = 4.5 inches
Time Increment	t = 0.0001 sec.
Finite Boundary Size	Depth = 130"
	Width = 130" to 203" depending on wheel spacing

The only difference between each of the cases is the tandem wheel spacing. One of the cases corresponds to the single wheel case, m = 0 (or m = ∞), and the other two cases correspond to tandem tracking wheel configurations with wheel spacings of 1.05 D and 1.7 D, where D is the tire carcass outside diameter. In order to minimize the influence of the finite boundary on the sinkage when the wheel spacings are changed, the distances between the finite boundaries and the edges of the applied surface pressure strips are maintained constant by changing the width of the finite region.

Results of Test Cases and Discussions

The results of the single wheel case show the correct sinkage pattern. Shown in Figure 32 is a graph of the vertical deflection of the soil surface at various times (or stages of travel) plotted against a coordinate, $\bar{x}$, which is stationary with respect to the moving tire. The high sinkage indicated by curves B and C corresponding to lapse times of 0.015 second and 0.025 second are due to the rapid rise of the applied pressure causing the overshoot of deflection. Curves E F, and G corresponding to lapse times of 0.040, 0.050, and 0.060 second show the sinkage trailing behind the applied pressure strip. They also indicate that the sinkage pattern is approaching a steady state. The steadier pattern seems to indicate a permanent sinkage ratio of $(Z_R/\ell) = 0.013$, which is equivalent to a permanent sinkage of $Z_R = 0.24$ inch, and an instantaneous sinkage ratio of $(Z/\ell) = 0.022$, which is equivalent to an instantaneous sinkage of $Z = 0.40$ inch.

The vertical deflection of the soil surface at various times for the other two cases, corresponding to wheel spacings of 1.05 D and 1.7 D, are shown in Figures 33 and 34. The leading and trailing wheels are plotted on separate graphs so that the same scale as that for the single wheel case (Figure 32), can be retained for comparison purposes. The abscissa coordinate is again $\bar{x}$, which is stationary with respect to the moving wheels, and $\bar{x}$ is taken to be zero at the center of the leading applied pressure strip. The surface deflection curves corresponding to lapse times earlier than 0.040 second are not shown because deflection curves have not reached steady patterns as indicated in the single wheel case.

Observation of the sinkage patterns in Figures 33 and 34 indicates that the surface deflection under the leading applied pressure strip is fairly steady for both cases. On the contrary, the surface deflection under the trailing applied pressure strips goes through large fluctuations for both cases. These large fluctuations may be due to the elastic rebound of the soils rolled over by the leading tire or an elastic wave generated by the

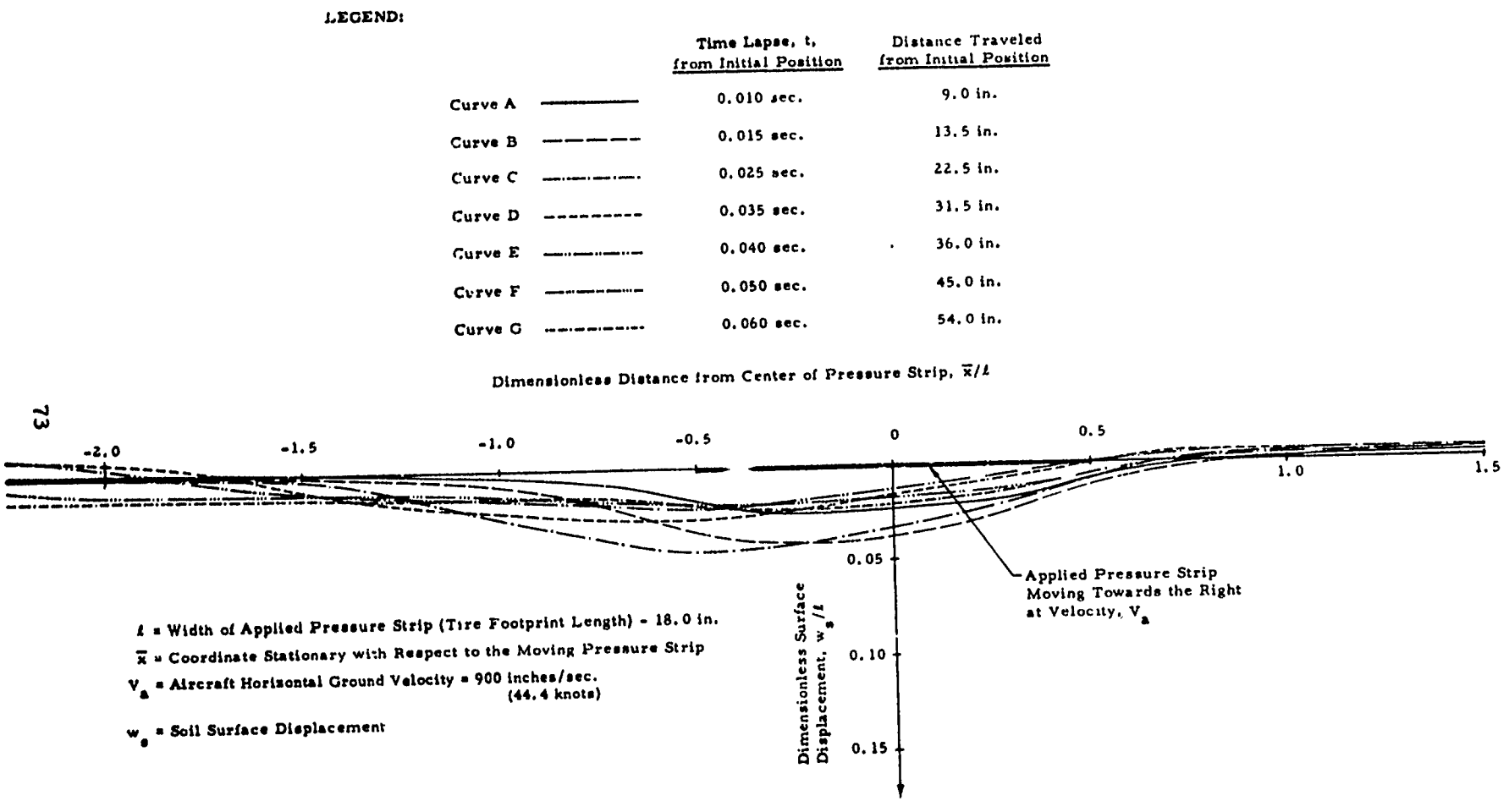

Figure 32. Deflection of the Soil Surface at Various Times for the Single Wheel Case

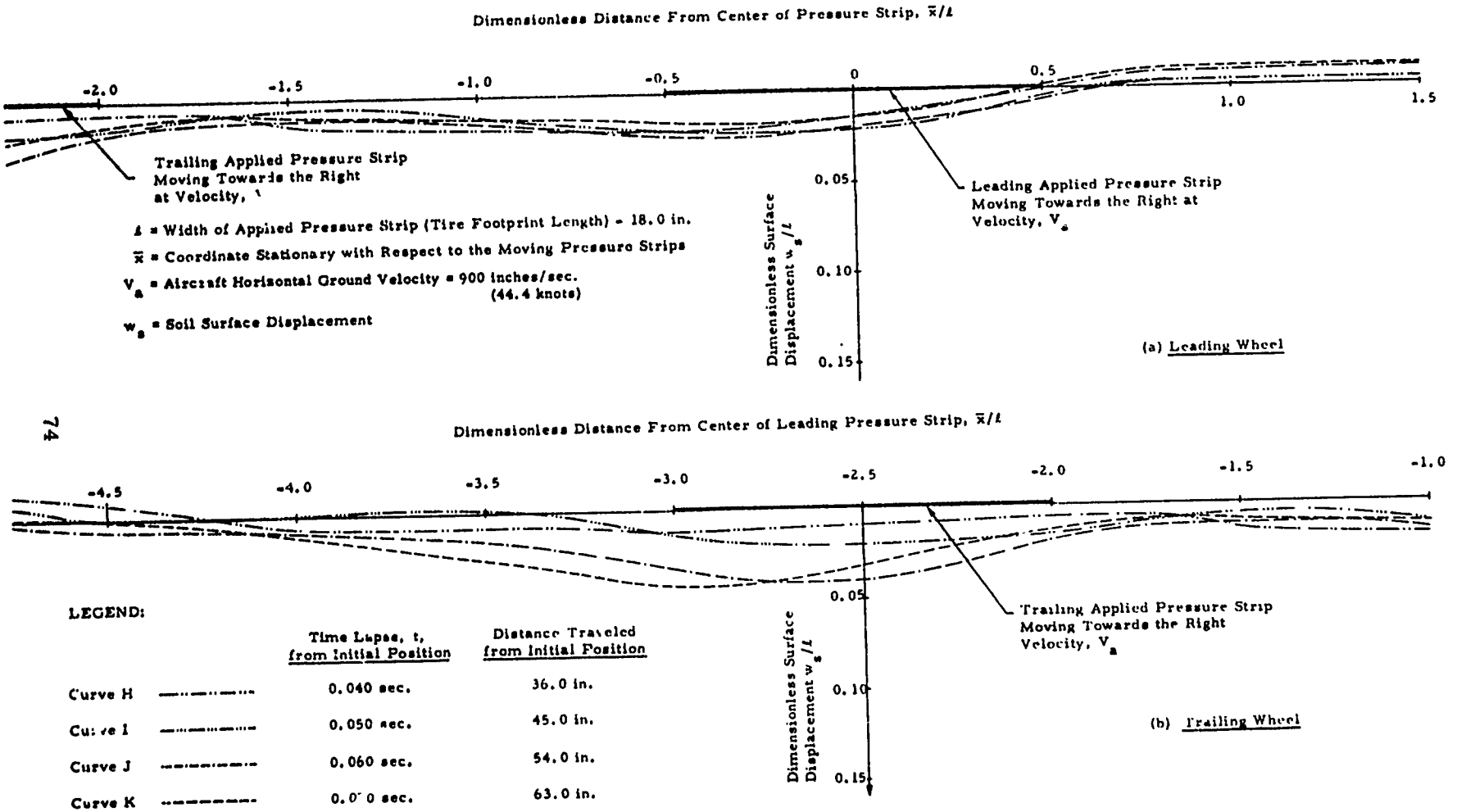

Figure 33. Deflection of the Soil Surface at Various Times for Tandem Wheel Spacing = 1.05 D

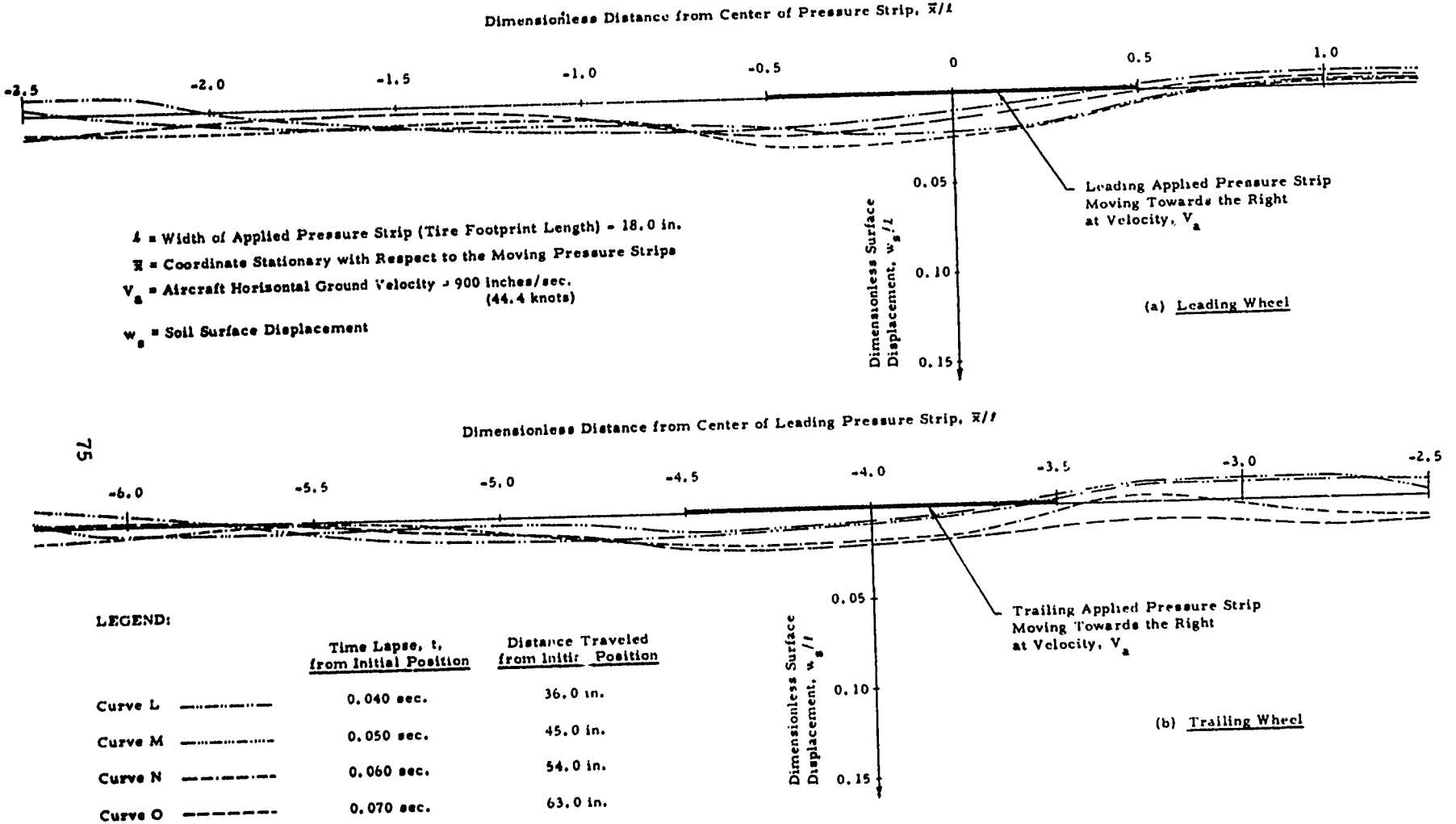

Figure 34. Deflection of the Soil Surface at Various Times for Tandem Wheel Spacing = 1.7 D

leading tire and reflected off the bottom finite boundary. A steadier sinkage pattern could possibly be attained for the trailing tire by running the computer program for a longer lapse time; however, it was not done because an unreasonable stress distribution starts to show due to the accumulation of computational error.

The results shown in Figures 33 and 34 were interpreted as follows. The instantaneous sinkages, Z, of the leading tire were obtained by averaging the peak deflections of the soil surface under the tire for lapse times of 0.040 to 0.070 seconds. The instantaneous sinkages, Z, of the trailing tire were obtained by averaging the differences between the peak soil surface level of the unloaded portion between the tires and the peak soil surface deflection under the trailing tire. In this way, the gross soil movement due to elastic rebound or wave may be canceled. The sinkages are summarized in Table XI.

From the instantaneous sinkage ratio, Z/D, the drag ratio, R/P, of the leading and trailing wheels were calculated from the drag-sinkage equations obtained in Phase II[2]. The drag ratios for both wheels were averaged and compared with the single wheel drag ratio. The results are also summarized in Table XI.

As indicated in the last column of Table XI, tandem wheel operation does not reduce significantly the drag load as compared to the single wheel operation. This was also the conclusion in the experimental test program performed as a separate effort of this research project[1].

The results show that the technique and computer program developed can be used for predicting tandem multiwheel effect quite successfully. The fluctuation of the sinkages is a weakness of the technique but the averaging procedure employed seemed to overcome it. The total computer time used for the three cases is approximately eight hours on the IBM 7094. Conversion to use the CDC 6600 would require approximately half an hour for each case. This long computer running time may limit somewhat the extensive utilization of the computer program.

TABLE XI

SINKAGES AND DRAGS FOR ROLLING TANDEM WHEELS

		Instantaneous Sinkage Ratio		Average Drag Ratio R/P	$\frac{(R/P)\ \text{Tandem}}{(R/P)\ \text{Single}}$
		Z/ℓ	Z/D		
Single Wheel	--	0.022	0.00925	0.0356	1.00
Tandem Wheel Spacing = 1.05D	Leading Wheel	0.022	0.00925	0.0348	0.98
	Trailing Wheel	0.021	0.00883		
Tandem Wheel Spacing = 1.7D	Leading Wheel	0.022	0.00925	0.0356	1.00
	Trailing Wheel	0.022	0.00925		

ℓ = Tire Footprint Length = 18.0 inches
D = Tire Outside Diameter = 42.8 inches
Z = Instantaneous Soil Sinkage
R = Rolling Drag
P = Vertical Load

B. HIGH SPEED VERTICAL PLATE TESTS

Introduction

As indicated previously, the full ground speed range of aircraft leads to tire/soil interaction loadings over a wide range of rates. One approximate way to estimate rates of loading in soil caused by tire/soil interaction is given by

$$r = \frac{ZV_a}{\ell} \tag{28}$$

where

r = rate of loading, in/sec

Z = soil sinkage, in

V_a = forward velocity of aircraft tire, in/sec

ℓ = contact footprint length of tire in soil, in.

For typical aircraft tires and sinkage conditions occuring in takeoff operations, the rate of loadings in soil as given by Equation (28) would probably exceed 100 inches per second. If the resistance to penetration in the soil changes significantly with the rate of loading then such a phenomena would have to be included in the equation of state for the soil.

Recently IITRI[3] conducted a series of vertical plate load tests with varying rates of loading (penetration) to examine this phenomena further. The results of these tests led IITRI to suggest that the typical sinkage-velocity curve for aircraft in a takeoff mode can be explained by changes in soil resistance to penetration which occur under varying rates of loading. Figure 35 shows a typical result for sand[3]. Reference to Figure 35 indicates that beginning from a static condition the soil first becomes stiffer as the rate increases (static to 15 in/sec) and then begins to undergo a period of decreasing stiffness (15 in/sec to 50 in/sec) as the rate of loading continues to increase. This decreasing stiffness reaches some minimum and again begins to increase at very high rates of loading (>50 in/sec).

Test Objective and Program

In an effort to further clarify the influence of penetration rate on the resistance of soil to penetration, a series of vertical plate tests were conducted in a clay and a sandy soil with variable rates of penetration. The purpose of the tests was to:

(a) Estimate the order of magnitude of influence of the rate of penetration on the soil resistance (stiffness) to penetration.

(b) To further investigate the penetration resistance phenomena shown by IITRI[3] as a possible explanation of the rolling drag-velocity relationship for aircraft tires operating on soil.

The initial series of test was run on Buckshot Clay, a very fine-grained clay obtained from the area around Vicksburg, Mississippi. The test program consisted of 22 different tests in which the rates of loading varied from 0.01 inches per second up to a maximum value of 40 inches per second. Table 12 gives a summary of these tests and the rate at which each was run.

Following the clay tests, a very similar series of tests was run on a riverwash sand which was obtained from the area around Dayton, Ohio. This series of tests consisted of 27 different tests which covered a rate of loading range identical to that of the clay tests. Table XIII gives a summary of the tests run on sand and the rates at which each was run.

In both clay and sand tests, the soil specimen was compacted into the test containers and a 3 inch diameter circular plate was penetrated into the sample to a depth of 3 inches by means of a hydraulic MTS loading system. The relationship between penetration and resistance was recorded on either an oscillograph recorder or on the recording system which is integral to the MTS system.

In performing these tests it was very important that the different test specimens could be consistently reproduced to the preselected conditions. It is obvious that if one test sample was of a higher density than another that

TABLE XII

PLATE TEST PROGRAM - CLAY

Test No.	Soil Type	Soil Stiffness CI (Desired)**	Rate of Plate Penetration (in/sec)
C-1A	Buckshot Clay	115.0	0.01
C-1B	"	"	0.01
C-2A	"	"	0.05
C-2B*	"	"	0.05
C-2C	"	"	0.05
C-3A*	"	"	0.10
C-3B*	"	"	0.10
C-3C	"	"	0.10
C-3D	"	"	0.10
C-4A	"	"	0.50
C-4B*	"	"	0.50
C-4C	"	"	0.50
C-5A	"	"	1.00
C-5B	"	"	1.00
C-6A	"	"	5.00
C-6B	"	"	5.00
C-7A	"	"	10.00
C-7B	"	"	10.00
C-8A	"	"	25.00
C-8B	"	"	25.00
C-9A	"	"	40.00
C-9B	"	"	40.00

* These tests were omitted from final calculations.

** Average soil penetration resistance over 0" to 6".

TABLE XIII

PLATE TEST PROGRAM - SAND

Test No.	Soil Type	Soil Stiffness* $CI_{2''}$ (desired)	Rate of Plate Penetration (in/sec)
S-1A	Riverwash Sand	51.0	0.01
S-1B	"	"	0.01
S-1C	"	"	0.01
S-2A	"	"	0.05
S-2B	"	"	0.05
S-2C	"	"	0.05
S-3A	"	"	0.10
S-3B	"	"	0.10
S-3C	"	"	0.10
S-4A	"	"	0.50
S-4B	"	"	0.50
S-4C	"	"	0.50
S-5A	"	"	1.00
S-5B	"	"	1.00
S-5C	"	"	1.00
S-6A	"	"	5.00
S-6B	"	"	5.00
S-6C	"	"	5.00
S-7A	"	"	10.00
S-7B	"	"	10.00
S-7C	"	"	10.00
S-8A	"	"	25.00
S-8B	"	"	25.00
S-8C	"	"	25.00
S-9A	"	"	40.00
S-9B	"	"	40.00
S-9C	"	"	40.00

* Soil Penetration Resistance at 2 inch penetration.

it would exhibit a higher resistance to penetration regardless of the rate of loading effects. In an effort to normalize the test results and to make the results independent of small variances in moisture and density, a series of cone penetrometer tests were performed on each test specimen prior to the actual plate test.

Test Setup

- MTS Loading System

The MTS tensile and fatigue machine is a single item closed-loop electro-hydraulic servo-activated testing machine with a maximum loading capacity of 75,000 pounds. The waveform applied to the soil was that of a ramp. Figure 36 shows the MTS system setup.

- Test Plate

The test plate is a 3 inch in diameter circular plate. Made out of aluminum, the plate has a thickness of 1/2 inch and has a 6 inch long aluminum shaft which has a diameter of 1-1/4 inches. The plate was designed so that it meets the dimensional requirements such that the distance to the nearest side of the test specimen container would be greater than three times the plate diameter and the distance to the bottom of the soil mass would be five times greater than the plate diameter. In addition to the plate, an aluminum extension was designed which would add 3 inches to the shaft length if needed. Figure 37 shows the test plate.

- Cone Penetrometer

The cone penetrometer was made out of stainless steel and had a 5 inch shaft whose diameter was 3/8 of an inch. The cone portion was 1-1/2 inches long and had a base of 0.80 inches in diameter (area = 0.5 in^2). The apex angle of the cone was 30 degrees (15 degrees on each side of the center line). The penetrometer tests were all run at a rate of 1.25 inches per second and were taken to a depth of 4-1/2 inches. Figure 37 shows the penetrometer used.

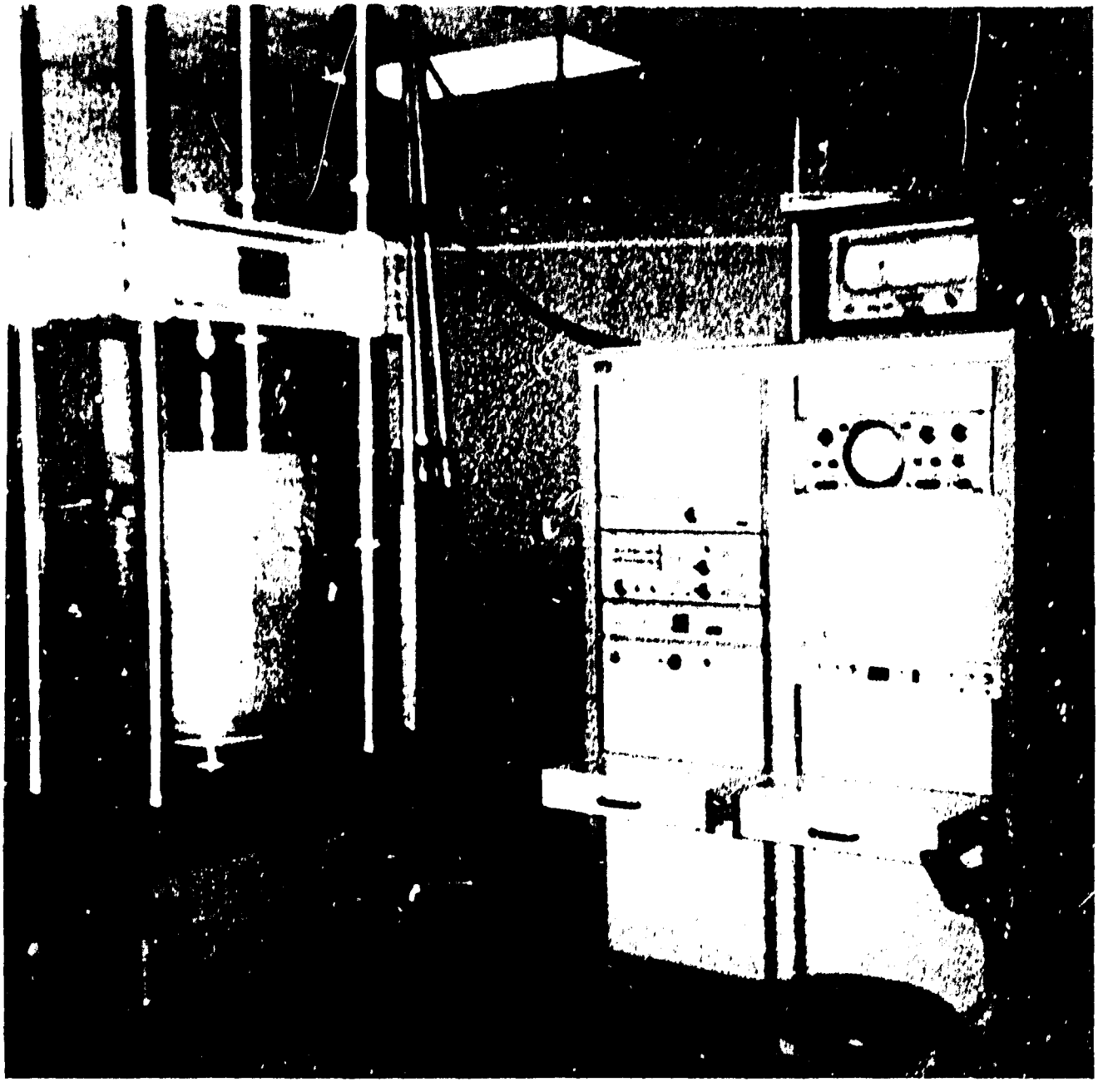

Figure 36. MTS Loading System

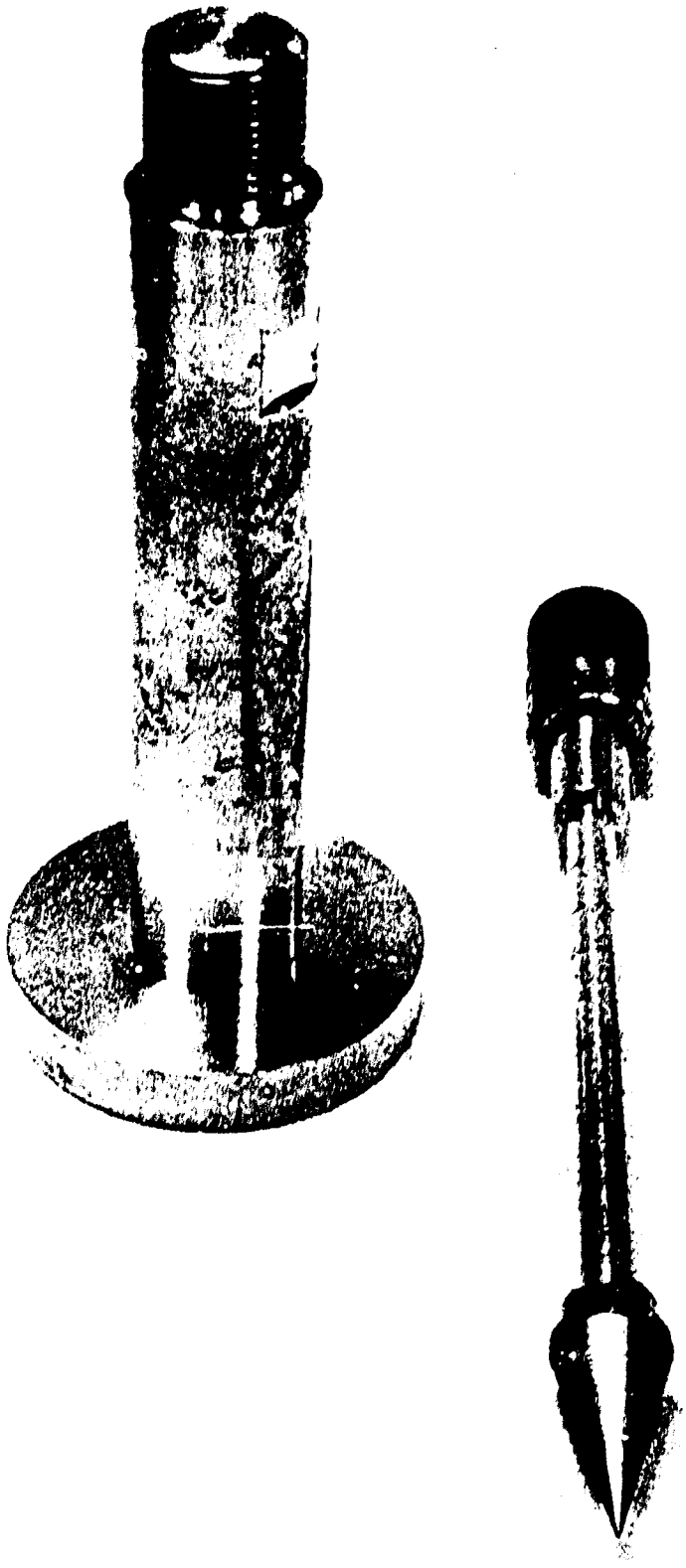

Figure 37. Test Plate and Cone Penetrometer

- Test Containers

The test containers were made from 25 inch high circular refuse containers. These containers were circular in cross-section with a base diameter of 19 inches and a top diameter of 22 inches. Support was added to the base of the containers in the form of two 3/4 inch plywood layers. In addition to these two layers, another layer of 3/4 inch plywood was added beneath the base so that the applied force would be transmitted directly to the soil mass.

- Recording System

The MTS recording system is integral to the MTS loading system and has a maximum recording rate of around 5 inches per second and contains no minimum rate limitations. The oscillograph recorder used during the clay tests is an 18 channel, type 5-114-PS recorder made by Consolidated Engineering Corporation. It has a paper speed range of 0.45 inches per second to 115.2 inches per second. The oscillograph recorder used during the sand test is an 18 channel, type 5-124 A recorder made by Consolidated Electrodynamic Corporation and has a paper speed range of .25 inches per second to 64.0 inches per second.

- Modified CBR Hammer

A modified CBR hammer was used to compact both the clay and sand specimens. This hammer had a 10 pound weight which dropped 18 inches onto a 3-7/8 inch circular plate. This hammer provides a compaction effort of 183.2 $lb\text{-}ft/ft^2$ per blow.

- Soil Classification

The two soils selected for testing were Buckshot Clay and riverwash sand. Extensive previous testing has been performed on the Buckshot Clay and its classification properties can be obtained from other literature sources. For comparison purposes, the grain size distribution of the Buckshot Clay is given in Figure 49 of Appendix I, and of the riverwash sand in Figure 51 of Appendix V.

Test Specimen Preparation and Uniformity Analysis

- Cone Penetration Tests

As indicated previously, the cone penetration test was used to determine the uniformity and strength of a sample prior to a plate test. The results of the cone penetrometer test were also used to normalize the results of the plate tests. If the strength of the soil can be represented by a cone index value which can be determined from the standard cone penetration test, then within certain limits, the soil's resistance to a penetrating plate can be made dependent upon only the rate of penetration by dividing the total soil resistance to the plate by this cone index value. The results of this procedure would provide an adequate method for comparing the effects related only to the rate of plate penetration.

The cone penetrometer was run at three different test locations chosen at even intervals in a region removed from the center of the sample. In the clay tests the tip of the cone was placed at the top of the sample and then penetrated to a depth of 4-1/2 inches. Both penetration depth (inches) and resistance (pounds) were recorded as shown in Figure 38. The definition of CI_{tot} for clay, together with a summary of the cone penetration results for clay is given in Appendix V.

In the sand tests the cone was penetrated 1-1/2 inches (to fully penetrate the cone) prior to the running of the cone penetration test. The cone was then penetrated an additional 4-1/2 inches while recording penetration depth and resistance as shown in Figure 39. Three cone penetration tests were performed on each sample and the definition of CI_{layer}, which was used in the normalizing procedure, is given in Appendix V together with a summary of the cone penetration results for sand.

- Clay Uniformity

In the construction of each test specimen, it was important that a systematic compaction procedure be used which would insure uniform

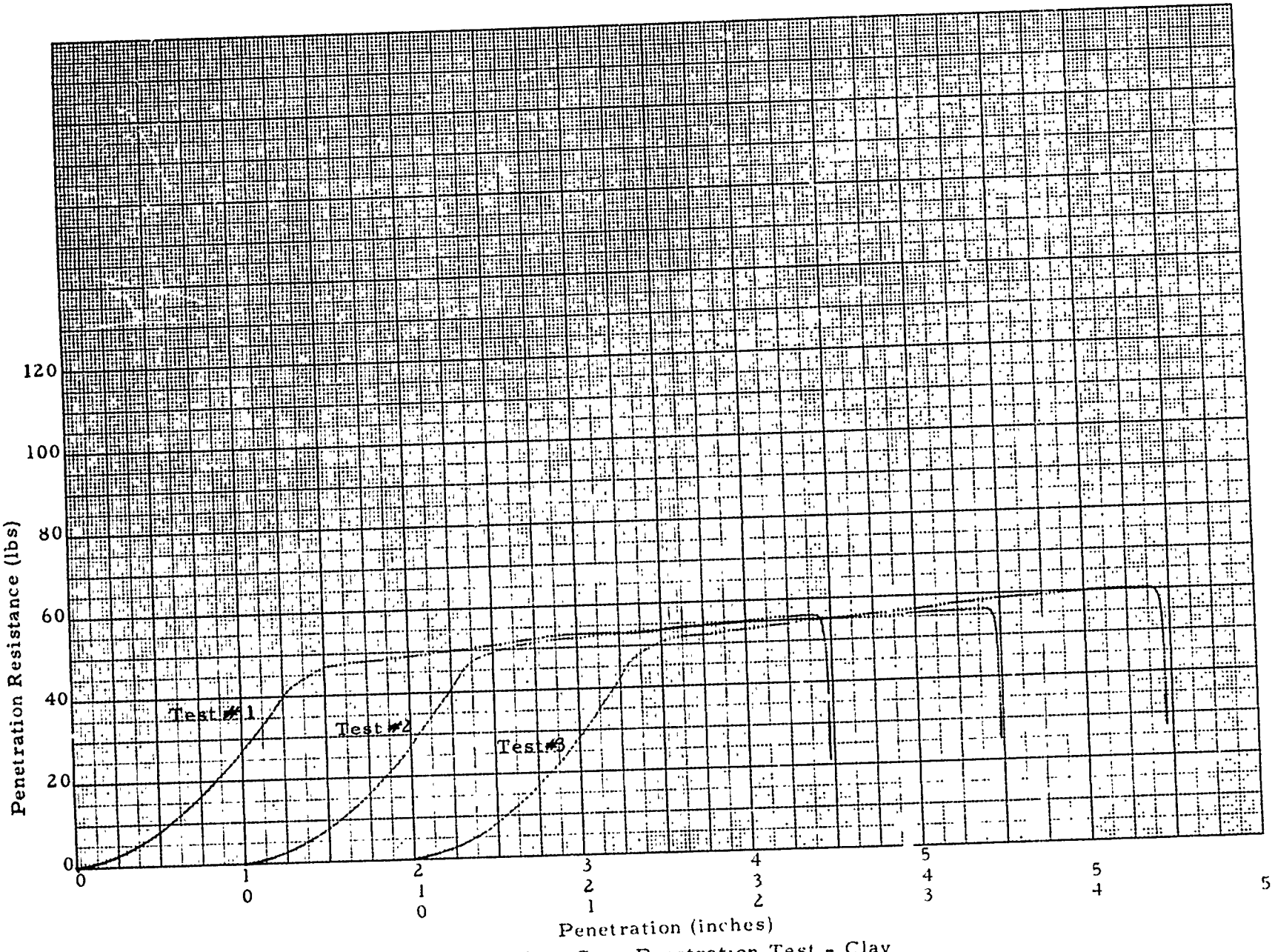

Figure 38 Cone Penetration Test - Clay

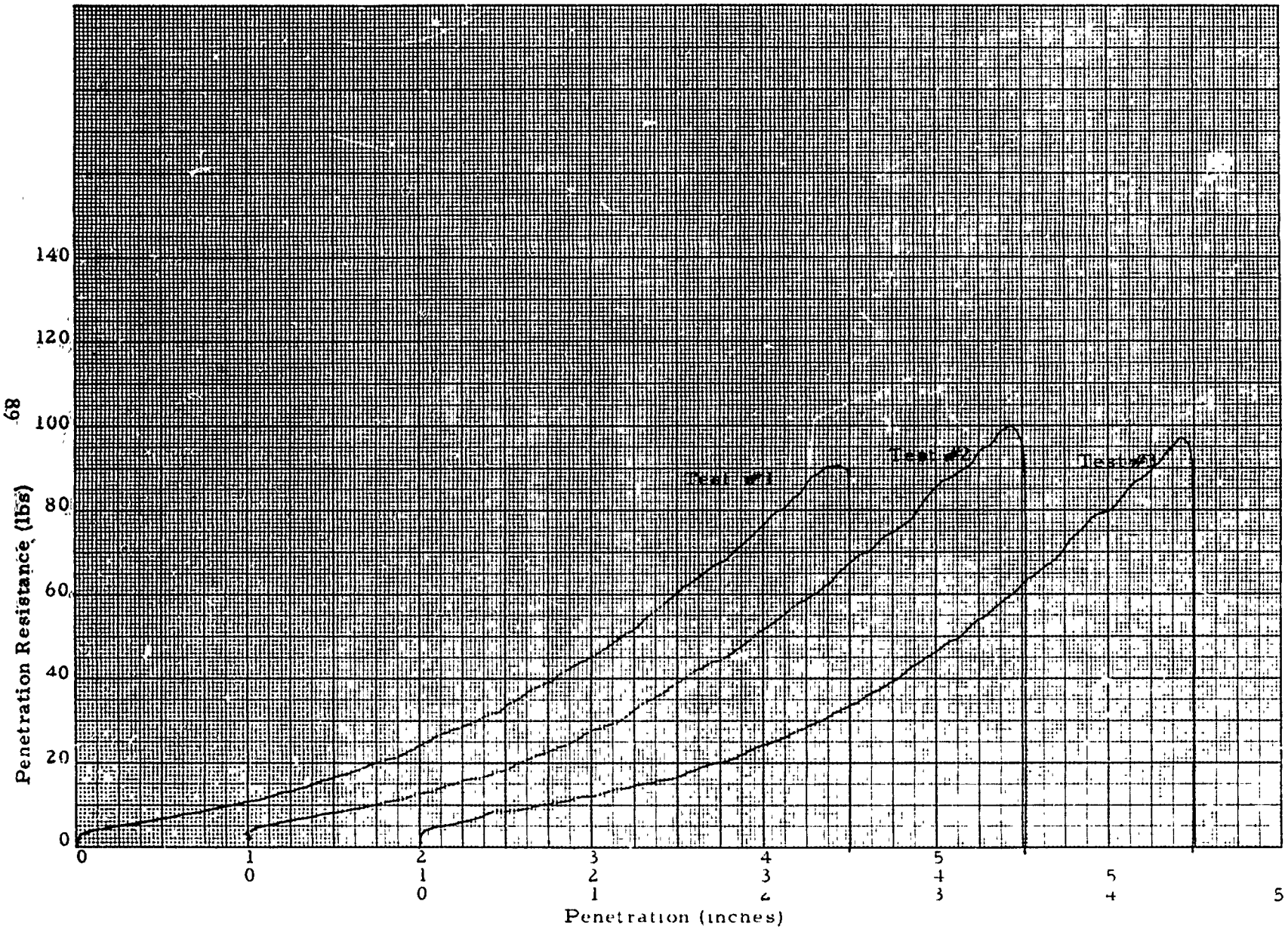

Figure 39. Cone Penetration Test - Sand

specimens throughout the test program. The specimens were compacted into the test containers by means of impact from a modified CBR hammer. The initial test specimens (Test C-3A, C-3B, C-4A, and C-4B) were compacted using 4 inch layers and 100 blows per layer. Subsequent to this several additional samples (C-2A, C-2B, C-5A, and C-5B) were prepared by recompacting the upper 8 inches in 2 inch lifts with 100 blows per layer. The results of the cone penetrometer test in all these samples indicated that they lacked the required uniformity. The results of Tests C-2A, C-3A, C-3B, and C-4B were not used in the subsequent analysis.

For all the remaining test specimens, the entire sample was built up in 2 inch lifts with 100 blows per layer. Samples were reused by recompacting only the upper 8 inches in 2 inch lifts. The results of the cone penetrometer tests on these subsequent samples as shown in Table 58 of Appendix V indicated the required uniformity had been attained by this compaction procedure.

- Sand Uniformity

All the sand specimens were built up using 2 inch lifts and 100 blows per layer. The samples were reused by recompacting only the upper 8 inches in 2 inch lifts. The results of the cone penetrometer tests on the sand specimens as shown in Table 60 of Appendix V indicated the required uniformity had been obtained for all samples within the test program.

Plate Test Results

- Clay

The loading plate tests were conducted immediately after the cone penetration tests. Figure 40 shows a test specimen immediately following a typical test in clay and Figure 41 shows the typical result of a plate penetration test in clay. The results of these tests can best be shown by a graph

Figure 40. Test Specimen Following Plate Penetration Test - Clay

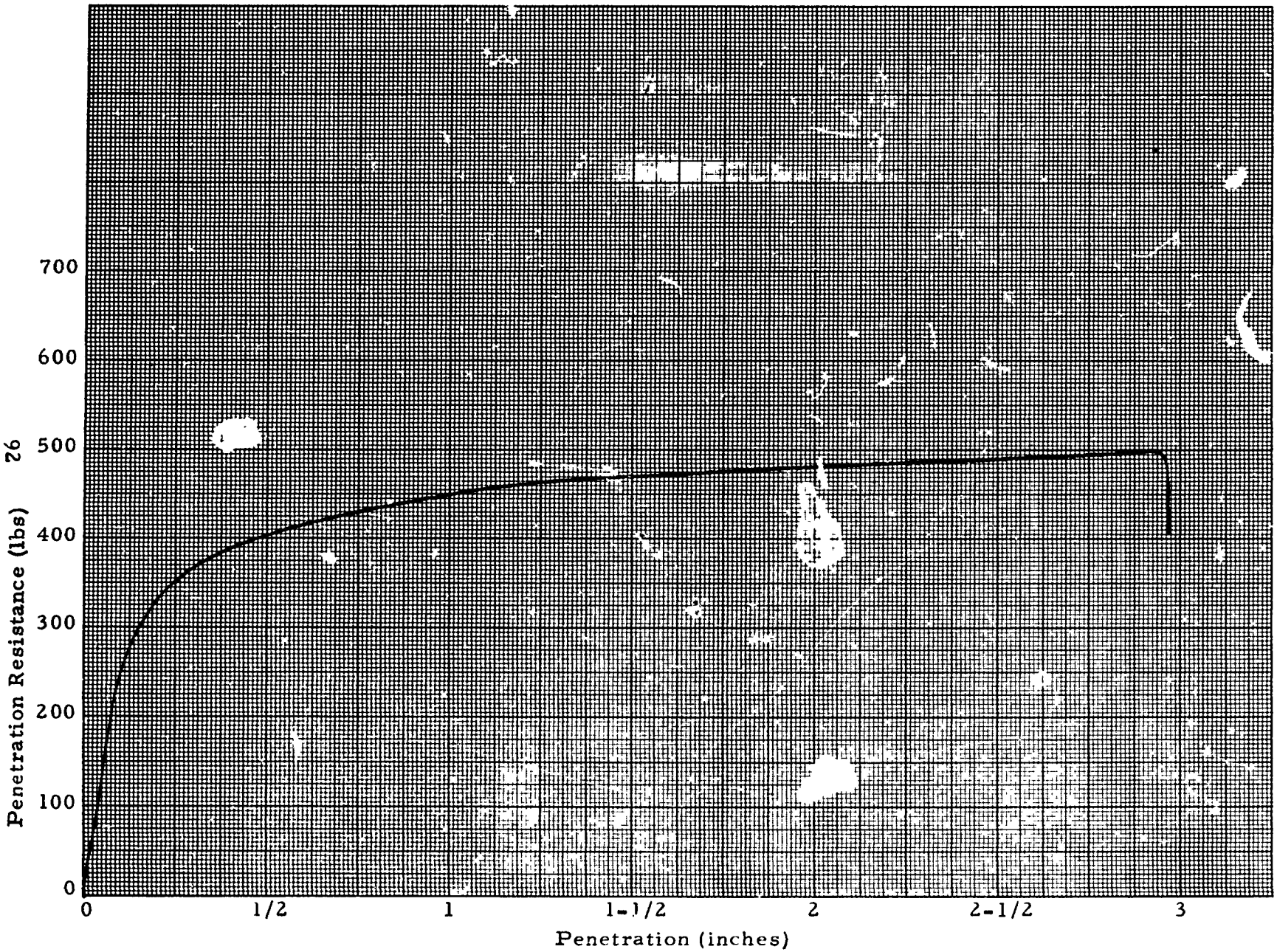

Figure 41. Typical Results of Plate Penetration Test - Clay

of the soil's resistance versus plate penetration for each tested rate of penetration. Such a graph is shown in Figure 42. Reference to Figure 42 shows that with the exception of Test 4, a trend exists in which an increase in the rate of penetration causes an increase in the soil's resistance. As discussed in the previous section, the test specimen used in Test 4 did not meet the desired uniformity, and thus, the results of this test are probably in error. Each data point shown in Figure 42 represents the average of at least two tests.

The results of the clay tests as shown in Figure 42 tend to agree with those obtained from previous rated plate penetration test conducted by IITRI[3] and others. The results of IITRI's tests also show increasing penetration resistance throughout their range of varying penetration rates (static to 40 in/sec). Although IITRI suggested that a decrease in penetration resistance might be observed in a portion of the rate range for plate sizes greater than the 1.95-in used in their test program, no such effect was observed for the 3-in diameter plate used in these tests.

The approximate equal spacing of the tests in Figure 42 suggests that a simple mathematical relationship may exist between the soil's resistance and the rate of penetration. To determine if such a relationship existed a graph of the soil's resistance to penetration versus the logarithm of the rate of penetration was developed at 1-1/2, 2, and 2-1/2 inches penetration. These graphs are shown in Figures 43 through 45. Each graph closely approximated a linear relationship on the semi-logarithmic plot and further investigation revealed that the slopes of these linear relationships were almost equal. By performing a Least Squares analysis, an equation was obtained for each graph. The constants in these equations which were approximately equal for all three cases, were combined to obtain one equation. As the rate of penetration increases, the soil's resistance also increases by the following equation.

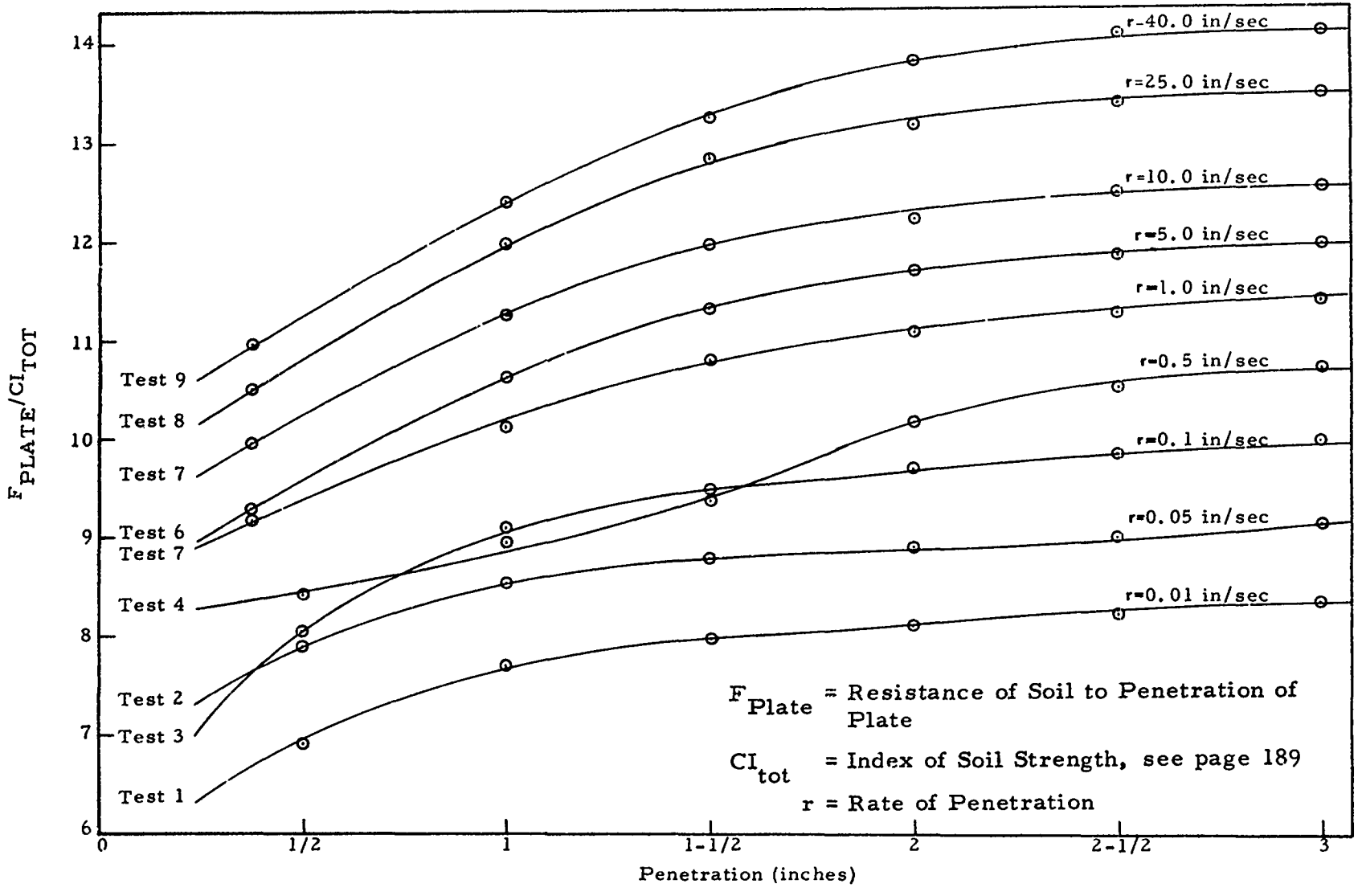

Figure 42. Results of Rate of Loading - Penetration Resistance Tests - Clay

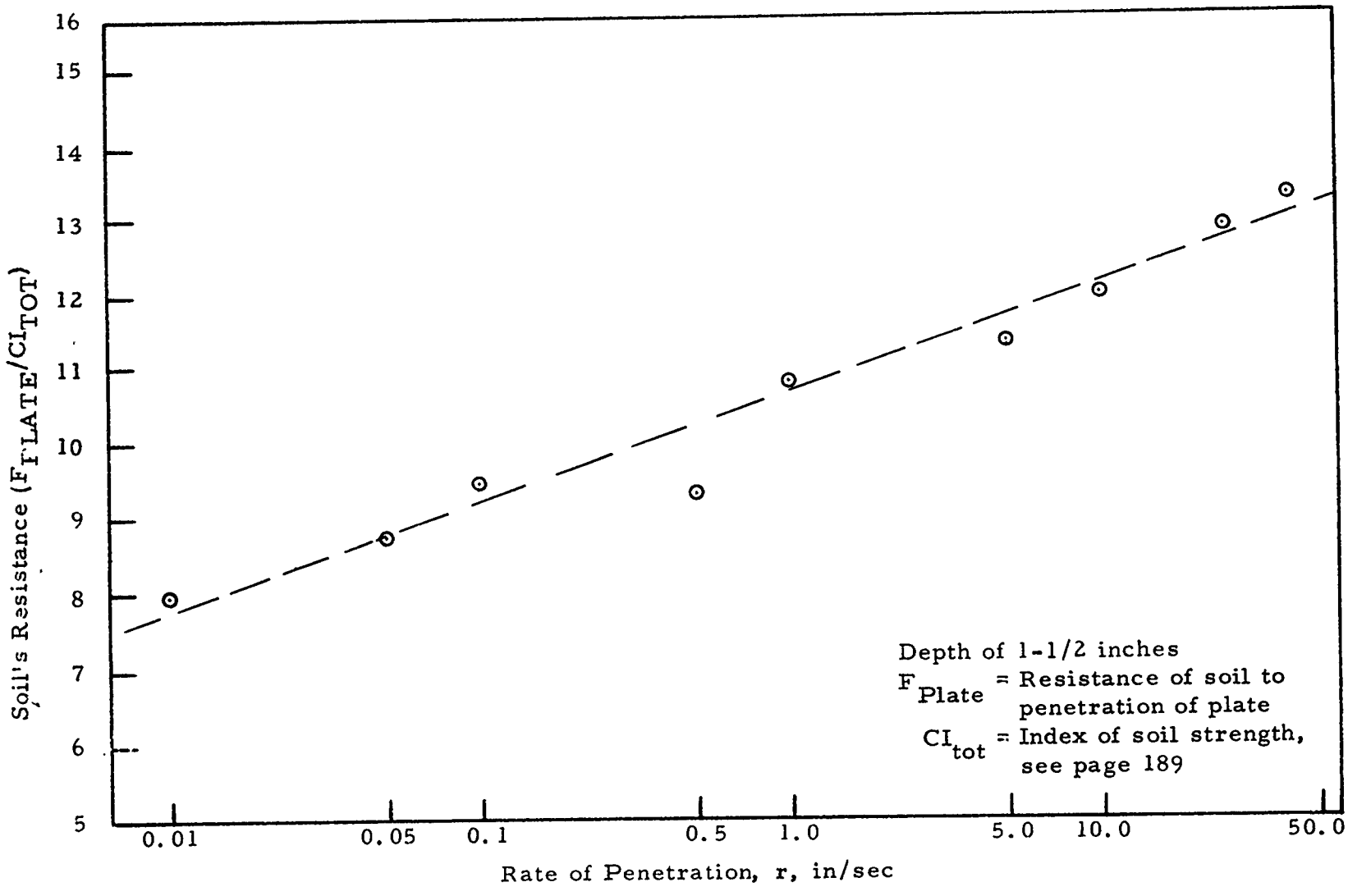

Figure 43. Variance of Soil's Resistance During Test - Clay

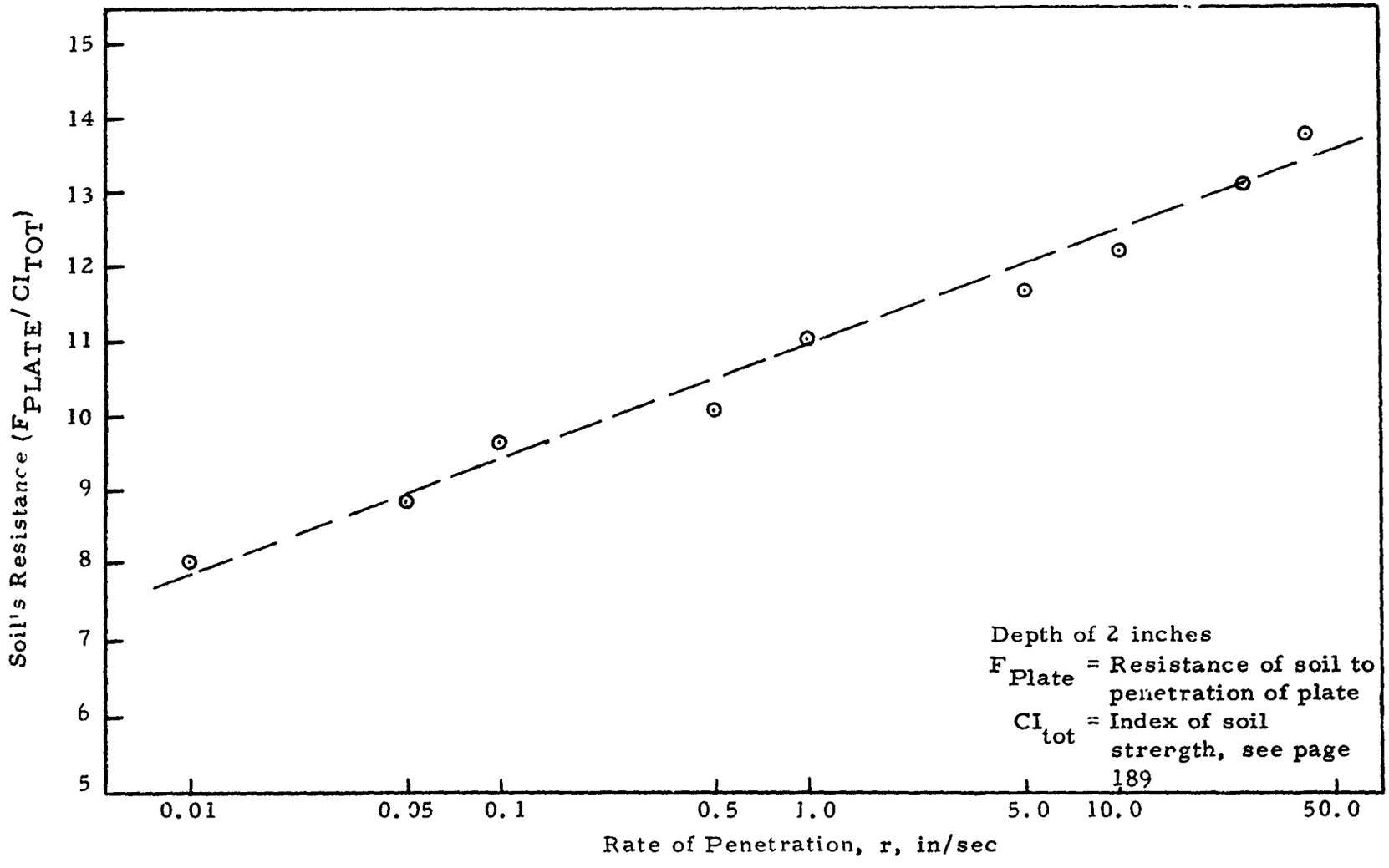

Figure 44. Variance of Soil's Resistance During Test - Clay

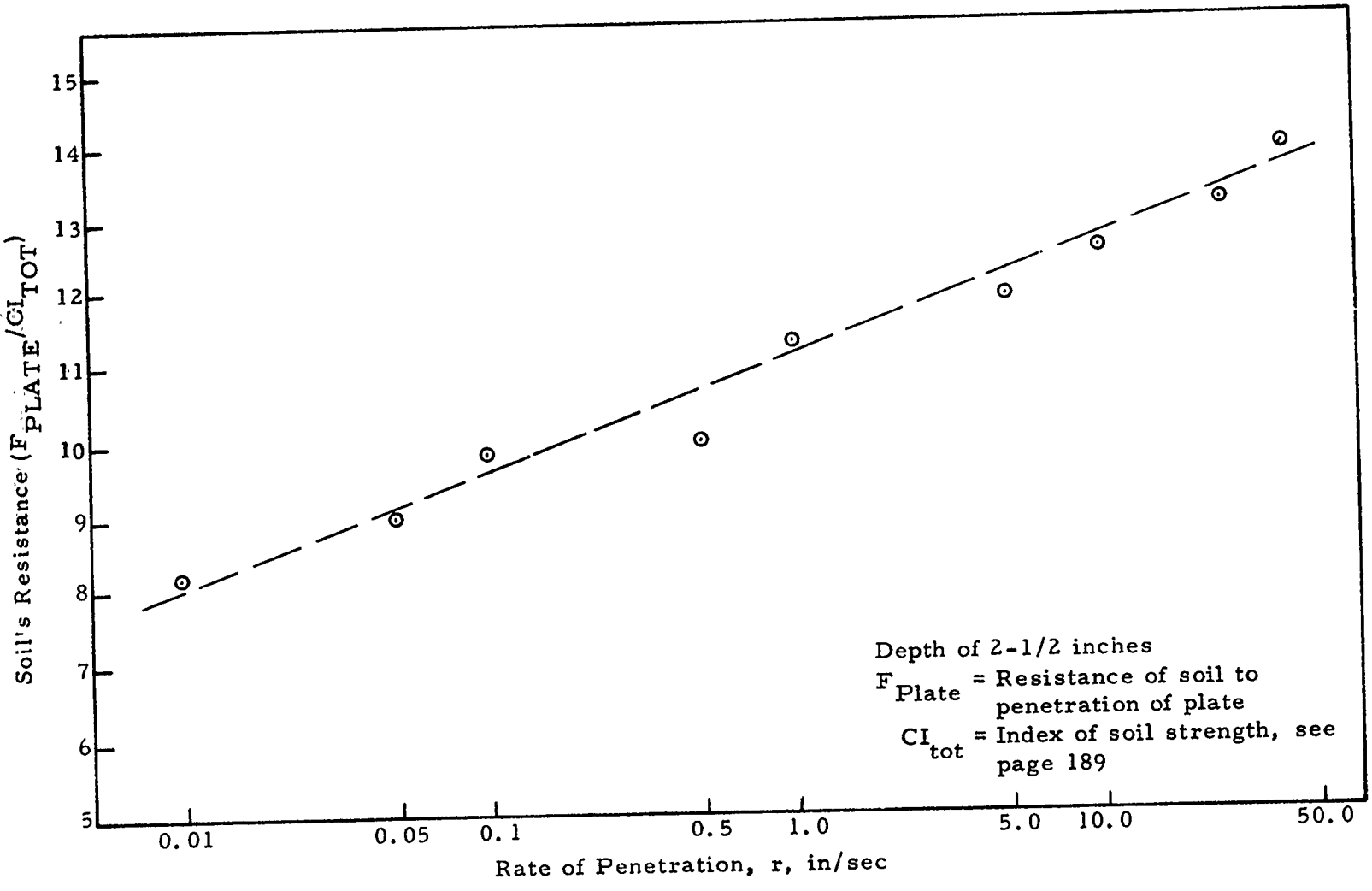

Figure 45. Variance of Soil's Resistance During Test - Clay

$$R_S = 0.68 \log r + 10.87 \quad (29)$$

where

R_S = soil's resistance = $\frac{F_{plate}}{CI_{tot}}$

where F_{plate} = resistance of plate (lbs)

CI_{tot} = Cone Index value (lbs/in^2)

r = rate of penetration (in/sec)

It should be mentioned that this equation was developed for the velocity range of approximately static to 40 inches per second, and is good for only Buckshot Clay for a penetration of a 3-inch diameter plate.

- Sand

The plate test results for the various penetration rates in sand were not as conclusive as those obtained in clay. The major difficulty that arose in the sand tests was that two different modes of failure were observed depending upon the rate of penetration. One mode was observed at rates of 10 inches per second and less, while another mode was observed for the rates of 25 and 40 inches per second. At 10 inches per second and less, the plate test results took the shape as shown in Figure 46. For these rates of loading, the force exerted on the plate increased almost linearly with the penetration. A similar analysis to that performed in clay was made and is shown in Figure 47. Reference to Figure 47 shows that at the slowest rates (Test 1 and 2), the plates experienced a lesser penetration resistance than at the intermediate rates (Tests 3, 4, and 5), and thus the soil's resistance increased over this range with an increase in rate. However, for Tests 6 and 7 (the higher rates) the soil's resistance to plate penetration showed a marked decrease when compared to the intermediate tests. Thus it may be summarized from Figure 47 that for the rate range of 0.01 inches per second to 10.0 inches per second that the sand shows a gradual increase

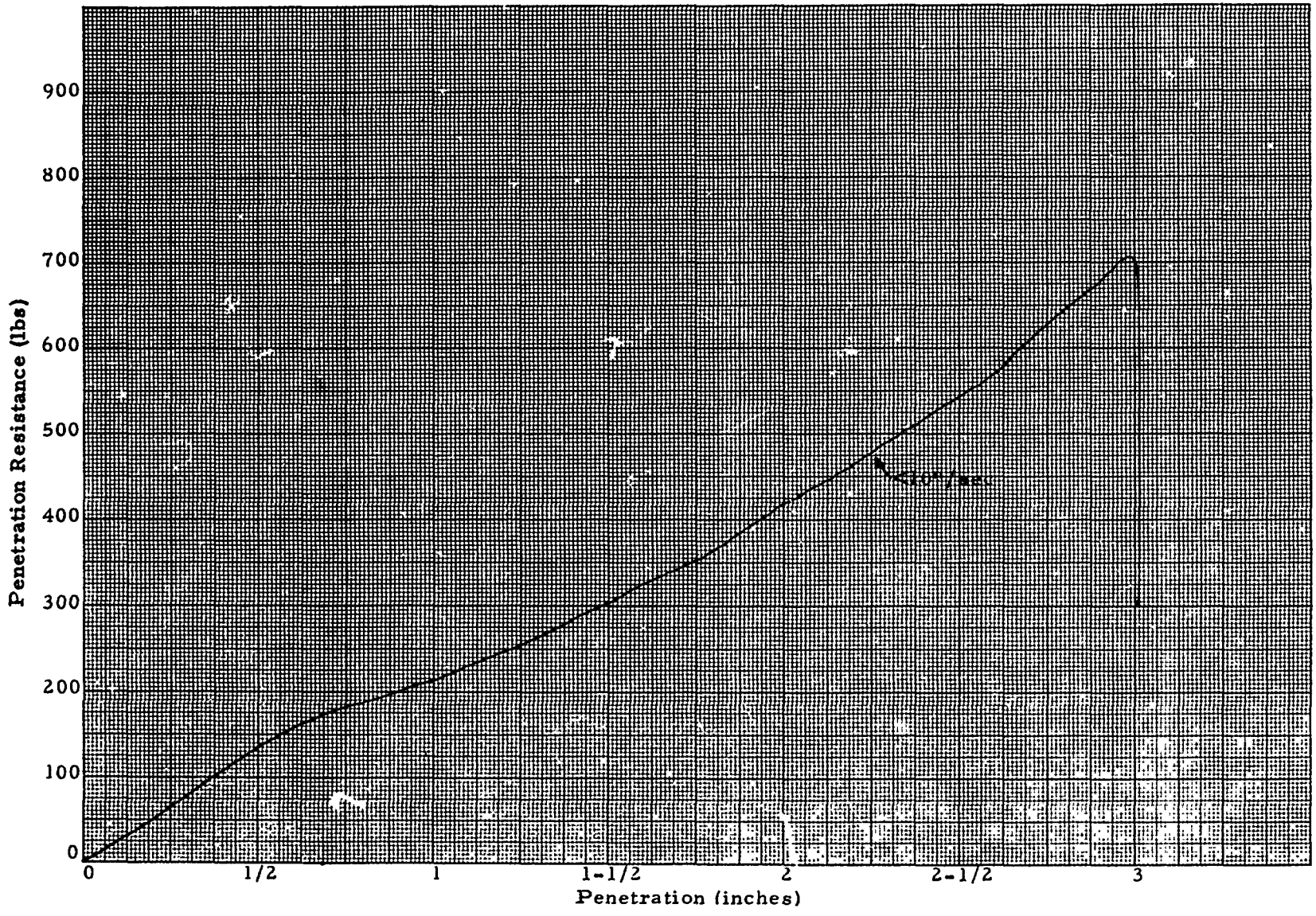

Figure 46. Typical Plate Penetration Test - Sand, <10"/sec

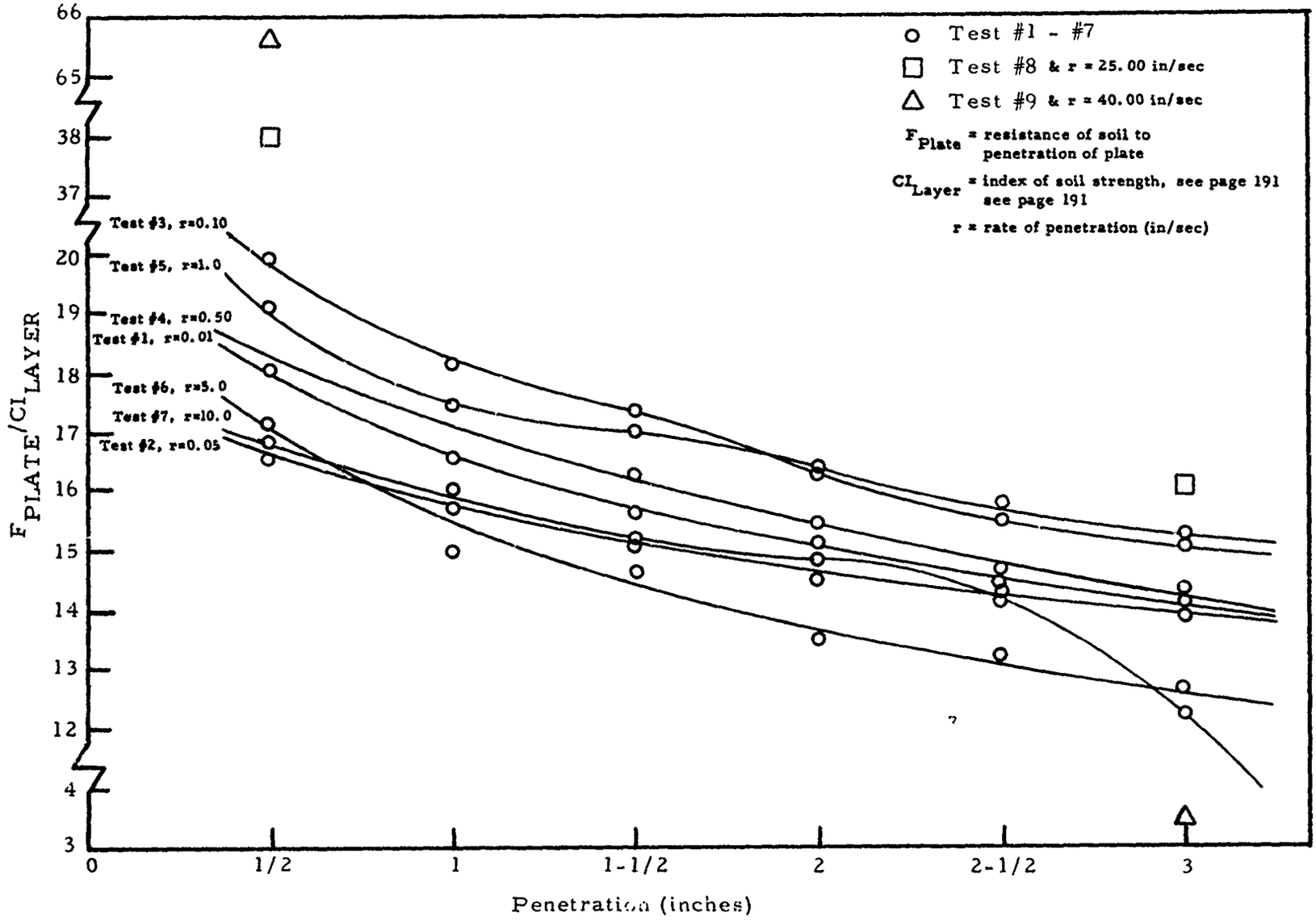

Figure 47. Results of Rate of Loading - Penetration Resistance Tests - Sand

in resistance to penetration with an increase in the rate of penetration, followed by a gradual decrease in penetration resistance for continuing increase in rate of penetration.

The results of Test 8 (rate = 25 in/sec) and Test 9 (rate = 40 in/sec) revealed that a different mode of failure occurred than for the slower rates of penetration. The result of Test 8 is shown in Figure 48. In both Test 8 and 9 an initial peak load value was obtained in the first half-inch of penetration. This was followed by a period of marked decrease in strength. In Test 8 a second peak value was obtained at about 2-1/2 inches of penetration but this second peak was not observed in the three-inch penetration of Test 9. It is not known what caused the change in mode of failure that produced the results of Tests 8 and 9, but it may have been due to the combination of the effects of excess pore air pressure and an impact-produced tension stress wave rebounding off the bottom of the test container. Reference to Figure 48 shows that this type of failure produces a soil's resistance which is considerably different from that obtained from the mode of failure associated with slower rates of penetration. One observation which should be made from Tests 8 and 9 is that the initial peak load found in Test 9 was greater than the initial peak load found in Test 8 (see Figure 47). This agrees with the results found by IITRI[3].

Conclusions

For the clay and sand soil tested in this program, the results of the rate of loading plate penetration tests have shown:

(1) The rate of penetration has considerable effect upon the resistance (or stiffness)of a soil to penetration.

(2) For a clay, the soil's normalized resistance (Resistance/Soil Strength) is directly proportional to the logarithm of rate of penetration. For Buckshot Clay and a 3-inch diameter plate, the soil's resistance can be described by Equation (29).

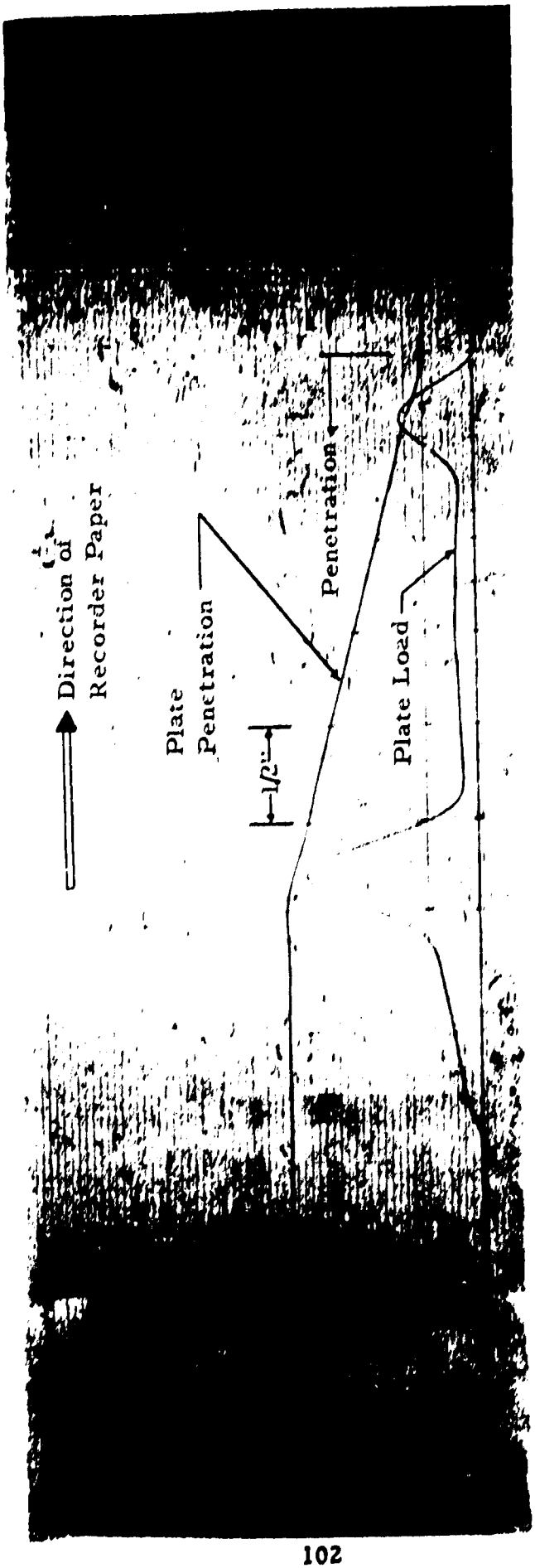

Figure 48. Plate Penetration Test, Test No. 8, Sand at 25.0"/sec

(3) For a sand, the mode of failure appears to be dependent upon the rate of penetration. This mode of failure has a large influence on the soil's resistance.

SECTION V
CONCLUSIONS AND RECOMMENDATIONS

A. CONCLUSIONS

The results of the Phase III - Part II research effort have shown that:

(1) Braking action of tires on soil leads to large increases in the braking drag ratio (R_B/P) and in some instances for the fully braked tire this ratio may approach or exceed one (1.0).

(2) The braking drag ratio continues to increase throughout the negative slip range for braked tires operating on both sand and clay.

(3) The ratio of braked tire sinkage to rolling tire sinkage ranges from 1.5 to 3.0 for clay type soils and 4.0 to 15.0 for sand type soils.

(4) The composite results of previous braking studies, the experimental braking verification tests, and the analytical results to date have led to preliminary braking analysis prediction equations which are suitable for a wide range of tire and soil parameters.

(5) Suitable experimental and/or analytical information is not currently available to permit a detailed analysis of high speed rolling drag effects in soil or to evaluate the effects of multipass operations on aircraft Nth pass drag or runway deterioration.

B. RECOMMENDATION FOR RESEARCH

Future research efforts for landing gear/soil interaction should be directed in the following areas:

(1) High speed (Region III) sinkage and drag performance for rolling and braked tires on soil.

(2) Landing gear loads and sinkage/drag interaction for turning operations in soil.

(3) Multiple pass (operations) effects as related to the prediction of Nth pass drag and runway deterioration, including an investigation of surface roughness and texture effects.

REFERENCES

1. Kraft, David C., Luming, Henry, and Hoppenjans, J. Richard, "Multiwheel Landing Gear-Soils Interaction and Flotation Criteria - Phase III, Part I," AFFDL-TR-71-12, Part I, Air Force Flight Dynamics Laboratory, Wright-Patterson AFB, Ohio, May 1971.

2. Kraft, David C., Luming, Henry, and Hoppenjans, J. Richard, "Aircraft Landing Gear-Soils Interaction and Flotation Criteria, Phase II," AFFDL-TR-69-76, Air Force Flight Dynamics Laboratory, Wright-Patterson AFB, Ohio, November 1969.

3. Crenshaw, B. M. and Butterworth, C. K., "Aircraft Landing Gear Dynamic Loads from Operation on Clay and Sandy Soil," AFFDL-TR-69-51, Air Force Flight Dynamics Laboratory, Wright-Patterson AFB, Ohio, February 1971.

4. Richmond, L. D., et al., "Aircraft Dynamic Loads from Substandard Landing Sites," AFFDL-TR-67-145, Air Force Flight Dynamics Laboratory, Wright-Patterson AFB, Ohio, September 1968.

5. Ladd, D., et al., "Aircraft Ground Flotation Investigation," AFFDL-TR-66-43, Air Force Flight Dynamics Laboratory, Wright-Patterson AFB, Ohio, August 1967.

6. Kraft, David C., "Analytical Landing Gear-Soils Interaction, Phase I," AFFDL-TR-68-88, Air Force Flight Dynamics Laboratory, Wright-Patterson AFB, Ohio, May 1968.

7. Freitag, Dean R., "Wheels on Soft Soils, an Analysis of Existing Data," Technical Report No. 3-670, U.S. Army Engineers Waterways Experiment Station, Vicksburg, Mississippi, January 1965.

8. "Aircraft Tires - Engineering Data," Third Edition, B. F. Goodrich Aerospace and Defense Products, Akron, Ohio.

9. Hay, D. R., "Aircraft Characteristics for Airfield Pavement Design and Evaluation," Technical Report AFWL-TR-69-54, Air Force Weapons Laboratory, Kirtland AFB, New Mexico, October 1969.

10. "Weight and Blast Data Relative to Runway Design," Systems Engineering Group (SEPIE), Research and Technology Division, Wright-Patterson AFB, Ohio, May 1964.

11. Kraft, David C. and Hoppenjans, J. Richard, "Design Procedure for Establishing Aircraft Capability to Operate on Soil Surfaces," AFFDL-TM-71-09-FEM, Air Force Flight Dynamics Laboratory, Wright-Patterson AFB, Ohio, September 1971.

12. Smith, Jerry L., "A Study of the Effects of Braking on Drag Force and Sinkage," unpublished report, Army Corps of Engineers, U.S. Army Engineers Waterways Experiment Station, Vicksburg, Mississippi.

13. Luming, Henry, "Multiwheel Vertical Pulse Load Analytical Sinkage Prediction Technique and Computer Program," UDRI-TR-70-22, University of Dayton, May 1970.

14. "Report on Traffic Tests with Flotation Type Landing Gear on the C-122 Aircraft," Ohio River Division Laboratories, U.S. Army Corps of Engineers, Mariemont, Ohio, 1953.

15. Wismer, R. D., "Performance of Soils Under Tire Loads," TR-3-666, Army Corps of Engineers, U.S. Army Engineers Waterways Experiment Station Vicksburg, Mississippi, February 1966.

16. Nuttal, C. J., "A Dimensionless Consolidation of WES Data on the Performance of Sand Under Tire Loads," AD-626-993, Army Corps of Engineers, U.S. Army Engineers Waterways Experiment Station, Vicksburg, Mississippi, 1965.

17. Hay, D. R., "C-141A Ground Flotaticn Test on Landing Mat and Unsurfaced Runways Civil Engineering Report," AFWL-TR-70-30, Air Force Weapons Laboratory, Kirtland, AFB, New Mexico, 1970.

18. Holm, I. C., "Multipass Behavior of Pneumatic Tires," Journal of Terramechanics, Vol. 6, No. 3, 1969.

19. Gray, D. H., "Evaluation of Aircraft Landing Gear Ground Flotation Characteristics for Operation from Unsurfaced Soil Airfields," ASD-TR-68-34, Wright-Patterson AFB, Ohio, 1968.

20. Luming, Henry, "Multiwheel Landing Gear-Soil Interaction - Phase III, Rolling Multiwheel Analytical Sinkage Prediction Technique and Computer Program," Interim Report, Technical Report UDRI-TR-71-08, University of Dayton Research Institute, Dayton, Ohio, April 1971.

21. Luming, Henry, "Multiwheel Vertical Pulse Load Analytical Sinkage Prediction Technique and Computer Program," Technical Report UDRI-TR-70-22, University of Dayton Research Institute, Dayton, Ohio, May 1970.

22. Luming, Henry, "Lumped-Parameter Approach to Axisymmetric Dynamic Soil Deformations," Proceedings of the Symposium on Applications of Finite Element Methods in Civil Engineering, November 13-14, 1969, Vanderbilt University, Nashville, Tennessee, pp. 642-662.

APPENDIX I

BRAKING VERIFICATION TESTS - SOIL TESTS AND PREPARATION

Classification

Both of the soils selected for the test program have been used extensively by WES in previous mobility studies and the classification properties have been reported previously. For comparison purposes, the grain size distribution and limits properties are given for the buckshot clay in Figure 49, and the grain size distribution for the mortar sand is shown in Figure 50.

California Bearing Ratio

The CBR is a plate bearing test using a three-square inch piston which is penetrated continuously into the soil to a depth of one-half inch while continuously recording the load resistance with depth. Annular surcharge weights are placed around the piston prior to its penetration. The ratio of the load at 0.1 inch penetration to that load supported by a standard well graded crushed gravel multiplied by 100 is defined as the CBR of the soil.

Cone Penetrometer Resistance

The mobility cone penetrometer is a rod device having a 30 degree cone tip and has a cross section base area of 0.5 square inch. The shaft is narrowed above the cone to minimize the friction between the side of the shaft and the hole. The cone penetrometer, which is pushed into the soil at a standard rate, measures the resistance to penetration (Cone Index) in pounds per square inch. The Cone Index is a measure of soil shear strength and its variation with depth. The CI value is usually given as the average resistance over the first 6 inches of depth.

Test Section Consistency

In order to demonstrate the consistency of each test section, Tables XIV and XV were prepared to compare the values of CI for the before and after test soil conditions. In addition to the CI data, the density values and moisture contents are also shown.

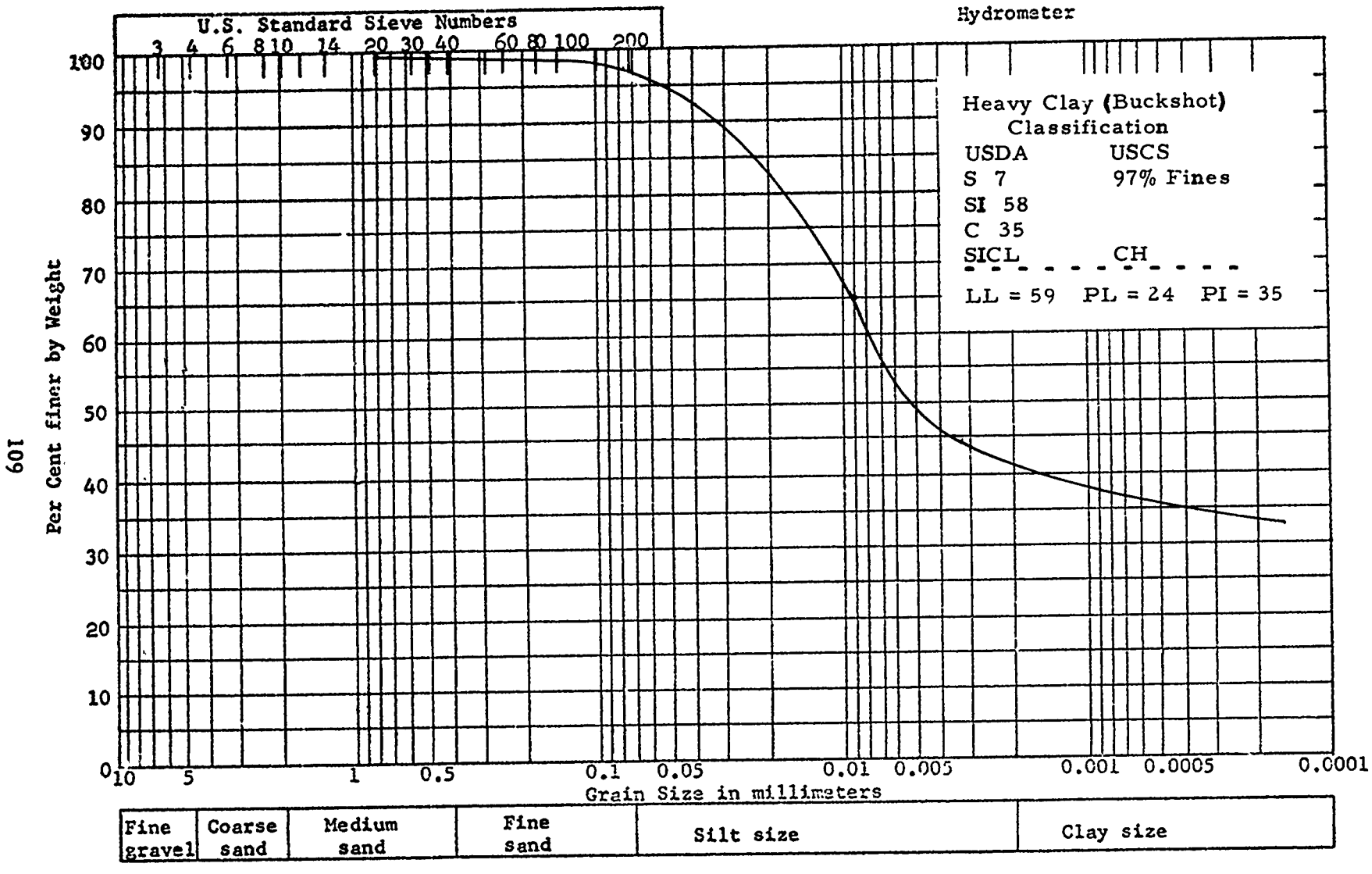

Figure 49. Grain Size Distribution - Buckshot Clay

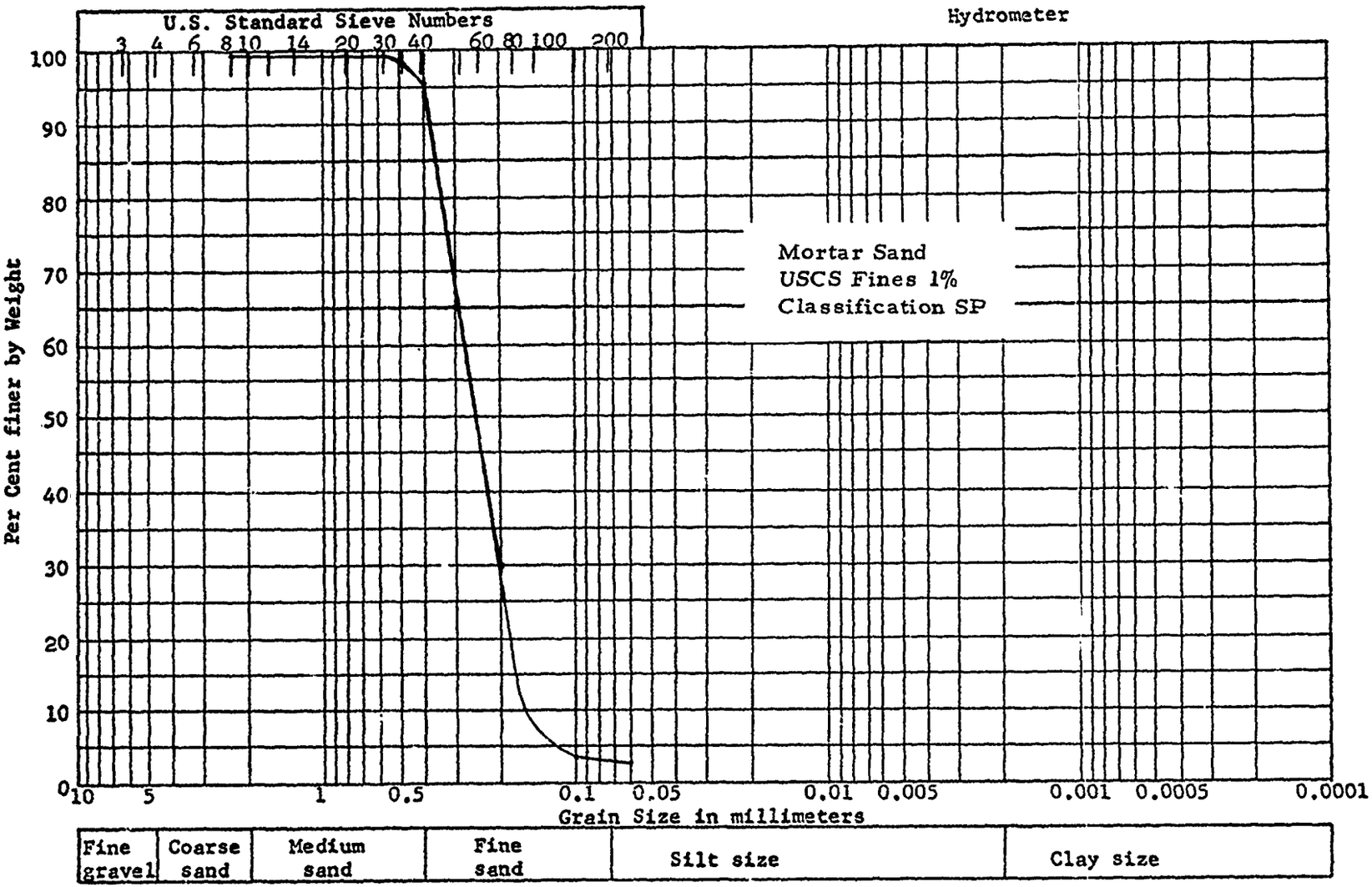

Figure 50. Grain Size Distribution - Mortar Sand

TABLE XIV

SOIL STRENGTH, STRENGTH CONSISTENCY, AND SOIL MOISTURE AND DENSITY DATA - BUCKSHOT CLAY

Test No.	Buckshot Clay					
	Before Test CI Avg	Before Test CI High	Before Test CI Low	Before Test Moisture % W	Before Test Dry Density pcf, γ_d	After Test CI Avg
1	39.9	41.8	37.1			
2	42.4	43.8	40.6	42.5 avg	76.4 avg	42.4
3	42.0	43.0	40.4			40.7
4	41.6	42.8	40.2			39.8
5	41.6	44.3	40.2	42.1 avg	77.6 avg	38.3
6	40.0	41.2	38.7			40.0
7	38.4	39.8	37.5			38.5
8	39.6	43.3	37.5	41.6 avg	78.2 avg	37.6
9	37.1	39.4	35.0			37.8
10	39.5	40.3	37.8			38.3
11	38.8	40.7	36.0			36.2
12	42.2	44.3	40.1			39.6
13	42.0	43.7	40.0	42.1 avg	77.1 avg	39.5
14	36.4	37.8	34.4			37.2
15	38.2	39.0	36.2	41.6 avg	77.6 avg	36.9
16	35.4	36.5	31.9			36.8
17	36.6	37.2	35.4			36.5
18	39.3	40.3	38.2	41.3 avg	77.9 avg	36.9
19	35.8	37.9	33.6			36.1
20	39.2	31.0	36.6			38.7
21	39.4	41.1	37.0	41.8 avg	77.5 avg	37.5
22	36.1	37.8	34.6			35.1
	39.2 avg			41.9 avg	77.5 avg	

TABLE XV

SOIL STRENGTH, STRENGTH CONSISTENCY, AND SOIL MOISTURE AND DENSITY DATA - MORTAR SAND

Test No.	Mortar Sand					
	Before Test CI Avg	Before Test CI High	Before Test CI Low	Before Test Moisture % W	Before Test Dry Density pcf, γ_d	After Test CI Avg
1	37.7	39.9	35.6			20.7
2	44.5	45.4	43.5	.08		22.4
3	43.2			.07		
4	41.0	42.6	39.4	.09	101.0	20.9
5	42.7	46.3	40.5	.13		22.5
6	42.1	43.3	40.4	.08		22.6
7	47.1	49.6	44.2	.13		24.6
8	47.0	48.3	45.5	.08		22.4
9	44.3	45.1	42.1	.11		20.6
10	47.6	48.8	45.8	.09		22.3
11	42.8	44.9	41.6	.08		21.9
12	46.5	50.1	45.1	.09		20.9
13	46.8	50.3	43.8	.10		26.8
14	44.2	45.4	41.7			24.6
15	45.1	47.1	43.9	.11	99.8	26.1
16	45.7	47.8	43.8	.09		24.6
17				.08		
18	39.8	45.7	36.6	.10		24.3
19	48.1	50.9	45.9	.13		23.7
20	42.2	45.4	38.5	.13		19.3
	44.1 avg			.10 avg	100.4 avg	

Soil Preparation

The buckshot clay was proce. sed, placed, and compacted at predetermined moistures and densities corresponding to the desired soil strength. The soil is first passed through a roller crusher and then placed in a pug mill where the soil-water mixing takes place at a selected moisture content. The soil is then placed in the soil carts in 6 inch layers with each layer compacted by pneumatic tired rollers. Previously developed empirical relationships between buckshot clay moisture content and compactive effort permitted the soil to be placed near the design soil conditions.

The mortar sand was prepared in an air dried condition. Different soil strengths were achieved by varying the density of placement of the soil. The sand was placed in uniform layers which were screened and vibrated on the surface as the filling progressed. Empirical relationships between the thickness of layer, vibratory effect, and soil density permitted the sand to be placed near the design soil conditions.

Test Procedures

The test procedures for running a single test in sand are:

(1) Loosen sand section by plowing
(2) Check weakened state by Cone Index tests
(3) Vibrate sand to desired soil strength
(4) Check strength by Cone Index tests
(5) Take final soil strength and surface elevation profile
(6) Calibration checks between recording station and computer
(7) Make a test run without load on test tires (in-air run)
(8) Load tire and check inflation pressure and deflection
(9) Run test
(10) Take post test soil strength and rut depth profile.

The test procedure for running a test in clay differs from the sand only in soil preparation techniques. The clay test bed has to be prepared

at least ten days in advance of a test so that the water content of the clay will stabilize as described above. The only preparation needed to run a test after the soil bed has been constructed involves smoothing the soil surface and measuring the soil strength and surface profiles. Steps (7) through (10) are then completed as in sand. Preparation for succeeding tests in the same clay soil bed can involve re-rolling and smoothing the soil surface. In both the sand and clay test procedure, a test is not run unless the desired soil strength and uniformity is attained during the preparation stages.

APPENDIX II

BRAKING VERIFICATION TESTS
CLAY AND SAND TEST DATA

TABLE XVI

BRAKED TEST RESULTS

Test No. 2 Tire Size 8:50-10

Soil Type Clay Tire Deflection 35 (d)

Soil Strength 42.4 (CI_{avg}) Carriage Speed 10 ft/sec (V_a)

Station	Slip % S	Load, lbs P	Drag, lbs R_B	Sinkage, in. Z	Torque, ft-lbs T'
23.6	10	1484	325	1.05	123
25.3	20	1483	500	1.25	240
25.9	30	1483	600	1.45	290
26.2	40	1485	650	1.60	315
26.4	50	1484	700	1.68	332
26.6	60	1480	750	1.75	353
26.8	70*	1470	790	1.85	375
27.1	80*	1460	850	2.00	380
27.4	90*	1460	890	2.00	368
29.5	100*	1490	840	1.95	289

* Carriage was slowing down at this point and velocity was not maintained.

TABLE XVII

BRAKED TEST RESULTS

Test No. 3 — Tire Size 8:50-10

Soil Type Clay — Tire Deflection 42 (d)

Soil Strength 42.0 (CI_{avg}) — Carriage Speed 10 ft/sec (V_d)

Station	Slip % S	Load, lbs P	Drag, lbs R_B	Sinkage, in. Z	Torque, ft-lbs T'
25.0	5	1690	280	1.17	58
28.0	10	1687	390	1.20	138
31.0	15	1685	500	1.29	219
	40				
	50				
	60				
	70				
	80				
	90				
	100				

TABLE XVIII

BRAKED TEST RESULTS

Test No. 4 Tire Size 8:50-10

Soil Type Clay Tire Deflection 42 (d)

Soil Strength 41.6 (CI_{avg}) Carriage Speed 10 ft/sec (V_a)

Station	Slip % S	Load, lbs P	Drag, lbs R_B	Sinkage, in. Z	Torque, ft-lbs T'
19.7	10	1705	385	.85	195
22.1	20	1705	570	1.05	280
24.0	30	1705	685	1.25	338
25.4	40	1705	735	1.50	370
26.2	50*	1705	780	1.70	388
26.7*	60	1705	840	1.75	380
26.9*	70	1705	880	1.80	370
	80				
	90				
	100				

* Carriage was slowing down at this point and velocity was not maintained.

TABLE XIX

BRAKED TEST RESULTS

Test No. 5 Tire Size 8:50-10

Soil Type Clay Tire Deflection 42 (d)

Soil Strength 41.6 (CI_{avg}) Carriage Speed 10 ft/sec (V_a)

Station	Slip % S	Load, lbs P	Drag, lbs R_B	Sinkage, in. Z	Torque, ft-lbs T'
	10				
22.7	20	1680	530	1.00	278
25.2	30	1680	705	1.25	345
26.7	40	1680	775	1.45	390
27.6	50	1680	810	1.65	405
28.0	60	1680	830	1.70	405
28.2	70	1681	840	1.85	405
28.6	80	1684	870	1.95	400
29.1	90	1684	910	2.05	388
31.0	100	1685	850	1.58	300

TABLE XX

BRAKED TEST RESULTS

Test No. 6 Tire Size 8:50-10

Soil Type Clay Tire Deflection 35(d)

Soil Strength 40.0 (CI_{avg}) Carriage Speed 10 ft/sec (V_a)

Station	Slip % S	Load, lbs P	Drag, lbs R_B	Sinkage, in. Z	Torque, ft-lbs T'
19.7	10	1490	380	1.05	205
23.0	20	1489	605	1.45	295
25.5	30	1485	680	1.75	335
27.0	40	1485	765	1.87	355
27.9	50	1485	840	1.95	370
28.5	60	1485	840	2.10	380
28.8	70	1470	880	2.20	380
29.0	80	1450	950	2.30	378
29.3	90	1450	1020	2.50	360
29.9	95	1460	1090	2.68	317
31.8	97	1490	930	1.90	290

TABLE XXI

BRAKED TEST RESULTS

Test No. 7 Tire Size 8:50-10

Soil Type Clay Tire Deflection 35 (d)

Soil Strength 38.4 (CI_{avg}) Carriage Speed 20 ft/sec (V_a)

Station	Slip % S	Load, lbs P	Drag, lbs R_B	Sinkage, in. Z	Torque, ft-lbs T'
21.6	10	1488	420	1.30	168
25.0	20	1490	600	1.50	268
27.2	30	1490	750	1.55	345
28.4	40	1480	840	1.85	370
29.2	50	1478	860	1.93	370
30.1	60*	1480	920	1.98	353
30.7	70*	1460	930	2.05	273
31.2	80*	1460	950	2.13	284
31.4	90*	1465	960	2.15	263
	100				

* Carriage was slowing down at this point and velocity was not maintained.

TABLE XXII

BRAKED TEST RESULTS

Test No. 8 Tire Size 8:50-10

Soil Type Clay Tire Deflection 42 (d)

Soil Strength 39.6 (CI_{avg}) Carriage Speed 20 ft/sec (V_a)

Station	Slip % S	Load, lbs P	Drag, lbs R_B	Sinkage, in. Z	Torque, ft-lbs T'
21.4	10	1690	435	1.00	160
25.8	20	1690	670	1.50	290
28.7	30	1650	850	1.70	380
29.5	40	1647	900	1.95	400
29.9	50	1670	970	2.20	412
30.2	60*	1680	1045	2.20	422
30.6	70*	1690	1060	2.15	430
30.9	80*	1685	1060	2.10	425
31.2	90*	1690	1030	2.05	410
	100				

* Carriage was slowing down at this point and velocity was not maintained.

TABLE XXIII

BRAKED TEST RESULTS

Test No. 9 Tire Size 8:50-10

Soil Type Clay Tire Deflection 42 (d)

Soil Strength 37 (CI_{avg}) Carriage Speed 5 ft/sec (V_a)

Station	Slip % S	Load, lbs P	Drag, lbs R_B	Sinkage, in. Z	Torque, ft-lbs T'
23.5	10	1678	440	1.45	140
27.7	20	1675	650	1.80	245
29.5	30	1673	825	2.08	275
30.4	40	1671	965	2.11	286
	50				
	60				
	70				
	80				
	90				
	100				

TABLE XXIV

BRAKED TEST RESULTS

Test No. 10 Tire Size 8:50-10

Soil Type Clay Tire Deflection 35 (d)

Soil Strength 39.6 (CI_{avg}) Carriage Speed 5 ft/sec (V_a)

Station	Slip % S	Load, lbs P	Drag, lbs R_B	Sinkage, in. Z	Torque, ft-lbs T'
	10				
19.5	20	1500	550	1.30	310
21.6	30	1497	700	1.55	327
23.1	40	1495	760	1.80	346
23.9	50	1493	840	2.05	350
24.4	60	1490	950	2.20	369
24.6	70	1490	1000	2.25	374
24.8	80	1490	1050	2.30	380
25.5	90	1490	1100	2.55	366
30.0	100	1490	1000	2.40	255

TABLE XXV

BRAKED TEST RESULTS

Test No. 11 Tire Size 8:50-10

Soil Type Clay Tire Deflection 35 (d)

Soil Strength 38.8 (CI_{avg}) Carriage Speed 5 ft/sec (V_a)

Station	Slip % S	Load, lbs P	Drag, lbs R_B	Sinkage, in. Z	Torque, ft-lbs T'
	10				
19.8	20	1478	580	1.40	295
21.7	30	1478	650	1.65	321
22.9	40	1478	740	1.80	330
23.5	50	1478	820	1.95	333
24.0	60	1478	880	2.05	335
24.6	70	1478	950	2.20	335
25.3	80	1475	1045	2.35	350
26.2	90	1475	1065	2.55	340
	100				

TABLE XXVI

BRAKED TEST RESULTS

Test No. 12 Tire Size 7:00-6

Soil Type Clay Tire Deflection 42 (d)

Soil Strength 42.2 (CI_{avg}) Carriage Speed 5 ft/sec (V_a)

Station	Slip % S	Load, lbs P	Drag, lbs R_B	Sinkage, in. Z	Torque, ft-lbs T'
22.8	10	1078	280	1.30	88
26.7	20	1076	410	1.25	148
28.6	30	1076	500	1.50	172
29.4	40	1076	560	1.75	173
29.6	50	1075	600	1.80	174
29.8	60	1075	640	1.85	175
30.1	70	1075	690	1.90	175
30.4	80	1075	740	1.95	175
30.8	90*	1075	757	2.05	170
	100				

* Carriage was slowing down at this point and velocity was not maintained.

TABLE XXVII

BRAKED TEST RESULTS

Test No. 13 Tire Size 7:00-6

Soil Type Clay Tire Deflection 35 (d)

Soil Strength 42.0 (CI_{avg}) Carriage Speed 5 ft/sec (V_a)

Station	Slip % S	Load, lbs P	Drag, lbs R_B	Sinkage, in. Z	Torque, ft-lbs T'
22.7	10	885	235	1.05	83
26.4	20	890	350	1.30	135
28.3	30	890	420	1.50	168
29.2	40	890	465	1.75	183
29.4	50	890	500	1.77	185
29.6	60	890	535	1.77	185
29.7	70	890	550	1.80	185
29.9	80	890	560	1.80	183
30.3	90	890	580	1.82	170
	100				

TABLE XXVIII

BRAKED TEST RESULTS

Test No. 14 Tire Size 7:00-6

Soil Type Clay Tire Deflection 35 (d)

Soil Strength 36.5 (CI_{avg}) Carriage Speed 10 ft/sec (V_a)

Station	Slip % S	Load, lbs P	Drag, lbs R_B	Sinkage, in. Z	Torque, ft-lbs T'
24.0	10	890	215	1.25	50
28.6	20	897	365	1.40	110
30.6	30	900	445	1.55	135
31.5	40	900	500	1.45	145
32.3	50	900	540	1.35	155
	60				
	70				
	80				
	90				
	100				

TABLE XXIX

BRAKED TEST RESULTS

Test No. 15 Tire Size 7:00-6

Soil Type Clay Tire Deflection 42 (d)

Soil Strength 38.2 (CI_{avg}) Carriage Speed 10 ft/sec (V_a)

Station	Slip % S	Load, lbs P	Drag, lbs R_B	Sinkage, in. Z	Torque, ft-lbs T'
26.0	10	1080	340	1.15	105
28.7	20	1077	460	1.40	146
29.6	30	1075	575	1.55	160
30.1	40	1075	610	1.65	168
30.7	50	1075	630	1.75	172
31.2	60	1070	650	1.90	180
31.6	70	1055	685	2.10	190
31.8	80	1045	730	2.20	180
32.0	90	1050	750	2.25	170
	100				

TABLE XXX

BRAKED TEST RESULTS

Test No. 16 Tire Size 7:00-6

Soil Type Clay Tire Deflection 35 (d)

Soil Strength 35.6 (CI_{avg}) Carriage Speed 20 ft/sec (V_a)

Station	Slip % S	Load, lbs P	Drag, lbs R_B	Sinkage, in. Z	Torque, ft-lbs T'
27.0	10	890	355	1.35	103
29.5	20	890	480	1.50	140
30.4	30	890	550	1.65	155
31.3	40	890	610	1.80	168
32.2	50	890	645	1.90	182
	60				
	70				
	80				
	90				
	100				

TABLE XXXI

BRAKED TEST RESULTS

Test No. 17 Tire Size 7:00-6

Soil Type Clay Tire Deflection 35 (d)

Soil Strength 36.6 (CI_{avg}) Carriage Speed 20 ft/sec (V_a)

Station	Slip % S	Load, lbs P	Drag, lbs R_B	Sinkage, in. Z	Torque, ft-lbs T'
24.8	10	885	300	1.33	85
27.9	20	885	470	1.40	162
29.3	30	880	580	1.60	193
29.9	40	880	615	1.75	200
30.3	50	880	645	1.80	215
30.4	60	875	660	1.85	220
30.6	70	870	670	1.90	220
30.8	80	870	690	1.95	210
31.4	90	880	710	2.00	187
	100				

TABLE XXXII

BRAKED TEST RESULTS

Test No. 18 Tire Size 7:00-6

Soil Type Clay Tire Deflection 42 (d)

Soil Strength 39.2 (CI_{avg}) Carriage Speed 20 ft/sec (V_a)

Station	Slip % S	Load, lbs P	Drag, lbs R_B	Sinkage, in. Z	Torque, ft-lbs T'
21.9	10	1100	390	1.23	123
23.3	20	1090	520	1.50	178
23.8	30	1080	650	1.65	190
24.1	40	1075	710	1.75	200
24.3	50	1070	745	1.85	203
24.5	60	1060	760	1.90	210
24.8	70	1057	800	1.95	215
25.1	80	1065	820	2.00	218
25.6	90	1080	850	2.05	210
28.4	100	1090	770	1.68	200
30.0	100	1078	835	2.15	170

TABLE XXXIII

BRAKED TEST RESULTS

Test No. 19 Tire Size 7:00-6

Soil Type Clay Tire Deflection 35(d)

Soil Strength 35.8 (CI_{avg}) Carriage Speed 10 ft/sec (V_a)

Station	Slip % S	Load, lbs P	Drag, lbs R_B	Sinkage, in. Z	Torque, ft-lbs T'
23.2	10	890	300	1.35	60
26.8	20	893	435	1.65	115
28.6	30	895	500	1.65	150
29.4	40	870	550	1.75	158
29.7	50	860	600	1.90	159
29.9	60	854	650	1.95	162
30.1	70	854	700	2.10	167
30.4	80	857	750	2.25	170
30.9	90	860	770	2.45	165
31.6	100	890	755	2.25	125

TABLE XXXIV

BRAKED TEST RESULTS

Test No. 20 Tire Size 8:50-10

Soil Type Clay Tire Deflection 35 (d)

Soil Strength 39.2 (CI_{avg}) Carriage Speed 20 ft/sec (V_a)

Station	Slip % S	Load, lbs P	Drag, lbs R_B	Sinkage, in. Z	Torque, ft-lbs T'
20.7	10	1475	410	1.30	138
23.2	20	1475	620	1.70	220
25.1	30	1475	860	1.85	390
26.3	40	1475	930	1.95	418
27.2	50	1460	960	2.00	455
27.7	60	1430	1050	2.25	480
27.8	70	1430	1060	2.35	475
27.9	80	1430	1130	2.60	455
28.4	90	1438	1170	2.65	405
30.3	100	1480	1150	2.40	337

TABLE XXXV

BRAKED TEST RESULTS

Test No. 21 Tire Size 8:50-10

Soil Type Clay Tire Deflection 42 (d)

Soil Strength 39.4 (CI_{avg}) Carriage Speed 20 ft/sec (V_d)

Station	Slip % S	Load, lbs P	Drag, lbs R_B	Sinkage, in. Z	Torque, ft-lbs T'
21.3	10	1680	540	1.20	250
23.0	20	1689	750	1.35	380
23.8	30	1680	895	1.50	450
24.3	40	1670	1050	1.65	505
24.7	50	1660	1150	1.85	530
25.0	60	1650	1200	2.00	525
25.2	70	1645	1240	2.30	520
25.5	80	1650	1260	2.55	505
25.8	90*	1665	1290	2.68	480
30.0	100*	1660	1280	2.50	425

* Carriage was slowing down at this point and velocity was not maintained.

TABLE XXXVI

BRAKED TEST RESULTS

Test No. 22 Tire Size 8:50-10

Soil Type Clay Tire Deflection 42 (d)

Soil Strength 36.1 (CI_{avg}) Carriage Speed 5 ft/sec (V_a)

Station	Slip % S	Load, lbs P	Drag, lbs R_B	Sinkage, in. Z	Torque, ft-lbs T'
19.9	10	1675	420	1.30	175
20.7	20	1680	600	1.65	220
21.5	30	1685	750	1.85	260
22.5	40	1675	920	2.30	290
22.7	50	1660	975	2.60	305
22.9	60	1657	1070	2.95	320
23.1	70	1653	1170	3.30	330
23.4	80	1650	1300	3.55	333
23.8	90	1625	1325	3.75	320
26.0	100	1610	1350	3.85	233

TABLE XXXVII

BRAKED TEST RESULTS

Test No. 1 Tire Size 8:50-10

Soil Type Sand Tire Deflection 35 (d)

Soil Strength 37.7 (CI_{avg}) Carriage Speed 5 ft/sec (V_a)

Station	Slip % S	Load, lbs P	Drag, lbs R_B	Sinkage, in. Z	Torque, ft-lbs T'
19.4	10	615	137	.40	15
21.2	20	605	205	.55	44
22.6	30	600	250	.75	65
23.6	40	595	293	1.00	80
24.9	50	594	345	1.57	97
26.7	60	588	405	2.50	122
28.2	70	583	460	3.45	140
30.4	80	580	515	4.25	165
	90				
	100				

TABLE XXXVIII

BRAKED TEST RESULTS

Test No. 2 Tire Size 8:50-10

Soil Type Sand Tire Deflection 42 (d)

Soil Strength 44.5 (CI_{avg}) Carriage Speed 5 ft/sec (V_a)

Station	Slip % S	Load, lbs P	Drag, lbs R_B	Sinkage, in. Z	Torque, ft-lbs T'
19.2	10	710	175	.40	16
20.9	20	707	235	.50	42
22.5	30	705	290	.70	66
24.5	40	700	355	1.15	95
26.5	50	695	420	1.75	126
28.0	60	685	475	2.55	150
29.1	70	682	510	3.25	166
30.6	80	682	560	3.90	190
32.3	90	675	620	4.65	212
	100				

TABLE XXXIX

BRAKED TEST RESULTS

Test No. 3 Tire Size 8:50-10

Soil Type Sand Tire Deflection 35 (d)

Soil Strength 43.2 (CI_{avg}) Carriage Speed 5 ft/sec (V_a)

Station	Slip % S	Load, lbs P	Drag, lbs R_B	Sinkage, in. Z	Torque, ft-lbs T'
21.8	10	988	235	.70	60
24.1	20	980	360	1.10	105
25.4	30	975	460	1.45	130
26.4	40	970	550	1.85	150
27.4	50	970	630	2.60	167
28.8	60	965	720	3.55	190
30.8	70	950	810	4.60	222
	80				
	90				
	100				

TABLE XL

BRAKED TEST RESULTS

Test No. 4 Tire Size 8:50-10

Soil Type Sand Tire Deflection 35 (d)

Soil Strength 41.0 (CI_{avg}) Carriage Speed 5 ft/sec (V_a)

Station	Slip % S	Load, lbs P	Drag, lbs R_B	Sinkage, in. Z	Torque, ft-lbs T'
20.8	10	1000	255	.70	78
22.9	20	1000	380	1.10	127
24.1	30	990	470	1.50	155
24.8	40	980	540	1.90	170
25.6	50	975	620	2.65	186
26.4	60	970	700	3.45	203
28.0	70	950	800	4.50	232
30.7	80	940	850	5.75	270
	90				
	100				

TABLE XLI

BRAKED TEST RESULTS

Test No. 5 Tire Size 8:50-10

Soil Type Sand Tire Deflection 35 (d)

Soil Strength 42.7 (CI_{avg}) Carriage Speed 10 ft/sec (V_a)

Station	Slip % S	Load, lbs P	Drag, lbs R_B	Sinkage, in. Z	Torque, ft-lbs T'
20.7	10	1010	230	.45	65
23.3	20	1000	370	.90	145
24.1	30	990	460	1.20	169
24.8	40	980	535	1.45	190
25.4	50	970	630	1.75	205
26.0	60	970	720	2.20	222
26.8	70	960	810	3.00	244
27.9	80	955	900	4.30	272
29.6	90	950	970	5.00	310
31.6	100	870	1030	5.50	360

TABLE XLII

BRAKED TEST RESULTS

Test No. 6 Tire Size 8:50-10

Soil Type Sand Tire Deflection 42 (d)

Soil Strength 42.1 (CI_{avg}) Carriage Speed 10 ft/sec (V_a)

Station	Slip % S	Load, lbs P	Drag, lbs R_B	Sinkage, in. Z	Torque, ft-lbs T'
19.7	10	700	180	.30	10
21.0	20	697	250	.50	45
22.1	30	690	310	.70	75
23.3	40	690	380	1.00	90
24.6	50	685	450	1.50	140
25.5	60	685	500	1.95	160
26.5	70	685	550	2.50	182
27.6	80	670	595	3.00	205
29.1	90	665	650	3.60	230
	100				

TABLE XLIII

BRAKED TEST RESULTS

Test No. 7 Tire Size 8:50-10

Soil Type Sand Tire Deflection 35 (d)

Soil Strength 47.1 (CI_{avg}) Carriage Speed 10 ft/sec (V_a)

Station	Slip % S	Load, lbs P	Drag, lbs R_B	Sinkage, in. Z	Torque, ft-lbs T'
22.1	10	605	180	.22	75
23.5	20	603	230	.35	100
24.5	30	600	275	.50	117
25.3	40	598	325	.70	135
26.0	50	595	370	.95	150
26.6	60	595	405	1.30	162
27.3	70	593	440	1.62	175
28.4	80	587	490	2.15	194
30.3	90	580	550	2.85	217
33.0	100	563	535	3.05	232

TABLE XLIV

BRAKED TEST RESULTS

Test No. 8 Tire Size 8:50-10

Soil Type Sand Tire Deflection 35 (d)

Soil Strength 47.0 (CI_{avg}) Carriage Speed 20 ft/sec (V_a)

Station	Slip % S	Load, lbs P	Drag, lbs R_B	Sinkage, in. Z	Torque, ft-lbs T'
22.0	10	590	190	.20	75
23.5	20	600	270	.30	120
24.5	30	590	335	.45	155
25.2	40	583	380	.55	177
25.8	50	588	420	.65	195
26.3	60	605	460	.75	210
26.9	70	580	493	.85	225
27.7	80	565	525	1.05	243
28.8	90	575	555	1.50	265
31.4	100	590	530	1.35	300

TABLE XLV

BRAKED TEST RESULTS

Test No. 9 — Tire Size 8:50-10

Soil Type Sand — Tire Deflection 42 (d)

Soil Strength 44.3 (CI_{avg}) — Carriage Speed 20 ft/sec (V_a)

Station	Slip % S	Load, lbs P	Drag, lbs R_B	Sinkage, in. Z	Torque, ft-lbs T'
	10				
20.8	20	685	220	.20	54
22.5	30	700	320	.53	98
24.2	40	700	430	.82	150
25.5	50	685	470	.75	198
26.3	60	690	510	.95	222
26.9	70	660	545	1.20	241
27.5	80	670	640	1.50	260
28.7	90	700	685	1.85	286
30.7	100	690	680	1.60	340

TABLE XLVI

BRAKED TEST RESULTS

Test No. 10 — Tire Size 8:50-10

Soil Type Sand — Tire Deflection 35 (d)

Soil Strength 47.6 (CI_{avg}) — Carriage Speed 20 ft/sec (V_a)

Station	Slip % S	Load, lbs P	Drag, lbs R_B	Sinkage, in. Z	Torque, ft-lbs T'
22.5	10	1000	320	.60	157
24.0	20	995	460	.85	225
25.4	30	990	570	1.15	285
25.7	40	980	650	1.40	296
26.2	50	970	720	1.60	315
26.6	60	965	760	1.85	330
27.1	70	960	820	2.20	345
27.9	80	960	990	2.70	367
29.1	90	990	1035	3.20	394
	100				

TABLE XLVII

BRAKED TEST RESULTS

Test No. 11 Tire Size 7:00-6

Soil Type Sand Tire Deflection 35 (d)

Soil Strength 42.8 (CI_{avg}) Carriage Speed 20 ft/sec (V_d)

Station	Slip % S	Load, lbs P	Drag, lbs R_B	Sinkage, in. Z	Torque, ft-lbs T'
22.9	10	390	105	.25	40
24.9	20	385	185	.35	64
25.8	30	380	220	.50	75
26.6	40	375	235	.75	90
27.1	50	365	250	.95	102
27.4	60	360	265	1.10	110
27.6	70	355	275	1.15	112
27.8	80	350	290	1.25	116
28.3	90	345	355	1.40	122
31.3	100	383	395	1.85	135

TABLE XLVIII

BRAKED TEST RESULTS

Test No. 12 Tire Size 7:00-6

Soil Type Sand Tire Deflection 42 (d)

Soil Strength 46.5 (CI_{avg}) Carriage Speed 20 ft/sec (V_a)

Station	Slip % S	Load, lbs P	Drag, lbs R_B	Sinkage, in. Z	Torque, ft-lbs T'
22.4	10	450	130	.20	30
24.5	20	445	220	.35	60
25.5	30	450	235	.47	75
26.1	40	445	260	.60	87
26.6	50	435	290	.75	95
26.9	60	420	320	.82	102
27.2	70	420	[illegible]0	.95	106
27.7	80	430	400	1.15	114
28.6	90	440	455	1.55	125
	100				

TABLE XLIX

BRAKED TEST RESULTS

Test No. 13 Tire Size 7:00-6

Soil Type Sand Tire Deflection 42 (d)

Soil Strength 46.8 (CI_{avg}) Carriage Speed 10 ft/sec (V_a)

Station	Slip % S	Load, lbs P	Drag, lbs R_B	Sinkage, in. Z	Torque, ft-lbs T'
22.9	10	457	145	.25	37
24.1	20	452	190	.50	50
24.6	30	445	225	.75	55
24.9	40	441	250	1.00	57
25.4	50	440	275	1.30	63
26.0	60	435	315	1.60	70
26.7	70	435	358	1.95	76
27.6	80	433	400	2.40	85
29.0	90	432	440	3.00	100
	100				

TABLE L

BRAKED TEST RESULTS

Test No. 14 Tire Size 7:00-6

Soil Type Sand Tire Deflection 35 (d)

Soil Strength 44.2 (CI_{avg}) Carriage Speed 10 ft/sec (V_a)

Station	Slip % S	Load, lbs P	Drag, lbs R_B	Sinkage, in. Z	Torque, ft-lbs T'
21.9	10	400	95	.40	30
23.6	20	403	145	.85	50
24.3	30	400	175	1.10	57
24.7	40	390	210	1.30	63
25.0	50	385	235	1.45	65
25.4	60	380	270	1.60	70
25.7	70	370	295	1.80	73
26.6	80	383	350	2.40	80
27.6	90	377	377	2.80	90
32.0	100	370	410	3.25	107

TABLE LI

BRAKED TEST RESULTS

Test No. 15 Tire Size 7:00-6

Soil Type Sand Tire Deflection 35 (d)

Soil Strength 45.1 (CI_{avg}) Carriage Speed 5 ft/sec (V_a)

Station	Slip % S	Load, lbs P	Drag, lbs R_B	Sinkage, in. Z	Torque, ft-lbs T'
	10				
20.4	20	400	145	.50	36
21.2	30	398	175	.75	42
21.7	40	385	200	1.00	46
22.1	50	375	225	1.20	50
22.5	60	375	248	1.55	53
23.5	70	380	290	2.45	60
24.8	80	375	335	3.70	70
26.5	90	370	370	4.40	82
31.8	100	385	430	4.68	124

TABLE LII

BRAKED TEST RESULTS

Test No. 16 Tire Size 7:00-6

Soil Type Sand Tire Deflection 42 (d)

Soil Strength 45.7 (CI_{avg}) Carriage Speed 5 ft/sec (V_a)

Station	Slip % S	Load, lbs P	Drag, lbs R_B	Sinkage, in. Z	Torque, ft-lbs T'
19.5	10	460	109	.35	17
20.6	20	450	150	.45	27
21.3	30	445	180	.65	35
22.0	40	440	213	.90	40
22.7	50	440	245	1.30	46
23.5	60	435	290	2.00	54
24.6	70	430	340	3.05	62
26.7	80	428	395	3.95	75
30.0	90	428	460	4.65	96
33.0	100	430	465	4.40	106

TABLE LIII

BRAKED TEST RESULTS

Test No. 18 Tire Size 8:50-10

Soil Type Sand Tire Deflection 42 (d)

Soil Strength 39.8 (CI_{avg}) Carriage Speed 10 ft/sec (V_a)

Station	Slip % S	Load, lbs P	Drag, lbs R_B	Sinkage, in. Z	Torque, ft-lbs T'
	10				
20.2	20	690	240	.40	35
22.0	30	687	300	.65	71
24.1	40	685	375	1.05	112
25.7	50	685	460	1.65	144
26.6	60	683	520	2.05	160
27.6	70	682	570	2.67	180
28.9	80	675	610	3.15	205
30.5	90	655	615	3.31	235
33.0	100	660	735	4.75	253

TABLE LIV

BRAKED TEST RESULTS

Test No. 19 Tire Size 8:50-10

Soil Type Sand Tire Deflection 42 (d)

Soil Strength 48.1 (CI_{avg}) Carriage Speed 20 ft/sec (V_a)

Station	Slip % S	Load, lbs P	Drag, lbs R_B	Sinkage, in. Z	Torque, ft-lbs T'
19.5	10	690	165	.15	17
22.9	20	695	300	.30	85
24.8	30	700	360	.50	128
26.5	40	700	420	.75	170
28.6	50	675	540	1.30	230
29.3	60	660	580	1.60	255
29.6	70	665	600	1.65	264
30.6	80	690	690	1.75	283
31.7	90	690	685	1.70	293
	100				

TABLE LV

BRAKED TEST RESULTS

Test No. 20 Tire Size 8:50-10

Soil Type Sand Tire Deflection 35 (d)

Soil Strength 42.2 (CI_{avg}) Carriage Speed 20 ft/sec (V_a)

Station	Slip % S	Load, lbs P	Drag, lbs R_B	Sinkage, in. Z	Torque, ft-lbs T'
21.0	10	593	155	.20	37
23.8	20	590	247	.35	90
25.8	30	603	320	.62	134
27.0	40	598	350	.70	166
27.9	50	575	380	.65	200
28.5	60	550	420	.85	225
29.1	70	545	535	1.00	246
29.8	80	555	573	1.20	264
30.7	90	573	585	1.60	275
	100				

APPENDIX III

GOVERNING EQUATIONS, LUMPED PARAMETER MODEL, AND NUMERICAL PROCEDURE FOR THE TWO-DIMENSIONAL PLANE STRAIN ROLLING MULTIWHEEL PROBLEM

Governing Equations

The equations of continuum elasticity and plasticity used in the lumped parameter iteration method are listed in this section in the form applicable to the lumped parameter model shown in Figure 22.

a. Dynamic Equations of Motion

$$\rho\ddot{U}(i,j) = \frac{\sigma_\eta(i+1,j+1) - \sigma_\eta(i,j)}{h/\sqrt{2}} + \frac{\tau_{\eta\zeta}(i,j+1) - \tau_{\eta\zeta}(i+1,j)}{h/\sqrt{2}} \qquad \text{(A-1a)}$$

$$\rho\ddot{V}(i,j) = \frac{\sigma_\zeta(i,j+1) - \sigma_\zeta(i+1,j)}{h/\sqrt{2}} + \frac{\tau_{\eta\zeta}(i+1,j+1) - \tau_{\eta\zeta}(i,j)}{h/\sqrt{2}} \qquad \text{(A-1b)}$$

where

U and V are the displacements in the η and ζ directions, respectively;

σ_η and σ_ζ are the normal stresses and $\tau_{\eta\zeta}$ is the shear stress;

ρ is the density of the soil;

h is the grid size; and

the dots indicate time derivatives, and i,j are indexing subscripts.

b. Quadrature Equations

$$U^t = U^{t-\Delta t} + (\Delta t)\dot{U}^{t-\Delta t} + \frac{(\Delta t)^2}{6}[2\ddot{U}^{t-\Delta t} + \ddot{U}^t] \qquad \text{(A-2a)}$$

$$V^t = V^{t-\Delta t} + (\Delta t)\dot{V}^{t-\Delta t} + \frac{(\Delta t)^2}{6}[2\ddot{V}^{t-\Delta t} + \ddot{V}^t] \qquad \text{(A-2b)}$$

$$\dot{U}^t = \dot{U}^{t-\Delta t} + \frac{\Delta t}{2}[\ddot{U}^{t-\Delta t} + \ddot{U}^t] \qquad \text{(A-2c)}$$

$$\dot{V}^t = \dot{V}^{t-\Delta t} + \frac{\Delta t}{2}[\ddot{V}^{t-\Delta t} + \ddot{V}^t] \qquad \text{(A-2d)}$$

where

Δt is the time increment, and superscript $(t-\Delta t)$ indicates the variables of the previous load increment.

c. Drucker-Prager Yield Criterion

The criterion states that if the yield function, f, as defined below is less than zero, the stress point is elastic, and if f is equal to or greater than zero, the stress point has yielded.

$$\text{Yield function} = f = \alpha_1 I + \sqrt{J - k} \tag{A-3}$$

where

$$I = \sigma_\eta + \sigma_\zeta + \sigma_\xi \tag{A-4}$$

$$J = \frac{1}{6}\left[(\sigma_\eta - \sigma_\zeta)^2 + (\sigma_\zeta - \sigma_\xi)^2 + (\sigma_\xi - \sigma_\eta)^2 + 6\tau_{\eta\zeta}^2 \right] \tag{A-5}$$

$$\sigma_\xi = \nu(\sigma_\eta + \sigma_\zeta) \tag{A-6}$$

$$\alpha_1 = \frac{2 \sin\phi}{\sqrt{3}(3 - \sin\phi)} \tag{A-7}$$

$$k = \frac{6\, c \cos\phi}{\sqrt{3}(3 - \sin\phi)} = \text{yield stress in shear} \tag{A-8}$$

c = cohesion

ϕ = friction angle

d. Incremental Strain-Displacement Relations

$$\Delta\epsilon_\eta(i,j) = \frac{\Delta U(i,j) - \Delta U(i-1,j-1)}{h/\sqrt{2}} \tag{A-9a}$$

$$\Delta\epsilon_\zeta(i,j) = \frac{\Delta V(i-1,j) - \Delta V(i,j-1)}{h/\sqrt{2}} \tag{A-9b}$$

$$\Delta\epsilon_\xi(i,j) = 0 \tag{A-9c}$$

$$\Delta\gamma_{\eta\zeta}(i,j) = \frac{\Delta U(i-1,j) - \Delta U(i,j-1)}{2h/\sqrt{2}} + \frac{\Delta V(i,j) - \Delta V(i-1,j-1)}{2h/\sqrt{2}} \tag{A-9d}$$

where $\Delta\epsilon_\eta$, $\Delta\epsilon_\zeta$, and $\Delta\epsilon_\xi$ are the normal strain increments,

$\Delta\gamma_{\eta\zeta}$ is the shear strain increment,

and $$\Delta U = U^t - U^{t-\Delta t} \tag{A-10a}$$

$$\Delta V = V^t - V^{t-\Delta t} \tag{A-10b}$$

e. Incremental Stress-Strain Relations

$$\Delta\sigma_\eta = \lambda\Delta\epsilon + 2G\Delta\epsilon_\eta - \beta Q\left(\frac{\sigma_\eta}{2\sqrt{J}} + B\right)\left(\frac{\Delta W}{2\sqrt{J}} + B\Delta\epsilon\right) \tag{A-11a}$$

$$\Delta\sigma_\zeta = \lambda\Delta\epsilon + 2G\Delta\epsilon_\zeta - \beta Q\left(\frac{\sigma_\zeta}{2\sqrt{J}} + B\right)\left(\frac{\Delta W}{2\sqrt{J}} + B\Delta\epsilon\right) \tag{A-11b}$$

$$\Delta\tau_{\eta\zeta} = 2G\Delta\gamma_{\eta\zeta} - \beta Q\left(\frac{\tau_{\eta\zeta}}{2\sqrt{J}}\right)\left(\frac{\Delta W}{2\sqrt{J}} + B\Delta\epsilon\right) \tag{A-11c}$$

where $$\Delta\epsilon = \Delta\epsilon_\eta + \Delta\epsilon_\zeta \tag{A-12}$$

$$B = \frac{1+\nu}{1-2\nu}\alpha - \frac{I}{6\sqrt{J}} \tag{A-13}$$

$$Q = \frac{4G}{1 + \frac{6(1+\nu)\alpha^2}{1-2\nu}} \tag{A-14}$$

λ = Lame's constant in Hooke's law = $\dfrac{E\nu}{(1+\nu)(1-2\nu)}$

G = Modulus of rigidity = $\dfrac{E}{2(1+\nu)}$

ΔW = Increment work done

$$= \sigma_\eta\Delta\epsilon_\eta + \sigma_\zeta\Delta\epsilon_\zeta + \tau_{\eta\zeta}\Delta\gamma_{\eta\zeta} \tag{A-15}$$

and $$\beta = \begin{cases} 1 \text{ if } f \geq 0 \text{ and } \Delta W > 0 \text{ (loading)} \\ 0 \text{ if } f \geq 0 \text{ and } \Delta W < 0 \text{ (unloading) or } f < 0 \text{ (elastic)} \end{cases}$$

Then the stresses at time t are:

$$\sigma_{\eta}^{t} = \sigma_{\eta}^{t-\Delta t} + \Delta\sigma_{\eta}^{t} \qquad \text{(A-16a)}$$

$$\sigma_{\zeta}^{t} = \sigma_{\zeta}^{t-\Delta t} + \Delta\sigma_{\zeta}^{t} \qquad \text{(A-16b)}$$

$$\tau_{\eta\zeta}^{t} = \tau_{\eta\zeta}^{t-\Delta t} + \Delta\tau_{\eta\zeta}^{t} \qquad \text{(A-16c)}$$

f. Stress Correction Equations for Perfectly Plastic Yielding

$$\sigma'_{\eta} = (1-\eta_c)\sigma_{\eta} + \eta_c\left[(1+6\alpha^2)\frac{I}{3} - 2\alpha k\right] \qquad \text{(A-17a)}$$

$$\sigma'_{\zeta} = (1-\eta_c)\sigma_{\zeta} + \eta_c\left[(1+6\alpha^2)\frac{I}{3} - 2\alpha k\right] \qquad \text{(A-17b)}$$

$$\tau'_{\eta\zeta} = (1-\eta_c)\tau_{\eta\zeta} \qquad \text{(A-17c)}$$

where $$\eta_c = \frac{J - (k-\alpha I)^2}{2J + 12\alpha^2 (k-\alpha I)^2} \qquad \text{(A-18)}$$

and σ'_{η}, σ'_{ζ}, and $\tau'_{\eta\zeta}$ are the corrected stresses.

Numerical Procedure for the Development of the Computer Program

For convenience in the numerical calculations, the above governing equations are first expressed in terms of dimensionless variables. The dimensionless variables are formed in the following manner: the variables having a dimension of stress are divided by the yield stress in shear, k (see Equation A-8); variables having a dimension of length are divided by the width, ℓ, of the applied surface pressure strip; and time is divided by a characteristic time h/V, which is the time required to travel between two mass points.

The rise time of the pressure-time curve is divided into a number of time increments, so the peak pressure is divided by this same number to get the pressure increment. For each increment of time, the stresses at the fictitious stress points in the plane (j = 1, in Figure 22) are changed by the pressure increment according to the pressure distribution. (Pressure increment becomes zero when peak load is attained.) Then the following steps are performed starting with the mass point at (i, j) = (2, 1):

(1) The accelerations $\ddot{U}$ and $\ddot{V}$ at time t are obtained by means of the dynamic equations of motion, Equation (A-1), using the most current stresses that are known at time t (if not known, those at time t-Δt are used).

(2) The accelerations at time t and the accelerations, velocities, and displacements at time t-Δt are then substituted into the quadrature equations, Equations (A-2), to give U, V, $\dot{U}$, and $\dot{V}$ at time t. Then the incremental displacements, ΔU^t and ΔV^t are obtained from Equations (A-10).

(3) The stresses at the two stress points immediately below the mass point (i, j) are recalculated according to the following steps for each stress point:

(a) The yield indicating table is checked to determine if the stress point had yielded. (Initially, the table would indicate all stress points to be elastic.)

(b) The incremental strains at time t are calculated using the incremental strain-displacement relations, Equations (A-9).

(c) The stress increments are then calculated from the incremental stress strain relations, Equations (A-11). The stresses at the time t are then calculated by Equations (A-16).

(d) The newly obtained stresses are then substituted into the yield criterion, Equation (A-3), to check if the stress point had yielded. The result is then recorded in the yield indicating table. Stress correction is performed using Equations(A-17), if it were required.

(4) Steps 1 through 3 are repeated for the rest of the mass points, proceeding from the left edge (i = 2) towards the right and then row by row downward.

(5) Using the new stresses obtained for all the stress points, steps 1 through 4 are repeated, thus starting the iteration cycle. This is done until the desired accuracy is reached.

(6) Steps 1 through 5 are repeated for the subsequent time increments, in which the applied pressure on the boundary is incremented according to the pressure-time curve.

APPENDIX IV

ROLLING MULTIWHEEL ANALYTICAL SINKAGE PREDICTION COMPUTER PROGRAM

with

A. Some Preliminary Remarks About the Computer Program

B. Procedure for Running the Computer Program

C. List of Symbols

D. Fortran Source Listing of the Computer Program

A. Some Preliminary Remarks About the Computer Program

(a) One of the input data items to the program is the time increment, DT. It is calculated prior to running the program, using the stability criterion discussed in the Phase II Final Report[1]. The following procedure should be followed:

- An approximate time increment satisfying the stability criterion is first obtained by the formula

$$(\Delta t)_{approx.} = \frac{h}{2c_1}$$

where h and c_1 are the grid size and the dilatational wave velocity, respectively.

- With the above approximate time increment as a guide, a smaller time increment, Δt, is chosen such that

$$n(\Delta t) = t_c = \frac{h}{V}$$

where n is an integer and V is the aircraft ground velocity. The symbol t_c is used for the time required for the loaded area to traverse between two consecutive mass points; t_c is also used as a characteristic time for non-dimensionalizing the time variable.

(b) The applied surface pressure was assumed to increase linearly to the peak pressure through the rise time, t_r, and was kept constant after t_r; t_r was taken to be 1.5 t_c.

(c) Since the computer time required to run through the total number of time increments is quite long, the computer program is written such that a small number of time increments may be run in one computer run. Magnetic tapes are used for saving results of one run for continuation in the next run. This can be done by specifying in the last data card the starting load increment number, LB, and the ending load increment number, LEN.

(d) The computer run is monitored by printing out the vertical normal stresses, the vertical displacements, and the yield indicating table of the

region under the load intermittently; the number of load increments skipped is given by the Index ILI. The vertical normal stresses, vertical displacements, and yield indicating table of the rest of the region are also printed out at a less frequent rate, and the number of load increments skipped in this case is given by IEI. The other stresses and displacements are not printed out because the volume of print-out would be prohibitively large; however, at a much less frequent rate all results of a load increment are saved on the output tape. The number of load increments skipped for this case is given by JLI. The indices ILI, IEI, and JLI are all input data specified in the last data card.

(e) Two magnetic tapes are required. They are set up as Units 9 and 10. They are used alternately as input and output tapes. The interchanging of the tapes is done by specifying the integers NTI and NTO, which are both input data items in the last data card. At the end of each run, all the results of the last load increment are recorded on the output tape, which already has the intermittent saving of all the results of the run. After this, all the previously saved results on the input tape are transferred over. This output tape then becomes the input tape in the continuation run. This rotation of tapes is necessary to avoid holding up a continuation run due to redundancy on the tape. The number of previous load increment results saved on the input tape is indicated by integer NT1. The position of the particular load increment results needed to make a continuation run is indicated by the integer NT2. The number of load increment results on the input tape that are to be transferred to the output tape is indicated by the integer NT3. NT1, NT2, and NT3 are input control indices specified in the last data card.

(f) The numerical value of each element of the yield indicating table supplies the following information:

(1) If $-1.0 < YIT < 0.0$, the stress point is elastic.

(2) If $-10.015 < YIT < -10.0$, the yield function is greater than zero but has not exceeded the tolerance for yielding (which is 0.015 in this case), thus, the stress point is still considered elastic.

(3) If $0.0 < YIT < 10.000$, the stress point has yielded and is loading, and no stress correction was applied. The digits to the right of the decimal point give the stress correction factor $(1 - \eta_c)$, which is a number between 0.0 and 1.0. The four digits left of the decimal point gives the value of the yield function which is a number between 0.0 and 1.0.

(4) If $30000.0 < YIT < 40000.0$, the yield function has exceeded the tolerances for stress correction, and stress correction has been applied, The digits other than the ten thousand place digit gives the same information as (3).

(5) If $20000.0 < YIT < 30000.0$, the yield function is negative but has not gone below the tolerance (-0.015) for becoming elastic again, thus, the stress point is still considered plastic. The digits other than the ten thousand place digit give the same information as (3).

(6) If $40000.0 < YIT < 70000.0$, the stress point is plastic and unloading. The digits other than the ten thousand place digit give the same information as (3).

(g) Before making a continuation run of the computer program, with the soil medium being still all-elastic, the value of the cohesion may be changed without affecting the results. However, since the stresses are normalized with respect to the yield stress in shear which is proportional to the cohesion, the values of the stresses must be converted by the conversion factor, CONV, during read-in of the tape data. This is done by specifying the control index ICV; if conversion is desired, ICV = 1; if conversion is not desired, ICV = 0. The value of the cohesion of the saved data on tape must also be specified as an input data.

(h) The tolerance for unloading is WOT specified in the second data card. A preliminary value for it may be calculated by the formula

$$\text{Tolerance for unloading} = \frac{(p_{max})^2 (\frac{\Delta t}{t_c})}{5(\lambda + 2G)}$$

where p_{max} is the peak contact pressure (tire vertical load/contact area), λ and G are the elastic constants, and Δt and t_c are defined in Item (a).

B. The Procedure for Running the Computer Program

(1) Specify on the first data card a title of length less than 24 characters including blank spaces.

(2) Specify the next four data cards:

Second Card - Specify five soil parameters: weight density (psf), Poisson's ratio, Young's modulus (psi), cohesion (psf), and friction angle (degree);

Third Card - Specify four load parameters: aircraft ground velocity (inches/sec), tire footprint length (inches), peak contact pressure (tire vertical load/contact area, psf), and tolerance for unloading (dimensionless);

Fourth Card - Specify computational parameters: space grid size in the x-direction (inches), space grid size in the y-direction (inches), time increment (seconds), number of grids in the x-direction, and number of grids in the y-direction (use 29);

Fifth Card - Specify the I-subscripts of the border mass points of the loaded areas. The first two is for the left pressure strip and the other two is for the right pressure strip.

(3) Specify on the sixth data card the value of the cohesion of the saved data on tape if conversion is desired. If conversion is not desired, a blank card must be supplied (see Item g).

(4) Prepare two magnetic tapes and set them up as Units 9 and 10. Specify on the second-to-last data card the tape numbers of these, arranged with the tape number for Unit 9 first.

(5) Specify the last data card. Sixteen integer numbers are required. Ten of them must be the following, the other four may be specified accordingly:

1 (LEN) (ILI) (IEI) (JLI) 0 0 0 0 1 9 10 0 0 1 100

LEN is the ending load increment number. It is necessary to have it equal to integral multiples of JLI. ILI , IEI, and JLI has already been discussed in Item (d). It is necessary to have JLI equal to integral multiple of ILI. It is suggested to use LEN = 50, ILI = 5, IEI = 5, and JLI = 50.

(6) To make a continuation run, the last data card is the only card needed to be changed. The information needed to change the card is always printed at the end of the preceding run. Only LEN is needed to be supplied by the operator.

C. List of Symbols

AL	Lame constant (λ) in psf; later becomes dimensionless (λ/k)
AP	Soil parameter (α_1)
BE	A variable in the plastic relation related to the stress invariants (B)
c	Cohesion (c) in psf
c_1	Dilatational wave velocity in fps (c_1)
c_2	Shear wave velocity in fps (c_2)
CONV	Conversion factor for cohesion (c); (see Remarks, Item g)
COI	Nondimensionalizing constant of the equation of motion
DFU, DFV	The value of the maximum percent convergence of η and ζ displacements between successive iterations among all the mass points
DT	Time increment (Δt) in seconds
DTT	Dimensionless time increment ($\frac{\Delta t}{t_c}$)
DU, DV	Percent convergence of the η and ζ displacements between successive iterations
E	Young's modulus (E) in psi
EX, EY, EXY	Strain increments ($\Delta\epsilon_\eta$, $\Delta\epsilon_\zeta$, and $\Delta\gamma_{\eta\zeta}$) at time t

FC	Yield function
FPL	Tire footprint length (ℓ) in inches; width of loaded area (b)
FMS, FMW, FMY	Variable format for printing out vertical stresses, vertical displacements, and yield indicating table
G	Shear modulus (G) in psi; later becomes dimensionless (G/k)
H	Grid size in the x-direction; the distance between mass points (h) in inches; later becomes dimensionless (h/ℓ)
HH	Twice the grid size (2h)
I	Index in the x-direction (i)
IBD(1), IED(1)	Limiting i-index for trailing loaded area
IBD(2), IED(2)	Limiting i-index for leading loaded area
IC	Index for controlling the particular surrounding stress point to be calculated
ICV	Conversion control index (see Remarks, Item g)
ILI	The number of load increments skipped in the print out
ILL	Load increment index
ILP	Index for controlling which load increment is to be printed out
IMV, MOV	Moving boundary control indices
ISF	I-subscript modifier for moving the finite region
IT	Iteration index
J	Index in the z-direction (j)
JA	Index for controlling, during the final iteration, the entry to program for checking if the stress point has yielded
JLI	The number of load increments skipped before partial results are saved on tape
LB	Starting load increment number for the particular computer run
LEN	Ending load increment number for the particular computer run
LPP	Index for indicating first plastic point occurring
M'	The number of grid points in the x-direction

N	The number of grid points in the downward direction (N')
NIT, NOT	Input-output magnetic tape unit numbers for saving results in continuation run
NLM	Number of load increments for the tire to move through a space grid, h
NT1, NT2, NT3	Control indices (see Remarks, Item e)
NTC	Load increments counter between two mass points
NTI, NTO	Input and output tape unit numbers
NTR	Number of load increments through the rise time
P	A constant in the plastic relation (Q)
PH	Stress correction factor (η_c)
PHI	Frictional angle (ϕ) in degrees; later becomes in radians
PI	Applied pressure increment during pressure increases
PKP	Peak surface pressure in psf (vertical load/contact area) (P_{max})
PO	Poisson's ratio (ν)
RAT	Stress correction factor ($1 - \eta$)
RHO	Weight density (ρ) in lb/ft^3
SI	The current applied surface pressure that is prescribed at the fictitious stress points
SIK	Dimensionless applied pressure increment
SJ	Second stress invariant of the stress tensor (J)
SS	First stress invariant of the stress tensor (I)
SX, SY, SXY	Normal and shear stresses in the (η, ζ) directions $(\sigma_\eta, \sigma_\zeta, \tau_{\eta\zeta})$ at time t
SXS, SYS, SXYS	The stresses of the previous iteration at the surrounding stress point being considered
SXT, SYT, SXYT	Normal and shear stresses in the (η, ζ) directions $(\sigma_\eta, \sigma_\zeta, \tau_{\eta\zeta})$ at time $t-\Delta t$
SZ	Vertical normal stress (σ_z) x 10^2; use for print-out purpose
SZZ	Normal stress in the direction normal to (η, ζ)
TC	Time required for tire to move through a space grid (h) in seconds. (Taken as characteristic time)
TM	Time in seconds (t)

U, UD, UDD	Displacement, velocity, and acceleration in the η-direction (U, $\dot{U}$, $\ddot{U}$) at time t
UB, VB	Temporary storage ior displacements at time t
UDB, VDB	Temporary storage for velocities at time t
UI	Displacement increment in the η-direction (ΔU) at time t
UPL	A variable for indicating unloading (β); UPL = -1.0 is not loading and UPL = 1.0 is unloading
UT, UDT, UDDT	Displacement, velocity, and acceleration in the η-direction (U, $\dot{U}$, $\ddot{U}$) at time t-Δt
V, VD, VDD	Displacement, velocity, and acceleration in the ζ-direction (V, $\dot{V}$, $\ddot{V}$) at time t
VA	Horizontal ground velocity, V_a, of aircraft in ips
VI	Displacement increment in the ζ-direction (ΔV) at time t
VT, VDT, VDDT	Displacement, velocity, and acceleration in the ζ-direction (V, $\dot{V}$, $\ddot{V}$) at time t-Δt
W	Vertical displacement (w) x 10^6 in z-direction, use for print-out purpose
WO	Incremental plastic work done (ΔW)
WOT	Unloading tolerance
YI	Yield indicating table at time t
YIT	Yield indicating table at time t-Δt
YS	Yield stress in skear (k) in psf

D. Fortran Source Listing of the Computer Program (see succeeding pages)

(Written for WPAFB IBM 7094 Computer. A version for the WPAFB CDC 6600 is available, but not listed here.)

```
$SETUP 9        (TAPE NO.)
$SETUP 10       (TAPE NO.)
$IBJOB          MAP,ALTIO

$IBFTC MMVSPC   M94,XR7
C   HENRY LUMING     UD RESEARCH INST.
C   PROGRAM FOR ROLLING MULTI-WHEEL ANALYTICAL SINKAGE PREDICTION
C   MAIN PROGRAM CALLING THE FOUR OVERLAID SUBROUTINES
       COMMON/DUMMY/ VD(49,29), UD(49,29),
      1               SX(49,29), SY(49,29), SXY(49,29),
      2               UT(49,29),UDT(49,29),UDDT(49,29), UI(49,29),
      3               VT(49,29),VDT(49,29),VDDT(49,29), VI(49,29),
      4              SXT(49,29),SYT(49,29),SXYT(49,29),YIT(49,29)
       COMMON/SDAT/ IM,DT,N,M,N1,M1,SI,SIK,CU1,HH,DTT,AL,GG,PU,C,
      1             CO3,P,AP,AAP,LPP,SQR2,WDT,NLM,NTR,IBD(2),IED(2)
       COMMON/CONTR/LB,LEN,ILI,ILP,IEI,IE,JLI,JLL,NT1,NT2,NT3,NTD,NTI,
      1             NII,NDT,NTC,NLD(20),IJB,MDV,IMV,ISF
       CALL SDAT1
       CALL SDAT2 ($99)
       CALL SCALC
       CALL PROUT
   99  STOP
       END



THE FOLLOWING IS A MAP SUB-PROGRAM TO DEFINE THE FILES FOR THE TAPE
   UNITS 8, 9, 10.

$IBMAP MMTAPE
       ENTRY    .UN08.
.UN08. PZE      UNIT08
UNIT08 FILE     ,B(1),READY,INOUT,BIN,BLK=256
       ENTRY    .UN09.
.UN09. PZE      UNIT09
UNIT09 FILE     ,B(2),READY,INOUT,BIN,BLK=256
       ENTRY    .UN10.
.UN10. PZE      UNIT10
UNIT10 FILE     ,B(3),READY,INOUT,BIN,BLK=256
       END



$ORIGIN         SEG1
$IBFTC MMDAT1   M94,XR7
       SUBROUTINE SDAT1
C   THIS SUBROUTINE READS IN PARAMETER DATA AND DOES SOME PRELIMINARY
C   CALCULATIONS.
       COMMON/DUMMY/ VD(49,29), UD(49,29),
      1               SX(49,29), SY(49,29), SXY(49,29),
      2               UT(49,29),UDT(49,29),UDDT(49,29), UI(49,29),
      3               VT(49,29),VDT(49,29),VDDT(49,29), VI(49,29),
      4              SXT(49,29),SYT(49,29),SXYT(49,29),YIT(49,29)
       COMMON/SDAT/ IM,DT,N,M,N1,M1,SI,SIK,CU1,HH,DTT,AL,GG,PU,C,
      1             CO3,P,AP,AAP,LPP,SQR2,WDT,NLM,NTR,IBD(2),IED(2)
```

```
      COMMON/CONTR/LB,LEN,ILI,ILP,IEI,IE,JLI,JLL,NT1,NT2,NT3,NTO,NTI,
     1             NII,NOT,NTC,NLU(20),IJB,MOV,IMV,ISF
      DIMENSION  TITLE(4)
C READ IN AND WRITE TITLE OF THE RUN.
      READ (5,129)  TITLE
      WRITE (6,144)  TITLE
C READ IN DATA - FIRST  READ CONSISTS OF SOIL PARAMETERS
C                SECOND READ CONSISTS OF LOAD PARAMETERS
C                THIRD  READ CONSISTS OF COMPUTATIONAL PARAMETERS
      READ (5,100) RHO,PO,E,C,PHI
      READ (5,101) VA,FPL,PKP,WOT
      READ (5,102) H,DT,M,N
      N1=N-1
      M1=M-1
C CALCULATE OTHER SOIL PARAMETERS AND PRINT THEM OUT FOR REFERENCE
      G=144.*E/(1.+PO)/2.
      C2=SQRT(G*32.2/RHO)
      C1=C2*(2.*(1.-PO)/(1.-2.*PO))**0.5
      AL=2.*PO*G/(1.-2.*PO)
      WRITE (6,103)
      WRITE (6,104) RHO,PO,E,G,C2,C1
      WRITE (6,105) C,PHI
      PHI=PHI*3.1415927/180.
      CC=(3.-SIN(PHI))*3.**0.5
      AP=2.*SIN(PHI)/CC
      AAP=AP*AP
      YS=6.*C*COS(PHI)/CC
      TC=H/VA
      NLM=TC/DT+0.001
      WRITE (6,106) AP,YS
      WRITE (6,111)
      WRITE (6,113) VA,FPL,PKP,NLM
      WRITE (6,107)
      WRITE (6,108) H,DT,M,N,WOT
      WRITE (6,109)
      WRITE (6,110) FPL,TC,YS
C NON-DIMENSIONALIZING ALL PARAMETERS AND CALCULATE SOME CONSTANTS THAT
C WILL BE USED IN THE LATER LOOPS
      AL=AL/YS
      G=G/YS
      GG=2.*G
      H=H/FPL
      SQR2=SQRT(2.)
      HH=H*SQR2
      FPL=FPL/12.
      DTT=DT/TC
      CO1=YS*TC*TC*32.2/(RHO*FPL*FPL)
      CO3= AP*(1.+PO)/(1.-2.*PO)
      P=GG/(0.5+3.*CO3*AP)
      DTG=DTT*GG
      DTP=DTT*P
      NTR=1.5*FLOAT(NLM)
      PI=-PKP/FLOAT(NTR)
      SIK=PI/YS
      PKPK=PKP/YS
      WRITE (6,115)  PKPK,PI,SIK,NTR
      RETURN
  100 FORMAT(F8.1,F6.2,3F8.1)
```

```
  101 FORMAT (2F10.3,F10.2,E10.2,2I5)
  102 FORMAT (F8.3,E12.6,2I5)
  103 FORMAT(1H1,19X,15HSOIL PROPERTIES)
  104 FORMAT(23X,/HDENSITY,17X,5HRHO =,F10.1,10H LBS/CU-FT/
     1        23X,14HPOISSONS RATIO,11X,4HPO =,F10.2/
     2        23X,14HYOUNGS MODULUS,12X,3HE =,F10.1,4H PSI/
     3        23X,13HSHEAR MODULUS,13X,3HG =,F10.1,10H LBS/SQ-FT/
     4        23X,29HSHEAR WAVE VELOCITY       C2 =,F10.1,7H FT/SEC/
     5        23X,29HDILATATIONAL WAVE VEL.    C1 =,F10.1,7H FT/SEC//)
  105 FORMAT(23X,8HCOHESION,15X,3HC =,F10.1,10H LBS/SQ-FT/23X,14HFRICTIO
     1N ANGLE,10X,5HPHI =,F10.1,4H DEG//)
  106 FORMAT(23X,29HFOR YIELD CRITERIA     ALPHA =,E16.8/49X,3HK =,E16.8,
     110H LBS/SQ-FT//)
  107 FORMAT(1H0,19X,24HCOMPUTATIONAL PARAMETERS)
  108 FORMAT(23X,10HSPACE MESH,
     116X,3HH =,F10.4,3H IN/23X,29HBASIC TIME INCREMENT      DT =,
     2F10.7,4H SEC//23X,11HNUMBER OF I,15X,3HM =,I4/23X,11HNUMBER OF J,
     315X,3HN =,I4/23X,29HUNLOADING TOLERANCE      WOT =,1PE10.2//)
  109 FORMAT(1H0,19X,50HCHARACTERISTIC PARAMETERS FOR NON-DIMENSIONALIZI
     1NG)
  110 FORMAT (23X,36HLENGTH -- FOOTPRINT LENGTH    = FPL =,F10.2,3H IN/
     1        23X,36HTIME   --       H/VA         = TC  =,F10.5,4H SEC/
     2        23X,36HSTRESS -- SHEAR YIELD STRESS = K   =,F10.2,10H LBS/
     3SQ-FT///)
  111 FORMAT (1H0,19X,15HLOAD PARAMETERS)
  112 FORMAT (1H///)
  113 FORMAT (23X,29HAIRCRAFT GROUND VELOCITY VA =,F10.3,7H IN/SEC/
     1        23X,29HTIRE FOOTPRINT LENGTH   FPL =,F10.3,3H IN/
     2        23X,29HPEAK APPLIED PRESSURE   PKP =,F10.1,10H LBS/SQ-FT/
     3        23X,29HNO. OF LOAD INCREMENTS  NLM =,I3//)
  115 FORMAT (1H0,19X,24HPRESSURE RISE PARAMETERS/
     1             23X,38HDIMENSIONLESS PEAK PRESSURE          =,1PE16.7/
     2             23X,38HPRESSURE INCREMENTS --DIMENSIONED    =,0PF16.5,
     310H LBS/SQ-FT/45X,16HDIMENSIONLESS  =,1PE16.7/
     4             23X,38HNO. OF INCREMENTS IN RISE TIME = NTR =,I10///)
  129 FORMAT (4A6)
  144 FORMAT (1H1////1H0,47X,42HMULTI-WHEEL MOVING LOAD SINKAGE PREDICTI
     1ON//59X,4A6)
      END
```

```
$ORIGIN        SEG1
$IBFTC MMDAT2  M94,XR7
      SUBROUTINE SDAT2 (*)
C  THIS SUBROUTINE CONTINUES SUBROUTINE SDAT1 AND ZEROES ARRAYS OR
C  READS DATA FROM TAPE.
      COMMON/DUMMY/ VD(49,29), UD(49,29),
     1              SX(49,29), SY(49,29), SXY(49,29),
     2              UT(49,29),UDT(49,29),UDDT(49,29), UI(49,29),
     3              VT(49,29),VDT(49,29),VDDT(49,29), VI(49,29),
     4             SXT(49,29),SYT(49,29),SXYT(49,29),YIT(49,29)
      COMMON/SDAT/ IM,DT,N,M,N1,M1,SI,SIK,CO1,HH,DTT,AL,GG,PO,C,
     1             CO3,P,AP,AAP,LPP,SQR2,WOT,NLM,NTR,I8D(2),IED(2)
      COMMON/CONTR/LB,LEN,ILI,ILP,IEI,IE,JLI,JLL,NT1,NT2,NT3,NTO,NTI,
     1             MT,NOT,NTC,NLO(20),IJB,MOV,IMV,ISF
```

```
C READ IN LIMITING INDICES FOR LOADED AREA AND CALCULATE APPLIED
C PRESSURE INCREMENT, SIK.
      READ (5,141)  IB1,IEN1,IB2,IEN2
      WRITE (6,116) IB1,IEN1,IB2,IEN2
C READ IN THE VALUE OF THE COHESION OF THE TAPE DATA WHICH IS USED FOR
C  CONVERSION.
      READ (5,140) CT
C READ IN TAPE NUMBERS OF THE TAPE SETUP ON UNIT 9 AND 10,RESPECTIVELY
      READ (5,141) NIT,NOT
C READ IN STARTING LOAD INCREMENT NUMBER AND ENDING LOAD INCREMENT
C NUMBER, AND OTHER CONTROL INDICES.  CALCULATE THE PRINT CONTROL
C INDICES, THE TIME OF THE PULSE, AND THE INITIAL APPLIED PRESSURE  SI,
C AND PRINT OUT FOR REFERENCE.
      READ (5,141) LB,LEN,ILI,IEI,JLI,NTC,NT1,NT2,NT3,LPP,NTI,NTO,ICV
     1            ,MOV,IJB,IMV
      ILP=LB+ILI-1
      IE=LB+IEI-1
      JLL=LB+JLI-1
      BL=LB-1
      TM=BL*DT
      IF (LB.GT.NTR)  BL=NTR
      SI=BL*SIK
  171 WRITE (6,117)
      WRITE (6,118)  LB,LEN,SI,SIK,TM
      WRITE (6,135) LB,LEN,ILI,IEI,JLI,NTC,NT1,NT2,NT3,LPP,NTI,NTO,ICV
     1            ,MOV,IJB,IMV
      LN=(LB-1)/NLM
      ISF=0
      IF (LB.GT.IMV)  ISF=(LB-1-IMV)/NLM+1
      WRITE (6,142)  ISF
      IF (NTC.EQ.NLM)  LN=LN-1
      IBD(1)= IB1+1+LN
      IBD(2)= IB2+1+LN
      IED(1)=IEN1+1+LN
      IED(2)=IEN2+1+LN
C IF CONVERSION IS NEEDED, CALCULATE THE CONVERSION FACTOR FOR THE
C  STRESSES.
      IF (ICV.EQ.0) GO TO 159
      CONV=CT/C
  159 CONTINUE
      IF (LB.NE.1)  GO TO 164
C IF THIS IS THE VERY FIRST RUN, ALL STRESSES AND DISPLACEMENTS ARE
C FIRST SET EQUAL TO ZERO, AND THE YIELD INDICATING MATRIX IS SET TO BE
C ELASTIC
      DO 7 J=1,N
      DO 7 I=1,M
        UD(I,J)=0.
        VD(I,J)=0.
        UT(I,J)=0.
        VT(I,J)=0.
       UDT(I,J)=0.
       VDT(I,J)=0.
      UDDT(I,J)=0.
      VDDT(I,J)=0.
        UI(I,J)=0.
        VI(I,J)=0.
        SX(I,J)=0.
        SY(I,J)=0.
```

```
      SXY(I,J)=0.
       SXT(I,J)=0.
       SYT(I,J)=0.
      SXYT(I,J)=0.
    7 YIT(I,J)=-1.
      RETURN
C REARRANGE DESIGNATION OF UNIT OF TAPES DEPENDING ON  NTI  AND  NTO
  164 IF (NTI.EQ.9) GO TO 173
      ILL=NIT
      NIT=NOT
      NOT=ILL
  173 WRITE (6,138) NIT
C IF THIS IS A CONTINUATION RUN, THE STRESSES, DISPLACEMENTS, AND
C     YIELD INDICATING TABLE OF THE PRECEDING RUN ARE READ IN FROM INPUT
C     TAPE. DATA READ IN, IF NO REDUNDANCY OCCURRED, ARE SAVED IN DISK
C     UNIT 8 FOR TRANSFER TO OUTPUT TAPE.
      DO 162 I=1,NT1
      READ (NTI) UT,UDT,UDDT,UI,VT,VDT,VDDT,VI,SXT,SYT,SXYT,YIT
      ILL=SYT(1,1)
      WRITE (6,139)  ILL
      IF (I.NE.NT2)  GO TO 162
      WRITE (8)  UT,UDT,UDDT,UI,VT,VDT,VDDT,VI,SXT,SYT,SXYT,YIT
  162 CONTINUE
C READ FROM DISK UNIT 8 THE DESIRE STARTING STRESSES AND DISPLACEMENTS
C FOR THE CONTINUATION RUN.
      IF (NT2.EQ.0)  GO TO 175
      REWIND 8
  174 READ (8)   UT,UDT,UDDT,UI,VT,VDT,VDDT,VI,SXT,SYT,SXYT,YIT
      ILL=SYT(1,1)
  175 IF (ILL.NE.(LB-1))  RETURN 1
      REWIND NTI
      NT1=0
C EQUATE THE CURRENT DISPLACEMENTS AND STRESSES WITH THE PREVIOUSLY
C  SAVED DISPLACEMENTS AND STRESSES. MAKE STRESS CONVERSION IF THE TAPE
C  DATA IS NORMALIZED DIFFERENTLY.
      DO 8 J=1,N
      DO 8 I=1,M
      UD(I,J)=UDT(I,J)
      VD(I,J)=VDT(I,J)
      IF (J.NE.1)  GO TO 9
        SX(I,1)=0.
        SY(I,1)=0.
       SXY(I,1)=0.
       SXT(I,1)=0.
       SYT(I,1)=0.
      SXYT(I,1)=0.
      GO TO 8
    9 IF (ICV.EQ.0) GO TO 176
       SXYT(I,J)=SXYT(I,J)*CONV
        SYT(I,J)= SYT(I,J)*CONV
        SXT(I,J)= SXT(I,J)*CONV
  176   SX(I,J)= SXT(I,J)
        SY(I,J)= SYT(I,J)
       SXY(I,J)=SXYT(I,J)
    8 CONTINUE
      NT2=0
      REWIND 8
      RETURN
```

```
  116 FORMAT (20X,28HSTARTING LOAD BORDER INDICES//
     1        23X,27HIB1  IEN1   IB2  IEN2      //20X,516//)
  117 FORMAT (1H1,18X,34HPARAMETERS FOR THIS PARTICULAR RUN)
  118 FORMAT (23X,37HSTARTING LOAD INCREMENT NUMBER   LB =,I6/23X,37HEND
     1ING   LOAD INCREMENT NUMBER  LEN =,I6/23X,37HSTARTING SURFACE PRES
     2SURE         SI =,1PE17.7,16H (DIMENSIONLESS)/23X,37HPRESSURE (OR L
     3OAD) INCREMENT    SIK =,1PE17.7,16H (DIMENSIONLESS)/23X,13HSTARTIN
     4G TIME,20X,4HTM =,0PF12.7,4H SEC//)
  135 FORMAT (1H0,18X,32HLAST DATA CARD OF THIS RUN IS---//
     225X,77HLB  LEN  ILI  IEI  JLI  NTC  NT1  NT2  NT3  LPP  NTI  NTO
     3ICV  MOV  IJB  IMV//22X,16I5///)
  138 FORMAT (1H0,18X,11HTAPE NUMBER,I6,54H  CONTAINS THE RESULTS OF LOA
     1D INCREMENT NUMBER  ILL =//)
  139 FORMAT (23X,I5)
  140 FORMAT (5F11.2)
  141 FORMAT (1X,16I5)
  142 FORMAT (18X,34HBORDER INTERFACE LOCATION----ISF =,I3///)
      END



$ORIGIN        SEG1
$IBFTC MMCALC  M94,XR7
      SUBROUTINE SCALC
C  THIS SUBROUTINE DOES THE MAIN CALCULATIONS OF THE ITERATIONS, PRINTS
C  OUT NEEDED RESULTS, AND SAVES RESULTS ON TAPES.
      COMMON/DUMMY/ VD(49,29), UD(49,29),
     1              SX(49,29), SY(49,29), SXY(49,29),
     2              UT(49,29),UDT(49,29),UDDT(49,29), UI(49,29),
     3              VT(49,29),VDT(49,29),VDDT(49,29), VI(49,29),
     4             SXT(49,29),SYT(49,29),SXYT(49,29),YIT(49,29)
      COMMON/SDAT/ TM,DT,N,M,N1,M1,SI,SIK,CO1,HH,DTT,AL,GG,PO,C,
     1             CO3,P,AP,AAP,LPP,SQR2,NDT,NLM,NTR,IBD(2),IED(2)
      COMMON/CONTR/LB,LEN,ILI,ILP,IEI,IE,JLI,JLL,NT ,NT2,NT3,NTO,NTI,
     1             NIT,NDT,NTC,NLO(20),IJB,MOV,IMV,ISF
C THE FOLLOWING DATA STATEMENTS SUPPLY THE VARIABLE FORMATS.
      LOGICAL FRNT,LAST
      SJF(V1,V2,V3,V4)=SQRT(((V1-V2)**2+(V2-V3)**2+(V3-V1)**2)/6.+V4*V4)
C STARTING POINT OF MOST OUTER LOOP, FOR CALCULATION OF EACH LOAD
C  INCREMENTS.
      UPL=-1.
      IY=0
  169 DO 250 ILL=LB,LEN
      LPT=0
      TM=TM+DT
C  SET PRESCRIBED APPLIED SURFACE PRESSURE.
      NTC=NTC+1
      IF (NTC.LE.NLM)  GO TO 8
      NTC=1
      IF (MOV.EQ.1)  IJB=IJB+1
      DO 3 K=1,2
      IBD(K)=IBD(K)+1
    3 IED(K)=IED(K)+1
      IF (ILL.LE.IMV)  GO TO 8
      ISF=(ILL-IMV)/NLM+1
      DO 160 J=1,N
```

```
      SX(ISF,J)=0.
      SY(ISF,J)=0.
     SXY(ISF,J)=0.
     SXT(ISF,J)=0.
     SYT(ISF,J)=0.
    SXYT(ISF,J)=0.
      UI(ISF,J)=0.
      VI(ISF,J)=0.
    UI(ISF+1,J)=0.
    VI(ISF+1,J)=0.
      UT(ISF,J)=0.
      VT(ISF,J)=0.
160   YIT(ISF,J)=-1.
  8 RNT=FLOAT(NTC)/FLOAT(NLM)
    IF (ILL.LE.NTR)  SI=SI+SIK
    DO 13 K=1,2
     IB=IBD(K)
    IEN=IED(K)
    IF (IB.LT.IBD(1))  GO TO 13
    DO 11 I=IB,IEN
    IF (I.EQ. IB)  GO TO 4
    IF (I.EQ.IEN)  GO TO 5
    ASI=SI/2.
    GO TO 7
  4 ASI=(1.-RNT)*SI/2.
    GO TO 7
  5 ASI=RNT*SI/2.
  7  SX(I,1)=ASI
     SY(I,1)=ASI
    SXY(I,1)=ASI
    SXT(I,1)=ASI
    SYT(I,1)=ASI
    SXYT(I,1)=ASI
 11 CONTINUE
 13 CONTINUE
     IB=IBD(1)
    IEN=IED(1)-1
    MK=M
    IF (ISF.GT.0)  MK=ISF
C STARTING POINT OF THE ITERATION LOOP.
    JA=1
    IT=0
  6 IT=IT+1
    LAST=JA.EQ.2
    DFU=0.
    DFV=0.
C STARTING POINT FOR THE LOOP INCREMENTING EACH ROW GOING DOWNWARD
    DO 83 J=1,N1
    JP=J+1
    DO 83 IQ=2,M1
C THE FOLLOWING 8 STATEMENTS MODIFY THE I-INDEX FOR REVOLVING BOUNDARY
    I=IQ+ISF
    IF (I-M) 161,163,165
161 IP=I+1
    GO TO 9
163 IP=1
    GO TO 9
165 I=I-M
```

```
      IP=I+1
C CALCULATE, AT EACH MASS POINT, THE ACCELERATIONS FROM THE DYNAMIC
C EQUATIONS OF MOTION. THE PARTICULAR EQUATION TO USE DEPENDS ON THE
C LOCATION OF THE MASS POINT.
    9 UDD=CO1*(SX(IP,JP)-SX(I,J)+SXY(I,JP)-SXY(IP,J))/HH
      VDD=CO1*(SY(I,JP)-SY(IP,J)+SXY(IP,JP)-SXY(I,J))/HH
C CALCULATE THE DISPLACEMENTS AND VELOCITIES AT TIME  T  FROM THE
C QUADRATURE EQUATIONS.
   10 UB     =UT(I,J)+DTT*UDT(I,J)+DTT*DTT*(UDDT(I,J)*2.+UDD)/6.
      VB     =VT(I,J)+DTT*VDT(I,J)+DTT*DTT*(VDDT(I,J)*2.+VDD)/6.
      UDB     =UDT(I,J)+DTT*(UDDT(I,J)+UDD)/2.
      VDB     =VDT(I,J)+DTT*(VDDT(I,J)+VDD)/2.
      IF (IT.NE.1) GO TO 12
      UD(I,J)=UDB
      VD(I,J)=VDB
      GO TO 14
C AVERAGE WITH THE DISPLACEMENTS FROM THE PRECEDING ITERATION
   12 U=UI(I,J)+UI(I,J)
      V=VI(I,J)+VI(I,J)
      UB=(UB+U)/2.
      VB=(VB+V)/2.
      UD(I,J)=(UDB+UD(I,J))/2.
      VD(I,J)=(VDB+VD(I,J))/2.
C   10 CALCULATE THE DISPLACEMENT INCREMENTS
   14 UI(I,J)=UB-UI(I,J)
      VI(I,J)=VB-VI(I,J)
      IF (JA.NE.2) GO TO 17
      UDDT(I,J)=UDD
      VDDT(I,J)=VDD
   17 IF (IT.LE.2) GO TO 20
C CALCULATE THE PERCENT CONVERGENCE OF THE VERTICAL DISPLACEMENT
C BETWEEN THIS AND THE PRECEDING ITERATION.  LOCATE THE LARGEST PERCENT
C AND SAVE IF FOR LATER REFERENCE.
      IF (ABS(U).LT.1.0E-30.OR.ABS(V).LT.1.0E-30)  GO TO 20
      DU=ABS(UB/U-1.)
      DV=ABS(VB/V-1.)
      IF (DU.LE.DFU) GO TO 18
      DFU=DU
      ILU=ILL
      ITU=IT
      IU=I
      JU=J
   18 IF (DV.LE.DFV) GO TO 20
      DFV=DV
      ILV=ILL
      ITV=IT
      IV=I
      JV=J
C CALCULATE THE STRESSES OF THE TWO STRESS POINTS BELOW THE MASS POINT.
C  INDEX IC INDICATES WHICH STRESS POINT IS BEING CONSIDERED.
C       IC=1  IS THE ONE ON THE RIGHT
C       IC=2  IS THE ONE ON THE LEFT
   20 IC=1
      K=IP
      L=JP
   22 KM=K-1
      IF (KM.EQ.0)  KM=M
      LM=L-1
```

```
      FRNT=IC.EQ.1.AND.K.NE.MK
C SAVE THE STRESSES OF THE PRECEDING ITERATION.
       SXS= SX(K,L)
       SYS= SY(K,L)
      SXYS=SXY(K,L)
      YITS=YIT(K,L)
C CALCULATE THE STRAIN INCREMENTS.
       EX=(UI(K,L)-UI(KM,LM))/HH
       EY=(VI(KM,L)-VI(K,LM))/HH
      EXY=(UI(KM,L)-UI(K,LM)+VI(K,L)-VI(KM,LM))/HH/2.
      EE=AL*(EX+EY)
C CHECK THE YIELD INDICATING TABLE TO DETERMINE WHICH STRESS-STRAIN
C  RELATION TO USE.
      IF (YITS.GE.0..AND.YITS.LE.40000.) GO TO 35
C STRESS POINT IS ELASTIC.
       SX(K,L)= SXT(K,L)+GG*EX+EE
       SY(K,L)= SYT(K,L)+GG*EY+EE
      SXY(K,L)=SXYT(K,L)+GG*EXY
      GO TO 50
C  35 STRESS POINT IS PLASTIC.
   35 UPL=-1.
      WO=SXS*EX+SYS*EY+SXYS*EXY
      SZS=PO*(SXS+SYS)
      SS=SXS+SYS+SZS
      SJ=SJF(SXS,SYS,SZS,SXYS)
      BE=CO3-SS/SJ/6.
      SJ2=SJ*2.
      WE=(WO/SJ2+BE*EE/AL)*P
       SX(K,L)= SXT(K,L)+GG*EX+EE-(SXS/SJ2+BE)*WE
       SY(K,L)= SYT(K,L)+GG*EY+EE-(SYS/SJ2+BE)*WE
      SXY(K,L)=SXYT(K,L)+GG*EXY-SXYS*WE/SJ2
C  50 CHECK IF THE STRESS POINT HAS YIELDED.  THIS IS DONE ONLY FOR THE
C     FINAL ITERATION.  JA INDEX CONTROLS THE ENTRY.
   50 IF (.NOT.LAST)  GO TO 64
C CALCULATE THE YIELD FUNCTION
      SS=SX(K,L)+SY(K,L)
      SZZ=PO*SS
      SS=SS+SZZ
      SJ=SJF(SX(K,L),SY(K,L),SZZ,SXY(K,L))
      FC=AP*SS+SJ-1.
C CHECK IF THE YIELD FUNCTION IS GREATER THAN THE TOLERANCE ABOVE ZERO.
C AND MAKE THE APPROPRIATE CHANGE IN THE YIELD INDICATING TABLE
      IF (FC.GT.0.015) GO TO 55
      IF (YITS.LT.0.)  GO TO 53
      IF (FC.GT.-0.015) GO TO 55
   53 IF (FRNT)  GO TO 66
      YI=FC
      IF (FC.GT.0.) YI=-10.-FC
      GO TO 64
C 55 STRESS POINT HAS YIELDED. CHANGE CONTROL INDEX TO SAVE DATA OF THIS
C    LOAD INCREMENT ON TAPE.  CHANGE THE FORMAT OF THE YIELD INDICATING
C    TABLE PRINT OUT.
   55 IF (FRNT)  GO TO 58
      IF (LPP.NE.1) GO TO 56
      LPP=2
C CHECK FOR UNLOADING
   56 WO=SX(K,L)*EX+SY(K,L)*EY+SXY(K,L)*EXY
      IF (WO.LT.-WOT) GO TO 57
```

```
      IF (WO.GT.WOT.OR.YITS.LT.40000.) GO TO 58
   57 UPL=1.
C CALCULATE THE STRESS CORRECTION FACTOR.
   58 SSP=(1.-AP*SS)**2
      SJS=SJ*SJ
      PH=(SJS-SSP)/(2.*SJS+12.*AAP*SSP)
      PAK=PH*((1.+6.*AAP)*SS/3.-2.*AP)
      RAT=1.-PH
      FCJ=AINT(10000.*FC)
      IF (FC.LT.0.) FCJ=20000.-FCJ
      YI=FCJ+RAT
      IF (UPL.GT.0.)  YI=YI+40000.
      IY=1
C STRESS CORRECTION IS MADE BY THE FOLLOWING STATEMENTS ONLY IF THE
C YIELD FUNCTION IS GREATER THAN A TOLERANCE.
      IF (FC.LT.0.020) GO TO 64
      YI=YI+30000.
       SX(K,L)= SX(K,L)*RAT+PAK
       SY(K,L)= SY(K,L)*RAT+PAK
      SXY(K,L)=SXY(K,L)*RAT
   64 IF (FRNT)  GO TO 66
      IF (LAST)  YIT(K,L)=YI
      IF (IC.EQ.2)  GO TO 83
   66 K=1
      IC=2
      GO TO 22
   83 CONTINUE
      IF (IT.LE.2) GO TO 6
      WRITE (6,143)  DFU,ILU,ITU,IU,JU,DFV,ILV,ITV,IV,JV
      IF (LAST)  GO TO 85
C CHECK IF THE CONVERGENCE IS GOOD ENOUGH.  RETURN TO CALCULATE ANOTHER
C ITERATION IF NOT ACCURATE ENOUGH.
      IF ((DFU.GT.0.002.OR.DFV.GT.0.002).AND.IT.LT.7) GO TO 6
C IF ACCURATE ENOUGH, ADJUST  JA  INDEX AND CALCULATE FINAL ITERATION.
      JA=2
      GO TO 6
C THE FOLLOWING LOOP SAVES ALL THE DISPLACEMENTS AND STRESSES FOR THE
C CALCULATION OF THE NEXT TIME INCREMENT.
C WITHIN THIS LOOP, THE VERTICAL DISPLACEMENTS AND STRESSES ARE ALSO
C CALCULATED FROM THE DIAGONAL DISPLAEMENTS AND STRESSES.
   85 DO 90 J=1,N
      DO 90 I=1,M
      IF (I.EQ.(ISF+1))  GO TO 87
         UT(I,J)=  UT(I,J)+UI(I,J)
         VT(I,J)=  VT(I,J)+VI(I,J)
   87   UDT(I,J)=  UD(I,J)
        VDT(I,J)=  VD(I,J)
      IF (J.EQ.1) GO TO 90
   89   SXT(I,J)=  SX(I,J)
        SYT(I,J)=  SY(I,J)
       SXYT(I,J)= SXY(I,J)
   90 CONTINUE
      IF (LPP.LT.2)  GO TO  185
C THE STRESSES AND DISPLACEMENTS OF THE LOAD INCREMENT IN WHICH THE
C FIRST PLASTIC POINT OCCURS ARE SAVED ON THE OUTPUT TAPE.
      LPP=0
      WRITE (6,119)
      WRITE (6,143)  TM,ILL,IT
```

```
      LPT=1
      GO TO 245
  185 CONTINUE
  193 IF (ILL.LT.ILP) GO TO 250
C SAVE RESULTS ON MASS STORAGE FOR SUBROUTINE PROUT TO PRINT OUT LATER.
C SAVING IS DONE ONLY AT INCREMENTS OF ILI.
  245 NT2=NT2+1
      SXT(1,1)=TM
      SYT(1,1)=ILL
      SXYT(1,1)=IY
       SXT(2,1)=IBD(1)
       SYT(2,1)=IED(1)-1
      WRITE (8  ) UT,UDT,UDDT,UI,VT,VDT,VDDT,VI,SXT,SYT,SXYT,YIT
       SXT(1,1)= SX(1,1)
       SYT(1,1)= SY(1,1)
      SXYT(1,1)=SXY(1,1)
       SYT(2,1)= SY(2,1)
       SXT(2,1)= SX(2,1)
      JTM=ITIME(K)
      WRITE (6,143)  TM,JTM
      IF (LPT.EQ.1)  GO TO 185
      ILP=ILP+ILI
  250 CONTINUE
      REWIND 8
      RETURN
  119 FORMAT (3X,23HSTRESS POINT IS PLASTIC//)
  143 FORMAT (2X,2(E20.8,4I8))
      END
```

```
$ORIGIN        SEG1
$IBFTC MPROUT  M94,XR7
      SUBROUTINE PROUT
C   THIS SUBROUTINE IS FOR PRINTING OUT THE VERTICAL STRESSES, VERTICAL
C   DISPLACEMENTS, AND YIELD INDICATING TABLE IN THE REGION UNDER THE
C   LOADED AREA FOR MONITORING THE COMPUTER RUN.
      COMMON/DUMMY/ VD(49,29), UD(49,29),
     1               SX(49,29), SY(49,29), SXY(49,29),
     2               UT(49,29),UDT(49,29),UDDT(49,29), UI(49,29),
     3               VT(49,29),VDT(49,29),VDDT(49,29), VI(49,29),
     4              SXT(49,29),SYT(49,29),SXYT(49,29),YIT(49,29)
      COMMON/SDAT/ TM,DT,N,M,N1,M1,SI,SIK,CO1,HH,DTT,AL,GG,PO,C,
     1             CO3,P,AP,AAP,LPP,SQR2,WOT,NLM,NTR,IBD(2),IED(2)
      COMMON/CONTR/LB,LEN,ILI,ILP,IEI,IE,JLI,JLL,NT1,NT2,NT3,NTO,NTI,
     1             NIT,NOT,NTC,NLO(20),IJB,MOV,IMV,ISF
      DIMENSION  SZ(49,29), W(49,29)
      EQUIVALENCE  (SZ(1),SX(1)),(W(1),SY(1))
      DIMENSION  FMS(3),FMW(3),FMY(3)
      DATA FMS(1)/18H(1X,I2,12   F10.6)  /,
     1     FMW(1)/18H(1X,I2,12   F10.6)  /,
     2     FMY(1)/18H(1X,I2,12   F10.6)  /,
     3     FX5,FX4,FX3,FX2/6HF10.5),6HF10.4),6HF10.3),6HF10.2)/
     4    ,FX6/6HF10.6)/
      DO 240 K=1,NT2
      READ  (8  ) UT,UDT,UDDT,UI,VT,VDT,VDDT,VI,SXT,SYT,SXYT,YIT
```

```
       TM= SXT(1,1)
      ILL= SYT(1,1)
      IEN= SYT(2,1)
       IB= SXT(2,1)
       IY=SXYT(1,1)
      IF (ILL.NE.JLL)  GO TO 5
C THE INDEX  JLL  CONTROLS THE SAVING OF THE RESULTS OF A PARTICULAR
C     LOAD INCREMENT ON THE OUTPUT TAPE FOR LATER REFERENCE.  THE
C     INTERVAL IS GIVEN BY  JLI.  THE RESULTS OF THE LAST LOAD INCREMENT
C     IS ALSO SAVED FOR THE CONTINUATION RUN.
      JLL=JLL+JL1
      NT1=NT1+1
      NLO(NT1)=ILL
      WRITE (NTO) UT,UDT,UDDT,UI,VT,VDT,VDDT,VI,SXT,SYT,SXYT,YIT
    5 SXT(1,1)=0.
      SXT(2,1)=0.
      IF (IY.EQ.1)  FMY(3)=FX3
      DO 30 J=1,N
      DO 30 I=1,M
          W(I,J)=(UT (I,J)+VT(I,J))*1.0E06/SQR2
      IF (J.NE.1)  GO TO 25
      SZ(I,1)= SXT(I,1)*200.
      GO TO 30
   25 SZ(I,J)=((SXT(I,J)+SYT(I,J))/2.+SXYT(I,J))*100.
   30 CONTINUE
      JT=0
C SELECTION OF FORMAT FOR THE PRINT OUT.
      IF (ABS(SZ(IEN,1)).LT.10. )  GO TO 209
      IF (ABS(SZ(IEN,1)).LT.100.)  GO TO 208
      FMS(3)=FX4
      GO TO 212
  208 FMS(3)=FX5
      GO TO 212
  209 FMS(3)=FX6
  212 IF (ABS(W(IB+1,1)).LT.  100.)  GO TO 218
      IF (ABS(W(IB+1,1)).LT.10000.)  GO TO 216
      FMW(3)=FX2
      GO TO 238
  216 FMW(3)=FX4
      GO TO 238
  218 FMW(3)=FX6
  238 CONTINUE
C  PRINT OUT RESULTS IN THE PROPER FORMAT
      JB=IJB
      JE=JB+11
  239 WRITE (6,125)  ILL,   TM,(J,J=JB,JE)
      WRITE (6,FMS)  (J,( SZ(I,J),I=JB,JE),J=1,N)
      WRITE (6,126)  ILL,   TM,(J,J=JB,JE)
      WRITE (6,FMW)  (J,(  W(I,J),I=JB,JE),J=1,N)
      WRITE (6,136)  ILL,   TM,(J,J=JB,JE)
      WRITE (6,FMY)  (J,(YIT(I,J),I=JB,JE),J=1,N)
      IF (JT.EQ.1)  GO TO 240
      JB=JB+12
      JE=JE+12
      IF (JE.GE.M)  JT=1
      GO TO 239
  240 CONTINUE
      NT2=NT1
```

```
      WRITE (6,138) NOT
      DO 205 I=1,NT1
  205 WRITE (6,139) NLO(I)
C THE RESULTS FROM THE INPUT TAPE IS TRANSFERRED TO THE OUTPUT TAPE
C BEHIND THE OUTPUT OF THIS RUN.
      IF (NT3.EQ.0)  GO TO 199
      DO 210 I=1,NT3
      READ (NTI)  UT,UDT,UDDT,UI,VT,VDT,VDDT,VI,SXT,SYT,SXYT,YIT
      NT1=NT1+1
      ILL=SYT(1,1)
      WRITE (NTO) UT,UDT,UDDT,UI,VT,VDT,VDDT,VI,SXT,SYT,SXYT,YIT
      WRITE (6,139)  ILL
  210 CONTINUE
  199 NT3=NT1
      LEN=LEN+1
      ICV=0
      WRITE (6,137) LEN,ILI,IEI,JLI,NTC,NT1,NT2,NT3,LPP,NTO,NTI,ICV,MOV
     1              ,IJB,IMV
   99 RETURN
  125 FORMAT (49H1VERTICAL STRESS DISTRIBUTION (SZ*100.)  AT ILL =,I5,
     1            8H, TIME =,F10.6,5H  SEC//1X,I9,11I10//)
  126 FORMAT (   58H1VERTICAL DISPLACEMENT DISTRIBUTION (W*10.0E 06)  AT
     1 ILL =,I5,            8H, TIME =,F10.6,5H  SEC//1X,I9,11I10//)
  136 FORMAT (40H1YIELD INDICATING TABLE (YII)   AT ILL =,I5,
     1   8H, TIME =,F10.6,5H  SEC//1X,I9,11I10//)
  137 FORMAT (1HO,3X,71HFOR CONTINUING RUN, ONLY NEED TO CHANGE THE LAST
     1 DATA CARD AS FOLLOWS--//
     211X,77HLB  LEN  ILI  IEI  JLI  NTC  NT1  NT2  NT3  LPP  NTI  NTO
     3ICV  MOV  IJB  IMV//8X,I5,5X,15I5)
  138 FORMAT (1HO,18X,11HTAPE NUMBER,I6,54H  CONTAINS THE RESULTS OF LOA
     1D INCREMENT NUMBER  ILL =//)
  139 FORMAT (23X,I5)
      END
```

THE FOLLOWING IS A SAMPLE SET OF INPUT DATA FOR THE PROGRAM.

```
$DATA
SPACING FACTOR, N=2.5
   130.0  0.45  8950.0  2000.0     15.0
   900.0       18.0     24600.0   1.38E-04
   4.50   0.0001         39   29
   11   15   21   25
     400.00      500.00
 2456 2561
    1   50    5    5   50    0    0    0    0    1    9   10    0    0
$EOF
                                                                  1  100
```

APPENDIX V

HIGH SPEED VERTICAL PLATE TESTS
TEST RESULTS

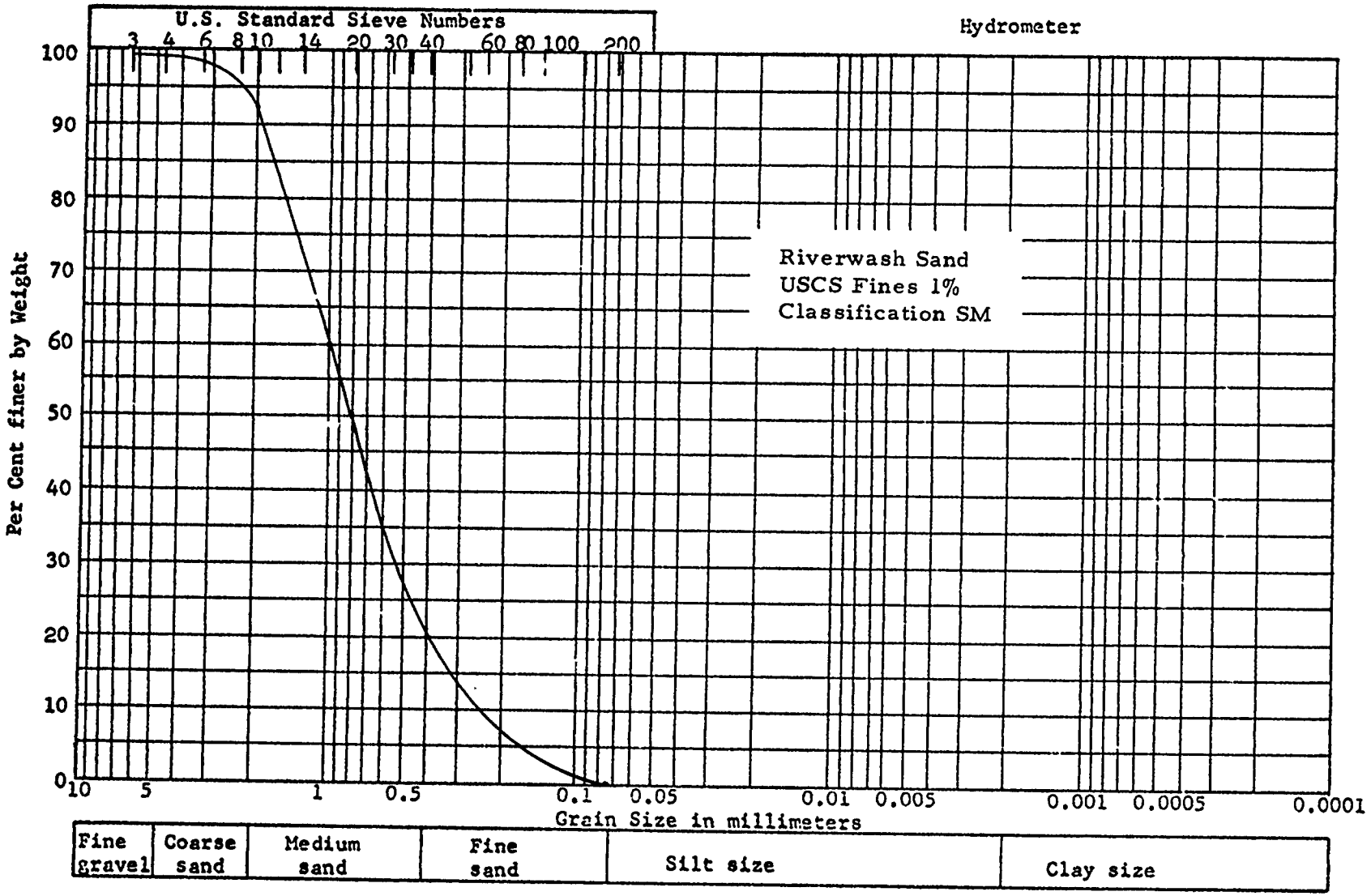

Figure 51. Grain Size Distribution - Riverwash Sand

TABLE LVI

MOISTURE - DENSITY - CONE INDEX SUMMARY - CLAY

Test No.	Percent Moisture W	Dry Density (lb/ft^3) γ_d	$CI_{tot.}$ (lb/in^2)
C-1A	29.89	85.69	121.8
C-1B	29.72	86.25	119.8
C-2A	28.96	75.13	137.7
C-2C	28.70	86.15	120.0
C-3C	28.31	90.02	108.7
C-3D	27.82	87.98	109.9
C-4A	29.72	71.56	99.7
C-4C	29.41	85.32	134.7
C-5A	29.46	78.98	141.7
C-5B	29.81	78.21	136.8
C-6A	30.35	81.38	102.9
C-6B	30.45	80.50	110.8
C-7A	29.80	81.59	109.3
C-7B	30.25	81.05	108.4
C-8A	29.16	88.91	120.8
C-8B	29.24	87.48	115.9
C-9A	29.25	87.19	109.2
C-9B	28.29	87.29	109.7

TABLE LVII

TYPICAL CONE PENETRATION RESISTANCE
WITH DEPTH CALCULATION

Test No. C-3D, Clay

Rate, r = 0.1 in/sec

Depth, inches	$R_{\#1}$ lbs	$R_{\#2}$ lbs	$R_{\#3}$ lbs	CI_{Layer}
1-1/2" + 1/2"	49	52	53	102.7
+ 1"	51	53.5	55	106.4
+ 1-1/2"	53	55	57	110.0
+ 2"	53.5	55	59	111.6
+ 2-1/2"	55	56	60	114.0
+ 3"	56	56	60	114.6

$$CI_{Layer} = \frac{R_{\#1} + R_{\#2} + R_{\#3}}{3 \cdot A_{Cone}}$$

where A_{Cone} = 0.50 sq. inches

$R_{\#1}$, $R_{\#2}$, $R_{\#3}$ represent the cone penetration resistance in pounds of three cone penetration tests taken per sample.

TABLE LVIII

UNIFORMITY OF SAMPLE PREPARATION - CLAY

Test No.	CI_{Layer}						CI_{tot}*
	$CI_{1/2"}$	$CI_{1"}$	$CI_{1-1/2"}$	$CI_{2"}$	$CI_{2-1/2"}$	$CI_{3"}$	
C-1A	117.7	120.7	124.7	125.7	123.0	120.7	121.8
C-1B	111.0	116.3	121.0	122.3	123.7	124.7	119.8
C-2A	114.7	148.3	147.5	138.6	129.3	122.6	137.7
C-2B**	131.7	133.3	129.0	130.7	131.3	123.3	129.9
C-2C	114.0	121.0	120.0	121.4	123.0	121.4	120.0
C-3A**	108.7	104.0	98.3	-	-	-	103.7
C-3B**	103.7	99.3	89.3	-	-	-	97.4
C-3C	105.0	107.7	108.7	109.0	110.7	111.3	108.7
C-3D	102.6	106.4	110.0	111.7	114.0	114.7	109.8
C-4A	109.0	98.7	91.3	-	-	-	99.7
C-4B**	112.5	104.0	96.0	-	-	-	104.1
C-4C	130.3	136.3	135.7	134.0	135.6	136.4	134.7
C-5A	132.6	134.7	141.6	142.7	147.0	149.6	141.7
C-5B	132.0	138.7	140.4	133.6	135.0	141.0	136.8
C-6A	98.4	100.7	103.0	104.7	105.0	106.0	102.9
C-6B	103.4	107.6	110.4	112.4	115.0	116.4	110.8
C-7A	104.7	109.4	110.7	110.7	110.0	110.4	109.3
C-7B	104.0	104.0	106.0	110.7	110.7	110.7	108.4
C-8A	113.6	119.6	122.0	122.3	123.4	124.0	120.8
C-8B	111.3	114.0	115.6	116.3	118.3	119.7	115.9
C-9A	103.7	107.0	109.4	110.7	111.4	113.0	109.2
C-9B	105.0	109.2	110.7	110.0	111.3	111.6	109.7

* $CI_{tot} = CI_{1/2"} + CI_{1"} + CI_{1-1/2"} + CI_{2"} + CI_{2-1/2"} + CI_{3"} \Big/ 6$

** These tests were omitted from final calculations.

TABLE LIX

MOISTURE - DENSITY - CONE INDEX SUMMARY - SAND

Test No.	Percent Moisture W	Dry Density (lb/ft^3) γ_d	$CI_{2''}$ (lb/in^2)
S-1A	4.96	119.76	49.0
S-1B	5.1[illegible]	120.55	48.0
S-1C	5.34	118.37	57.2
S-2A	5.48	115.90	51.4
S-2B	5.76	118.40	50.2
S-2C	5.76	120.74	52.0
S-3A	5.96	119.13	50.8
S-3B	5.69	115.65	49.3
S-3C	5.70	124.27	58.0
S-4A	5.90	119.10	50.8
S-4B	5.34	115.80	48.8
S-4C	5.83	120.86	50.6
S-5A	5.42	114.10	49.8
S-5B	5.66	113.40	50.6
S-5C	5.62	115.38	45.2
S-6A	5.64	123.06	56.4
S-6B	5.12	121.16	53.4
S-6C	4.95	120.66	52.0
S-7A	5.10	123.06	61.4
S-7B	5.23	124.65	51.4
S-7C	5.13	121.46	58.2
S-8A	4.58	122.29	49.6
S-8B	4.72	119.17	53.3
S-8C	4.81	119.94	47.1
S-9A	5.13	124.95	57.9
S-9B	4.83	118.53	61.7
S-9C	4.75	120.68	54.8

TABLE LX

UNIFORMITY OF SAMPLE PREPARATION - SAND

Test No.	CI_{Layer}					
	$CI_{1/2"}$	$CI_{1"}$	$CI_{1-1/2"}$	$CI_{2"}$	$CI_{2-1/2"}$	$CI_{3"}$
S-1A	12.7	22.1	33.7	49.0	68.3	91.9
S-1B	12.9	21.2	32.3	48.0	67.3	90.7
S-1C	16.2	26.5	40.5	57.2	80.0	104.9
S-2A	14.8	23.2	35.2	51.4	70.4	94.4
S-2B	13.2	21.8	33.8	50.2	67.8	91.2
S-2C	15.4	24.7	36.5	52.0	70.2	92.1
S-3A	13.5	21.9	34.0	50.8	71.4	97.2
S-3B	13.0	21.8	33.5	49.3	69.4	90.6
S-3C	17.1	27.7	41.3	58.0	75.8	100.1
S-4A	14.7	23.1	35.0	50.8	69.4	93.2
S-4B	14.9	22.7	33.6	48.8	69.5	92.4
S-4C	15.6	24.3	34.0	50.6	70.4	95.0
S-5A	14.5	23.5	34.7	49.8	69.7	97.3
S-5B	13.5	22.7	33.7	50.6	68.0	89.9
S-5C	12.0	20.4	31.5	45.2	64.3	90.8
S-6A	17.2	27.9	40.9	56.4	74.5	96.1
S-6B	15.0	23.8	36.9	53.4	72.4	95.7
S-6C	13.7	23.0	35.1	52.0	75.0	100.4
S-7A	16.4	27.7	42.7	61.4	86.1	111.3
S-7B	14.7	24.5	36.7	51.4	70.1	90.3
S-7C	15.1	25.1	39.4	58.2	82.9	110.8
S-8A	12.6	21.0	33.3	49.6	66.0	85.4
S-8B	14.5	23.4	36.2	53.3	72.9	94.3
S-8C	14.9	23.3	33.8	47.1	65.5	90.8
S-9A	15.3	25.7	39.0	57.9	80.4	108.1
S-9B	15.3	25.7	41.6	61.7	85.3	111.5
S-9C	15.6	25.8	38.7	54.8	76.5	104.0

APPENDIX VI

UNIVERSITY OF DAYTON TIRE/SOIL INTERACTION RESEARCH REPORTS AND COMPUTER PROGRAMS

A summary listing is given on the following pages of each report and each computer program developed by the University of Dayton under Air Force sponsorship (Air Force Flight Dynamics Laboratory, Vehicle Equipment Division) in the research program, "Landing Gear/Soils Interaction and Flotation Criteria."

The computer programs are available for use by other organizations with Air Force permission. Additional information may be secured by contacting:

Dr David C. Kraft
Dept. of Civil Engineering and Research Institute
University of Dayton
Dayton, Ohio 45409

Mr. George J. Sperry
Project Engineer, Vehicle Equipment Division (AFFDL/FEM)
Air Force Flight Dynamics Laboratory
Wright-Patterson Air Force Base, Ohio 45433

LANDING GEAR/SOILS INTERACTION AND FLOTATION CRITERIA PUBLICATIONS AND REPORTS

Kraft, David C., and Hoppenjans, J. R., Experimental Determination of Rolling-Multiple Wheel Performance in Soil, paper accepted for presentation at ISTVS 4th International Congress, Stockholm, Sweden, April 1972.

Kraft, David C., Luming, Henry, and Hoppenjans, J. Richard, Multiwheel Landing Gear - Soils Interaction and Flotation Criteria - Phase III, Part I, AFFDL-TR-71-12, Part 1, Air Force Flight Dynamics Laboratory, Wright-Patterson Air Force Base, Ohio, May 1971.

Kraft, David C., and Luming, Henry, Multiple Rolling Tire Sinkage and Drag Interaction Effects, paper presented at the Joint ISTVS-SAE Meeting, Detroit, Michigan, January 1971.

Luming, Henry, Analytical Aircraft Landing Gear-Soil Interaction - Phase III, Rolling Single Wheel Analytical Sinkage Prediction Technique and Computer Program, AFFDL-TR-70-142, Air Force Flight Dynamics Laboratory, Wright-Patterson Air Force Base, Ohio, September 1970.

Kraft, David C., Liguori, Albert E., Hoppenjans, J. Richard, Twin-Vertical Plate Verification Tests, Test Report, UDRI-TR-70-27, University of Dayton Research Institute, Dayton, Ohio, May 1970.

Luming, Henry, Multiwheel Vertical Pulse Load Analytical Sinkage Prediction Technique and Computer Program, UDRI-TR-70-22, University of Dayton Research Institute, Dayton, Ohio, May 1970.

Kraft, D. C., Luming, H., and Hoppenjans, J. R., Aircraft Landing Gear-Soils Interaction and Flotation Criteria, Phase II, AFFDL-TR-69-76, Air Force Flight Dynamics Laboratory, Wright-Patterson AFB, Ohio, November 1969.

Luming, Henry, Finite Element Approach to Axisymmetric Dynamic Soil Deformations, Symposium on Application of Finite Element Methods in Civil Engineering, Vanderbilt University, Nashville, Tennessee, November 1969.

Kraft, David C., Flotation Performance of Aircraft Tires on Soil Runways, Journal of Terramechanics, Vol. 6, No. 1, 1969.

Kraft, David C., Preliminary Single Wheel Relative Merit Index, UDRI-TR-69-16, University of Dayton, Dayton, Ohio, May 1969.

Kraft, David C., Analytical Landing Gear-Soils Interaction, Phase I, AFFDL-TR-68-88, Air Force Flight Dynamics Laboratory, Wright-Patterson Air Force Base, Ohio, August 1968.

LANDING GEAR/SOILS INTERACTION A' D FLOTATION CRITERIA COMPUTER PROGRAMS

Title of Computer Program: Transient Loading-Sinkage Analysis, Computer Program - 1

Brief Description: The computer program calculates the instantaneous (time-dependent) sinkage into a soil medium of a rolling aircraft tire. The rolling aircraft tire loading is simulated as a dynamic pulse loading applied in a vertical direction through a mass at the interface. The duration of the pulse is varied to simulate different forward velocities of the tire. The soil medium is assumed to be elastic and the load is applied as a uniform pressure over a circularly loaded area. The input parameters are the magnitude of

the mass, shape of load pulse, duration of pulse, radius of loaded area, intensity of pressure, soil density, and soil shear modulus.

Computer Language: Fortran IV - (IBM)

Equipment: The computer program was originally written for use on the IBM 7094 at Wright-Patterson Air Force Base, Dayton, Ohio.

Reference: Kraft, David C., "Analytical Landing Gear-Soils Interaction - Phase I," AFFDL-TR-68-88, Air Force Flight Dynamics Laboratory, Wright-Patterson Air Force Base, Ohio, August 1968.

Title of Computer Program: Flotation Index-Operations Index, Computer Program - 2

Brief Description: The computer program calculates the flotation capacity of single and multiple wheel landing gear configurations for operation on unprepared (soil) runways. The flotation capacity is expressed by the Flotation Index (FI) and Operations Index (OI) which are calculated based on sinkage and drag. The FI is the drag ratio of a given aircraft based on specified operating conditions. The OI is the ratio of sinkage to load at the same operating conditions. Current program results include flotation ratings of all currently used aircraft tires on cargo, bomber, and fighter type aircraft. These results permit aircraft designers to select tires and landing gear configurations for optimum flotation (minimum drag). Program was revised 6-70.

Computer Language: Fortran IV - (IBM)

Equipment: The computer program was originally written for use on the IBM 7094 at Wright-Patterson Air Force Base, Dayton, Ohio.

Reference: Kraft, David C., Luming, Henry, and Hoppenjans, J. R., "Aircraft Landing Gear-Soils Interaction and Flotation Criteria - Phase II," AFFDL-TR-69-76, Air Force Flight Dynamics Laboratory, Wright-Patterson Air Force Base, Ohio, November 1969.

Title of Computer Program: Sinkage Wheel Stationary Pulse Load-Sinkage Prediction, Computer Program - 3

Brief Description: This computer program calculates the instantaneous sinkage into a soil medium caused by a rolling aircraft tire. The interface contact of the rolling tire is simulated by a stationary circular surface contact pressure which is uniform over the contact area and varies with time in the form of a pulse. The magnitude of the pressure changes in the same manner as the pressure experienced by a soil particle near the surface of the soil as the tire rolls over it. The soil is assumed to be an elastic-plastic material with elastic deformation governed by Hooke's law, the plastic deformations governed by an incremental stress-strain relation which is based on the normality flow rule, and the plastic yielding governed by the Drucker-Prager yield criterion with no strain-hardening. The input soil parameters are the density, the Young's modulus, the cohesion, and the friction angle. The numerical method used in solving the boundary value problem is the lumped parameter iteration method. This method uses an axisymmetric lumped parameter model to approximate the continuous medium and an iterative procedure to calculate the displacements and the stresses at the discrete points of the model.

Computer Language: Fortran IV - (IBM)

Equipment: This computer program was originally written for use on the IBM 7094-DCS at Wright-Patterson Air Force Base, Dayton, Ohio. It has a 32K-word core capacity.

Reference: Kraft, David C., Luming, Henry, and Hoppenjans, J. R., "Aircraft Landing Gear-Soils Interaction and Flotation Criteria - Phase II", AFFDL-TR-69-76, Air Force Flight Dynamics Laboratory, Wright-Patterson Air Force Base, Ohio, November 1969.

Title of Computer Program: Rolling Single Wheel Sinkage Prediction, Computer Program - 4

Brief Description: This computer program calculates the instantaneous sinkage into a soil medium caused by a rolling aircraft tire. The interface contact of the rolling tire is simulated by a surface contact pressure which is applied uniformly over an area equivalent to the tire footprint area and is moved across the surface at the aircraft horizontal ground velocity. The magnitude of the uniform pressure increases over a finite rise time from zero to a pressure equal to the vertical tire load divided by the contact area. The soil medium is assumed to be an elastic-plastic material with elastic deformations governed by Hooke's law, the plastic deformations governed by an incremental stress-strain relation which is based on the normality flow rule, and the plastic yielding governed by the Drucker-Prager yield criterion with no strain-hardening. The input soil parameters are the density, the Young's modulus, the cohesion, and the friction angle. The numerical method used in solving the boundary value problem is the lumped parameter iteration method. This method uses a three-dimensional lumped parameter model to approximate the continuous medium and an iterative procedure to calculate the displacements and stresses at the discrete points of the model. An input-output scheme is also used for utilizing the limited core capacity for the three-dimensional problem.

Computer Language: Fortran IV - (IBM)

Equipment: This computer program was originally written for use on the IBM 7094-DCS at Wright-Patterson Air Force Base, Dayton, Ohio. It has a 32K-word core capacity.

Reference: Luming, H., "Analytical Landing Gear-Soil Interaction - Phase III, Rolling Single Wheel Analytical Sinkage Prediction Technique and

Computer Program," AFFDL-TR-70-142, Air Force Flight Dynamics Laboratory, Wright-Patterson Air Force Base, Ohio, September 1970.

Title of Computer Program: Multiwheel Stationary Pulse Load Sinkage Prediction, Computer Program - 5

Brief Description: This computer program calculates the instantaneous sinkage into a soil medium caused by a pair of rolling twin aircraft tires. If the sinkages for various twin-wheel spacings were calculated and compared with the corresponding single-wheel sinkage, twin wheel effects of aircraft landing gear configurations could be obtained for use in flotation studies. The interface contacts of the rolling twin tires are simulated by two stationary surface pressure strips which are uniformly distributed and vary with time in the form of a pulse. The magnitude of the pressure changes in the same manner as the pressure experienced by a soil particle near the surface of the soil as the tire rolls over it. The soil is assumed to be an elastic-plastic material with elastic deformations governed by Hooke's law, the plastic deformations governed by an incremental stress-strain relation which is based on the normality flow rule, and the plastic yielding governed by the Drucker-Prager yield criterion with no strain-hardening. The input soil parameters are the density, the Young's modulus, the cohesion, and the friction angle. The numerical method used in solving the boundary value problem is the lumped parameter iteration method. This method uses a plane-strain two dimensional lumped parameter model to approximate the continuous medium and an iterative procedure to calculate the displacements and stresses at the discrete points of the model.

Computer Language: Fortran IV - (IBM)

Equipment: This computer program was originally written for use on the IBM 7094-DCS at Wright-Patterson Air Force Base, Dayton, Ohio. It has a 32K-word core capacity.

Reference: Luming, Henry, "Multiwheel Landing Gear-Soil Interaction - Phase III, Multiwheel Vertical Pulse Load Analytical Sinkage Prediction Technique and Computer Program," R&D Computer Program Report, Report No. UDRI-TR-70-22, University of Dayton Research Institute, Dayton, Ohio, May 1970.

Title of Computer Program: Rolling Tandem Wheel Sinkage Prediction, Computer Program - 6

Brief Description: This computer program calculates the instantaneous sinkage into a soil medium caused by a pair of free-rolling tandem-tracking aircraft tires. If the sinkages for various tandem-wheel spacings were calculated and compared with the corresponding single-wheel sinkage, tandem wheel effects of aircraft landing gear configurations could be obtained for use in flotation studies. The interface contacts of the rolling tandem tires are simulated by two surface pressure strips which are applied uniformly over areas with width equal to the tire footprint length. The pressure strips are moved across the surface at the aircraft horizontal ground velocity. The magnitude of uniform pressure increases over a finite rise time from zero to a pressure equal to the vertical tire load divided by the contact area. The soil is assumed to be an elastic-plastic material with elastic deformations governed by Hooke's law, the plastic deformations governed by an incremental stress-strain relation which is based on the normality flow rule, and the plastic yielding governed by the Drucker-Prager yeild criterion with no strain-hardening. The input soil parameters are the density, the Young's modulus, the cohesion, and the friction angle. The numerical

method used in solving the boundary value problem is the lumped parameter iteration method. This method uses a plane-strain two dimensional lumped parameter model to approximate the continuous medium and an iterative procedure to calculate the displacements and stresses at the discrete points of the model.

Computer Language: Fortran IV - (IBM and CDC)

Equipment: This computer program was originally written for use on the IBM 7094-DCS at Wright-Patterson Air Force Base, Dayton, Ohio. It has a 32K-word core capacity. A version for use on the CDC-6600 at Wright-Patterson Air Force Base is also available.

Reference: Luming, Henry, "Multiwheel Landing Gear-Soil Interaction - Phase III, Rolling Multiwheel Analytical Sinkage Prediction Technique and Computer Program," R&D Computer Program Report, Report No. UDRI-TR-71-08, University of Dayton Research Institute, Dayton, Ohio, April 1971.

Title of Computer Program: Braked Wheel Sinkage Prediction Computer Program

Brief Description: This computer program calculates the instantaneous sinkage of a braked aircraft tire into a soil runway. The loading applied to the soil surface is simulated by a uniform vertical pressure acting simultaneously with a uniform horizontal shear which is given as a percentage of the vertical load. The load is applied over an area with width equal to the tire footprint length. The soil is assumed to be an elastic-plastic matrix with elastic deformations governed by Hooke's Law, the plastic deformations governed by an incremental stress-strain relation which is based on the normality flow rule, and the plastic yielding governed by the Drucker-Prager yield criterion with no strain hardening. The input soil parameters are the density, Young's modulus, cohesion, and friction angle. The soil is assumed to be in a state of plane strain and is modeled by a two-dimensional

lumped parameter approach. An iterative procedure is utilized to compute the displacements and stresses at the discrete points of the model.

Computer Language: Fortran IV

Equipment: This computer program was written for use on the CDC 6600 digital computer at Wright-Patterson Air Force Base.

Reference: Bogner, Fred K., "Braked Wheel Sinkage Prediction Technique and Computer Program" (in preparation).

UNCLASSIFIED
Security Classification

DOCUMENT CONTROL DATA - R&D
(Security classification of title, body of abstract and indexing annotation must be entered when the overall report is classified)

1 ORIGINATING ACTIVITY (Corporate author)	2a. REPORT SECURITY CLASSIFICATION
University of Dayton Research Institute 300 College Park Avenue Dayton, Ohio 45409	Unclassified 2b GROUP

3. REPORT TITLE

MULTIWHEEL LANDING GEAR - SOILS INTERACTION AND FLOTATION CRITERIA - PHASE III. PART II

4 DESCRIPTIVE NOTES *(Type of report and inclusive dates)*

Final Report

5. AUTHOR(S) *(Last name, first name, initial)*

Kraft, David C.; Luming, Henry; Hoppenjans, J. Richard; and Bogner, Fred

6. REPORT DATE	7a. TOTAL NO. OF PAGES	7b. NO. OF REFS
January 1972	201	22

8a. CONTRACT OR GRANT NO.	9a ORIGINATOR'S REPORT NUMBER(S)
F33615-70-C-1170 b. PROJECT NO. c. d.	9b. OTHER REPORT NO(S) *(Any other numbers that may be assigned this report)* AFFDL-TR-71-12, PART II

10. AVAILABILITY/LIMITATION NOTICES

Distribution limited to U. S. Government agencies only; test and evaluation; statement applied February 1972. Other requests for this document must be referred to AF Flight Dynamics Laboratory (AFFDL/FEM), Wright-Patterson AFB, Ohio 45433.

11. SUPPLEMENTARY NOTES	12. SPONSORING MILITARY ACTIVITY
	AF Flight Dynamics Laboratory (AFFDL/FEM) Wright-Patterson AFB, Ohio 45433

13. ABSTRACT

The design and utilization of military aircraft in forward area situations has required a continual investigation of those factors which define the aircraft flotation performance and operations capability on semi- and unprepared soil runways. This report summarizes these efforts conducted under Phase III - Part II of a continuing research program in landing gear/soil interaction.

Phase III - Part II consisted primarily of a comprehensive investigation of the flotation variable of braking and how braked tire/soil interaction influences flotation performance. A series of full scale braked tire tests were conducted in a sand and clay type soil. An analytical study of braked tire/soil interaction was also made using a lumped parameter technique to simulate the soil. The results of these investigations resulted in two braking analysis equations which can be used to predict the braked tire drag ratio, ~~R_B/P (where R_B = braked drag force, R = vertical tire load)~~, for aircraft type tires operating in sand and clay type soils.

Additional studies were also made, on a preliminary basis, of the flotation variables of multipass and speed. An update of the Aircraft Flotation/Operation Summary Guide, initially presented in the Phase III - Part I Final Report, is also presented.

DD FORM 1 JAN 64 1473

UNCLASSIFIED
Security Classification

UNCLASSIFIED
Security Classification

14. KEY WORDS	LINK A		LINK B		LINK C	
	ROLE	WT	ROLE	WT	ROLE	WT
Aircraft Flotation; Aircraft Ground Surface Drag; Aircraft Tire Sinkage; Soil Mechanics; Dynamic Loading of Soil; Lumped Parameter Iteration Method; Computer Program; Aircraft Tire Braking Effects on Soil Runways; Aircraft Multipass Operation on Soil; Aircraft Ground Speed.						

INSTRUCTIONS

1. ORIGINATING ACTIVITY: Enter the name and address of the contractor, subcontractor, grantee, Department of Defense activity or other organization *(corporate author)* issuing the report.

2a. REPORT SECURITY CLASSIFICATION: Enter the overall security classification of the report. Indicate whether "Restricted Data" is included. Marking is to be in accordance with appropriate security regulations.

2b. GROUP: Automatic downgrading is specified in DoD Directive 5200.10 and Armed Forces Industrial Manual. Enter the group number. Also, when applicable, show that optional markings have been used for Group 3 and Group 4 as authorized.

3. REPORT TITLE: Enter the complete report title in all capital letters. Titles in all cases should be unclassified. If a meaningful title cannot be selected without classification, show title classification in all capitals in parenthesis immediately following the title.

4. DESCRIPTIVE NOTES: If appropriate, enter the type of report, e.g., interim, progress, summary, annual, or final. Give the inclusive dates when a specific reporting period is covered.

5. AUTHOR(S): Enter the name(s) of author(s) as shown on or in the report. Enter last name, first name, middle initial. If military, show rank and branch of service. The name of the principal author is an absolute minimum requirement.

6. REPORT DATE: Enter the date of the report as day, month, year; or month, year. If more than one date appears on the report, use date of publication.

7a. TOTAL NUMBER OF PAGES: The total page count should follow normal pagination procedures, i.e., enter the number of pages containing information.

7b. NUMBER OF REFERENCES: Enter the total number of references cited in the report.

8a. CONTRACT OR GRANT NUMBER: If appropriate, enter the applicable number of the contract or grant under which the report was written.

8b, 8c, & 8d. PROJECT NUMBER: Enter the appropriate military department identification, such as project number, subproject number, system numbers, task number, etc.

9a. ORIGINATOR'S REPORT NUMBER(S): Enter the official report number by which the document will be identified and controlled by the originating activity. This number must be unique to this report.

9b. OTHER REPORT NUMBER(S): If the report has been assigned any other report numbers *(either by the originator or by the sponsor)*, also enter this number(s).

10. AVAILABILITY/LIMITATION NOTICES: Enter any limitations on further dissemination of the report, other than those imposed by security classification, using standard statements such as:

(1) "Qualified requesters may obtain copies of this report from DDC."

(2) "Foreign announcement and dissemination of this report by DDC is not authorized."

(3) "U. S. Government agencies may obtain copies of this report directly from DDC. Other qualified DDC users shall request through _____."

(4) "U. S. military agencies may obtain copies of this report directly from DDC. Other qualified users shall request through _____."

(5) "All distribution of this report is controlled. Qualified DDC users shall request through _____."

If the report has been furnished to the Office of Technical Services, Department of Commerce, for sale to the public, indicate this fact and enter the price, if known.

11. SUPPLEMENTARY NOTES: Use for additional explanatory notes.

12. SPONSORING MILITARY ACTIVITY: Enter the name of the departmental project office or laboratory sponsoring *(paying for)* the research and development. Include address.

13. ABSTRACT: Enter an abstract giving a brief and factual summary of the document indicative of the report, even though it may also appear elsewhere in the body of the technical report. If additional space is required, a continuation sheet shall be attached.

It is highly desirable that the abstract of classified reports be unclassified. Each paragraph of the abstract shall end with an indication of the military security classification of the information in the paragraph, represented as *(TS)*, *(S)*, *(C)*, or *(U)*.

There is no limitation on the length of the abstract. However, the suggested length is from 150 to 225 words.

14. KEY WORDS: Key words are technically meaningful terms or short phrases that characterize a report and may be used as index entries for cataloging the report. Key words must be selected so that no security classification is required. Identifiers, such as equipment model designation, trade name, military project code name, geographic location, may be used as key words but will be followed by an indication of technical context. The assignment of links, rules, and weights is optional.

GPO 886-551

☆U.S.Government Printing Office: 1972 — 759-086/384

UNCLASSIFIED
Security Classification